THE EFFECTS OF INCREASING STEP RATE ON ACHILLES TENDON STRESS
DURING RUNNING

By

KATHRYN A. FARINA

A DISSERTATION

Presented to the Department of Human Physiology
and the Division of Graduate Studies of the University of Oregon
in partial fulfillment of the requirements
for the degree of
Doctor of Philosophy

March 2022

DISSERTATION APPROVAL PAGE

Student: Kathryn A. Farina

Title: The Effects of Increasing Step Rate on Achilles Tendon Stress During Running

This dissertation has been accepted and approved in partial fulfillment of the requirements for the Doctor of Philosophy degree in the Department of Human Physiology by:

Michael E. Hahn, Ph.D.	Chairperson
Andrew R. Karduna, Ph.D.	Core Member
Nicholas L. Strasser, M.D	Core Member
Robert E. Guldberg, Ph.D.	Institutional Representative

and

Krista Chronister	Vice Provost of the Division of Graduate Studies

Original approval signatures are on file with the University of Oregon Division of Graduate Studies.

Degree awarded March 2022

DISSERTATION ABSTRACT

Kathryn A. Farina

Doctor of Philosophy

Department of Human Physiology

March 2022

Title: The Effects of Increasing Step Rate on Achilles Tendon Stress During Running

Achilles tendon injuries are one of the most common running related injuries. Injuries to the Achilles tendon are painful, often involve long recovery and rehabilitation, and many patients are non-responsive to current treatments. One hypothesis for development of injury involves the combined action of frontal plane rearfoot motion and tibial rotation during the stance phase of running, leading to damage, and possible injury, within the tendon tissue if not given adequate time to recover. Targeting these actions of rearfoot motion may alter stress in the tendon, possibly decreasing injury risk, or providing alternate avenues of rehabilitation by addressing underlying movement patterns. The purpose of this dissertation was to evaluate how increasing step rate during running affects motion at the rearfoot and how changes in rearfoot motion affect stress in the Achilles tendon in healthy and injured runners.

This dissertation was divided into three projects. Project 1 involved twenty healthy runners running with +5% and +10% increases in step rate on a force-instrumented treadmill, while motion capture data were collected. Results indicated increasing step rate significantly reduced peak rearfoot angles in the sagittal and frontal plane and reduced tibial internal rotation in the transverse plane. Project 2 used these previously collected data

in a generic calcaneus and Achilles tendon finite element model to estimate changes in Achilles tendon stress as a result of increasing step rate. Conflicting results were observed, as the finite element model produced increased stress in the Achilles tendon with increased step rate but calculating stress with cross sectional area showed decreases in stress. Project 3 repeated procedures from Projects 1 and 2; however, runners with Achilles tendon injury were recruited for this final study, with magnetic resonance imaging scans of their injured leg used to create subject-specific finite element models. The results showed no significant differences in Achilles tendon stress with increased step rate, however results were variable between subjects. The results of this dissertation indicate increasing step rate significantly affects rearfoot motion; however, constraints in the finite element models and high subject variability led to inconclusive results concerning how increasing step rate affects Achilles tendon stress.

CURRICULUM VITAE

NAME OF AUTHOR: Kathryn A. Farina

GRADAUTE AND UNDERGRADUATE SCHOOLS ATTENDED

    University of Oregon, Eugene, OR
    Appalachian State University, Boone, NC
    High Point University, High Point, NC

DEGREES AWARDED

    Doctor of Philosophy, Human Physiology, 2022, University of Oregon
    Master of Science, Exercise Science, 2018, Appalachian State University
    Bachelor of Science, Exercise Science, 2016, High Point University

AREAS OF SPECIAL INTEREST

    Lower extremity biomechanics
    Footwear biomechanics
    Running biomechanics

PROFESSIONAL EXPERIENCE:

    Manager, Concept Excellence—Advanced Creation Testing & Quality, adidas, 2021 - Present

    Human Performance Specialist and Administrator, Bowerman Sports Science Center, University of Oregon, 2019 - 2021

    Graduate Employee, University of Oregon, 2018 - 2021

    Graduate Teaching Assistant, Appalachian State University, 2016 - 2018

    Sales Associate, Nike Factory Store, 2018

    Sales Associate, Crozet Running Store, 2014 - 2018

    Research Assistant, Human Biomechanics and Physiology Laboratory, High Point University, 2013 - 2016

GRANTS, AWARDS, AND HONORS

    Outstanding Doctoral Student Presentation Award, Northwest Biomechanics

Symposium, 2021

William and Genera Fieldman Scholarship, Department of Human Physiology, University of Oregon, 2021

Ursula (Sue) Moshberger Scholarship, Department of Human Physiology, University of Oregon, 2020

First Year Merit Award, Department of Human Physiology, University of Oregon, 2019

Graduate Student Award, Appalachian State University, 2018

Office of Student Research Graduate Research Grant, Appalachian State University, 2018

American Society of Biomechanics Student Travel Award, 2018

North Carolina Tuition Scholarship, Appalachian State University, 2016-2018

Division I Student Athlete (Track & Field / Cross Country), Appalachian State University & High Point University, 2012-2017

Student Travel Grant, High Point University, 2015, 2016

Summer Undergraduate Research Institute Scholarship, High Point University, 2015

Big South Conference Cross Country All-Conference Academic Team, 2013

Presidential Scholarship, High Point University, 2012

Millis Scholar Athlete, High Point University, 2012-2016

PUBLICATIONS

Farina KA, Hahn ME (2022). Increasing step rate affects rearfoot kinematics and ground reaction forces during running. Biology 11, 8.

Strasser NL, Farina KA (2021). Haglund's Syndrome and Insertional Achilles tendinopathy. Operative Techniques in Sports Medicine 29.

Farina KA, Needle AR, van Werkhoven H (2021). Continuous tracking of foot strike pattern during a maximal 800-meter run. Sensors 21, 5782.

Farina KA, Kandah BA, Sowers NM, Moore GM (2021). Bone marrow aspirate concentrate injection of the Achilles tendon in a competitive distance runner. Journal of Musculoskeletal Research 24.

van Werkhoven H, Farina KA, Langley MH (2019). Using a soft conformable foot sensor to measure changes in foot strike angle during running. Sports 7, 184.

Farina KA, Wright AA, Ford KR, Wirfel LA, Smoliga JM (2017). Physiological and biomechanical responses to running on lower body positive pressure treadmills in healthy populations. Sports Medicine 47, 261-275.

ACKNOWLEDGEMENTS

I cannot express my gratitude and thanks to my advisor, Dr. Mike Hahn, enough. I always enjoy our talks about running, life, and science. You have encouraged and supported me in everything I could have ever wanted to do and have helped me grow more than you know as a researcher and person. I cannot think of a better role model to have as an advisor, and I will forever be grateful you accepted me into the BSSC family (and didn't kick me out when my dog tried to eat your chickens).

To my wonderful committee—thank you for all the support and agreeing to take on this journey with me. To Dr. Andy Karduna: thank you for always being willing to help with any request, and your encouragement these past few years. To Dr. Bob Guldberg: thank you for your expertise and wisdom and the many thought-provoking questions in our discussions. To Dr. Nick Strasser: thank you for being a part of this process, and always being willing to chat about the clinical aspects of this project—I have thoroughly enjoyed our brainstorming sessions and learning more about the clinical side of Achilles tendon injuries. Thank you all for your time, flexibility, and willingness to help me in completing this project.

Thank you to the current and former members of the BSSC—I could not have asked for a better lab group to be a part of and learn from, and this dissertation would not have been possible without you all. To Seth Donahue: thank you for the fun times sharing an office together, listening to angsty music and life talks, and your willingness to help with any problems. To Dr. Mike McGeehan: thank you for always lending a hand, or an ear, and for the many dog running excursions. To Dr. Evan Day: thank you for all your

DEDICATION

To my family, friends, and mentors—this would not have been possible without your encouragement, guidance, and support; and to my partner, Vinny—thank you for never letting me give up.

TABLE OF CONTENTS

LIST OF FIGURES

LIST OF TABLES

CHAPTER I

INTRODUCTION

Background and Significance

Introduction

Running is an injury laden sport, with the incidence of developing a running

related injury (RRI) ranging from 20-79% in a one year period [1]. Unfortunately, the

running injury cycle is quite challenging, as runners who experience a RRI are often at

increased risk for developing another RRI [2]. RRIs are multifactorial [3,4] and

addressing the specific injury site may not address other underlying mechanisms that

could be putting the runner at increased risk of injury or could have contributed to current

injury. Gait retraining has gained attention as a modality to both recover from and

prevent future RRIs through learning, adopting, and retaining a new motor pattern [5].

Approaches for gait retraining have primarily centered around visual or auditory

feedback, using mirrors [6], real-time data graphs [7–9], or metronomes [10,11]. These

interventions have targeted adjusting specific movement patterns that may be a

contributing factor to development of the injury, such as altering hip frontal plane motion

in the case of patellofemoral pain [9] or iliotibial band syndrome [8]. With promising

results of reducing pain and allowing runners to return to full training loads, gait

retraining has become a common intervention in rehabilitation for a variety of RRIs.

Despite its prevalence in RRI diagnoses, Achilles tendinopathy (AT) is one injury

that has not been targeted for gait retraining interventions. A challenging condition, AT is

characterized by pain and swelling in and around the tendon, representing a failed healing

response [12]. Disorganized production of tenocytes, the main cell type in the tendon,

1

cellular deterioration, and disruption of the collagen fibers are often present in the tendinopathic tendon [12]. It has been reported that 1 in 20 recreational runners develop AT [13], and its incidence may be more common in competitive runners [14,15]. The exact etiology for the development of AT is unknown, but one theory involves the combined action of frontal plane rearfoot motion and tibial rotation during the stance phase of running [16,17]. Following the overuse pattern for development of other RRIs, excessive motion in one segment disrupting normal motion at another segment may cause wear and tear on a structure over time, leading to development of injury. In the case of AT, this theory suggests excessive frontal plane motion of the rearfoot during stance may cause torsional forces to act upon the Achilles tendon when conflicting with rotation of the tibial segment, and over time, and with insufficient recovery, could lead to the development of tendinopathy [16,17].

Currently, the leading methods for rehabilitation of AT involve progressive loading of the tendon through eccentric, or heavy load, resistance training [18]; however, the injury is prone to recurrence [19], and these loading protocols may be ineffective in a number of patients [14,20]. Given the promising results of gait retraining in correcting problematic movement patterns associated with other RRIs, targeting excessive rearfoot movement for AT rehabilitation may be justified as another method of therapeutic intervention. Finding a proper method of gait retraining that alters rearfoot movement, and subsequently modifies loads and stress in the Achilles tendon is key to determining if gait retraining may be beneficial for AT management.

Anatomy of the Achilles Tendon and Implications for Injury Development

The Achilles tendon is thought to be one of the strongest in the human body with the capability to withstand near eight times body weight during running [21]. Without the Achilles tendon, cost of transport would substantially increase, as the Achilles tendon provides essential energy storage and return [22]. The Achilles tendon attaches the triceps surae muscle group, encompassing the medial and lateral heads of the gastrocnemius and soleus muscle, to the posterior aspect of the calcaneus. Tendon fibers derived from the gastrocnemius descend and converge while rotating around the fibers of the soleus, and ultimately attach to the calcaneus on the lateral side, while those of the soleus attach on the medial side. The spiraling of the tendon fascicles contributes to the tendon's strength, as this spiraling allows less fiber buckling when the tendon is relaxed, and decreased deformation when the tendon is stressed [23]. Although this spiraling may reduce fiber distortion and inter-fiber friction, the twisting of the tendon fibers has also been thought to contribute to increased shear stress in the tendon when it is placed under load [23–25].

Like other tendons in the human body, the Achilles tendon is made up primarily of collagen fibers, and functions to transmit forces from muscle to bone [26]. At rest, the tendon's collagen fibers are crimped and with increased strain, begin to flatten [26]. Once the tendon is strained up to 2%, the tendon deforms in a linear fashion, but once the strain exceeds 4%, microscopic failure can begin to occur [26]. When this microscopic failure occurs, or even when the tendon is stressed within physiological limits, cumulative damage may build up within the tissue [26,27]. If not given adequate time to repair, this cumulative damage can lead to injury [26,27].

Achilles Tendinopathy

Achilles tendinopathy is a common RRI, with reports of 5-34% of all runners developing Achilles tendon pain or tendinopathy [28,29]. A painful condition, AT results from a failed healing response producing disorganization of the tendon fibers, cellular deterioration, and weakening of the tendon structure [12]. This failed healing response is often the product of a mismatch between cell recovery and breakdown, where damage to the tendon exceeds repair, and leads to a state of degeneration in the tendon [12].

Although this cycle of degeneration is thought to be the mechanism of injury to the tendon, the exact etiology setting the tendon on this downward spiraling path is debated. Microtrauma within the tendon could be the result from non-uniform stress, which may produce increased frictional forces between fibrils, or concentrated loading leading to localized fiber damage [26,27]. One theory for the development of AT in runners involves the combined actions of frontal plane rearfoot motion and tibial rotation [16,17]. In normal running gait, a slightly supinated foot makes contact with the ground and the calcaneus everts as the subtalar joint begins to pronate, causing the talus to move medially and adduct, thus internally rotating the tibia due to the tight articulations between the subtalar, talocrural, and tibiotalar joints [17]. Similarly, once the foot moves into midstance, the foot begins to supinate and the knee extends to prepare for the foot leaving the ground, causing the tibia to externally rotate [17]. When a mismatch arises in the timing of these coupling events, or one segment displays excessive motion, rotation of the tibia may conflict with rearfoot eversion, and cause increased stresses to be placed on other soft tissues or bones [16]. This conflicting motion between the start of tibial external rotation with knee extension and prolonged rearfoot eversion over time could

4

lead to increased loading on certain areas of the Achilles tendon, and lead to injury development [16].

Once the tendon falls into a state of disrepair, it is often a long road of recovery due to the innate nature of low metabolic activity in tendon tissue, resulting in slow healing processes [26]. Despite these challenges faced with returning the tendon to a healthy state, it is generally accepted that the tendon needs a loading environment to stimulate collagen synthesis and repair [18,30]. For this reason, efforts at AT rehabilitation have been centered on eccentric, isometric, or heavy load resistance training [18]. In addition, progressive loading appears to be an important factor in AT management, which may include increasing load, repetitions, or complexity of task by moving from more static to dynamic exercises [31–33]. Some patients report resolutions in tendon pain with this type of progressive loading; however, this progression could take upwards of 12 months to return to full activity [34–36], and as many as 45% of patients are reported to not respond to treatment [14,20]. Additionally, AT is prone to recurrence [19,33,37], suggesting patients may be returning to activity too quickly, or the stimulus received in rehabilitation was not sufficient to prepare the tendon for the increased demands of activity.

Characteristics of Runners with Achilles Tendinopathy

Lending to the theory of a mismatch between the timing of rearfoot motion and tibial rotation, runners presenting with AT have been reported to exhibit increased eversion, or time of eversion, in the rearfoot compared to healthy controls [38–41]. As increased motion in one body segment may influence another, or result in

overcompensation of movement to reach a desired point [42], runners with AT have also been found to remain in greater external tibial rotation throughout the stance phase, compared to controls [43]. The authors of this study found this increased external rotation of the tibia to be related to the femur remaining more internally rotated and noted this could place additional stress on the Achilles tendon. These alterations in more proximal segments could stem from motion more distally, and in this case, the authors speculated that control at the distal tibia, linked to that of rearfoot movement, could be lacking [43].

Rearfoot eversion during the stance phase of running supplements the complex movements of pronation and supination in order to absorb shock upon landing and prepare the foot to push-off the ground [44,45]. When the foot pronates in the first part of stance, the tibia is also forced to internally rotate [16]. Internal rotation of the entire lower limb allows for rearfoot eversion and pronation to occur, which lets the foot remain flexible to help absorb shock at impact with the ground [46]. As the foot moves through stance and supinates, it must become a rigid lever to enable efficient push off from the ground, the tibia externally rotates, and the hip extends to allow for external rotation of the femur [45]. It can be seen how the whole lower limb is connected throughout gait, and if one area is not able to function correctly, or is mistimed, deleterious effects can occur at many other points along the chain. It has been proposed that control of the hip musculature influences distal lower limb movement, including rearfoot motion [45,47–49]. In runners with AT, reductions in gluteal muscle activation, prime controllers of hip frontal and transverse plane movement [46], have been observed [50,51], and could influence movement at the foot due to the musculoskeletal linkage described above .

Similarly, increases in hip external rotation moment, impulse, and hip adduction impulse have also been found in runners with AT [52].

Runners with AT appear to be affected throughout the kinetic chain. The root of what causes a runner to develop AT can likely not be attributed to a single factor; however, combinations of movement patterns that could stem from proximal (hip function) or distal (rearfoot movement) mechanisms may contribute to placing increased stress or strain on the Achilles tendon. In effect, modifying one aspect of gait will cause changes elsewhere in the lower limbs. Therefore, a gait retraining intervention for runners with AT should be designed with the interdependence of the lower limb, as a whole, kept in mind.

Gait Retraining for Running Injury

Overuse RRIs often experience this cycle of inadequate time for repair coupled with cumulative damage eventually leading to injury. Gait retraining has successfully been used to address a variety of RRIs which are thought to stem from repetitive movement of misaligned structures over time. The methods of gait retraining have centered around altering step rate or foot strike pattern [53–55], or types of real-time external feedback to adjust motion in the form of visual or auditory cues [7,56–59]. Most notably, gait retraining has been used to treat patellofemoral pain syndrome [6,9,11,60–63], but has also been used to treat conditions such as iliotibial band syndrome [8,10,64,65], tibial stress fractures or bone stress syndrome [66,67], and lower-leg compartment syndrome [68,69]. In these previous studies, focus has been on modifying gait to reduce stress or load on certain structures, such as decreasing ground reaction

forces in the case of tibial stress fractures [67], or decreasing motion that may be considered excessive at a segment, such as decreasing hip adduction angles in the case of patellofemoral pain syndrome [9].

Increasing step rate is a popular method for gait retraining because it is easy to implement, can be done outside of a lab environment, and has shown good results in the management of some RRIs. Although there have been many studies that have used step rate manipulations as an intervention, few studies have evaluated non-sagittal plane motion at the rearfoot. Altering stride length, thereby jointly altering step rate, has produced a trend of decreased peak ankle eversion with decreased stride length (increased step rate) [70]. Increasing step rate has yielded decreases in hip adduction angle, peak hip adduction angle, and hip internal rotation moment [53,71,72], factors implicated in the development of patellofemoral pain syndrome and iliotibial band syndrome [73,74]. Increasing step rate has also been shown to increase gluteal muscle activity [54], a feature thought to be lacking in those with AT [50,51]. One study evaluated a +5% increase in step rate on Achilles tendon stress and strain using tendon cross sectional area from ultrasound and an estimated Achilles tendon force from musculoskeletal modeling, and found a decrease in tendon stress accompanied the increase in step rate [75]. These authors did not evaluate frontal plane mechanics at the ankle, but attributed the reduction in tendon stress and strain to a decrease in center of mass vertical displacement, along with foot placement closer to the center of mass at initial contact [75]. Given the possible link between increased rearfoot eversion and AT, more research is needed to determine the effects of altering rearfoot motion on Achilles tendon stress distribution.

Connecting Changes in Gait and Achilles Tendon Stress

Although evaluating the effects of changes in rearfoot motion are important and may be helpful in better understanding the etiology of AT development, it is also important to assess how this altered motion may affect loading and stress in the Achilles tendon. It has been reported that calcaneus angle appears to have an influence over stress distribution within the Achilles tendon [76]. Additionally, excessive loading is likely one of the major factors in the development of AT [18], and increased Achilles tendon force has been shown to accompany increases in tendon stress [77,78], which could increase vulnerability of the tendon to injury. Therefore, it is important to examine changes in loading and stress distribution as a result of altering step rate.

Finite element (FE) modeling is a method that has previously been used in estimating stress in the Achilles tendon under static and dynamic conditions [79–86]. This technique involves dividing a geometric structure of interest into many elements, for which material property and boundary conditions may be applied, thereby reducing the complexity of the object. This then leads to an understanding of the mechanical properties, such as displacements, strains, and stresses of each element, estimated using mathematical computations, and applied to the object as a whole [87]. Previous investigations using FE modeling of the foot and ankle complex have primarily focused on stresses within the bony structures [88–101]. Of those looking specifically at the Achilles tendon, the majority have been focused on either static conditions [85,102], conditions in which little movement is involved [79,83,84,86], such as heel raises, or conditions in which only a select few time points are analyzed (such as at heel-strike) [80,82]. Stress in the calcaneus [92] and metatarsal heads [103] through the stance phase

of running has been estimated, but Achilles tendon stress not evaluated. Additionally, the

effects of different foot strike patterns and loading conditions, on plantar foot ligaments,

muscles, and soft tissue at the heel pad have been evaluated using a FE modeling

approach, but also did not include the Achilles tendon [104,105]. There is therefore a

need to evaluate the Achilles tendon under more dynamic conditions to better understand

stress distribution in the tendon during running.

General and Specific Aims

   The overall goal of this dissertation was to investigate the effects of altering step

rate on rearfoot motion, and how this affects stress in the Achilles tendon, in both healthy

runners and runners with Achilles tendon injury. This work will help to improve

understanding of the complex mechanisms at play in the development of AT, and the

potential alternate avenues of recovery from the injury. To reach this goal, three specific

aims were addressed.

Specific Aim 1. Evaluate the effects of altering step rate on rearfoot motion. Modifying

step rate is a method used in gait retraining to alter frontal plane motion at both the hip

and knee joints. Few investigations have evaluated the effects of increasing step rate on

kinematics at the rearfoot. It is hypothesized that increasing step rate will decrease peak

rearfoot eversion.

Specific Aim 2. Determine changes in stress distribution and magnitude within the

Achilles tendon during running as a result of altering step rate. It is unknown if changing

step rate will alter stress distribution, or magnitude, in the Achilles tendon, and if these changes are related to a concomitant change in rearfoot motion. Finite element modeling will be used in determining the effects of varying step rate on stress through the Achilles tendon. It is hypothesized that increasing step rate will decrease peak von Mises stress in the Achilles tendon, and peak stress will be moved laterally with a decrease in rearfoot eversion.

Specific Aim 3. Identify if altering step rate affects rearfoot motion and Achilles tendon stress in runners with Achilles tendon pain. Runners with Achilles tendon pain may exhibit excessive rearfoot eversion compared to healthy controls. It is unknown if runners with AT will alter rearfoot eversion as a result of modifying step rate, and how this will affect stress in the Achilles tendon. In addition, tendon stress may be altered differently in runners with Achilles tendon pain or could divert stress away from injured areas in the tendon (if a runner is experiencing pain on the medial side of the tendon, peak stress could be moved laterally). It is hypothesized altering step rate in runners with Achilles tendon pain will show similar effects to those seen in the previous Aims, where an increase in step rate will decrease peak rearfoot eversion and peak stress in the Achilles tendon.

The completion of these aims will provide a better picture of how stress is distributed throughout the Achilles tendon as a result of increasing step rate. Using subject-specific models will provide a picture of how an injured tendon responds to alterations in step rate and rearfoot kinematics. These data will set a foundation for future

research into individualized modeling of the Achilles tendon, and new areas to explore for alternate methods of rehabilitation for Achilles tendon injuries.

Organization of Dissertation

This dissertation is written in a journal style format, where chapters III-V have been or will be submitted for publication to peer-reviewed journals. The following explains how these chapters fit together into a coherent body of work. A bridge paragraph explaining the flow of studies is included at the conclusion of Chapters III and IV.

The current chapter (Chapter I) provides background information regarding functional anatomy of the Achilles tendon, injury to the Achilles tendon and prevalence in runners, possible mechanisms that may influence Achilles tendon injury in runners, and current rehabilitation methods for Achilles tendon injury in runners. In addition, the use of finite element modeling to explore how altering aspects of foot motion affects Achilles tendon stress is discussed. This chapter provides the case for the significance of and need for this research. Chapter II will detail the methodology utilized for each study. Chapter III addresses Specific Aim 1 and describes the initial study in which an intervention of increasing step rate during running was used, and how these changes in step rate affect rearfoot motion. Chapter IV details the use of a finite element model of the Achilles tendon and calcaneus together with the previously collected data from Chapter III to estimate changes in stress in the Achilles tendon to address Specific Aim 2. Chapter V then uses methods previously discussed in Chapters III and IV to address Specific Aim 3, in which it was necessary to evaluate how runners with Achilles tendon pain responded to changes in step rate, and how this affected tendon stress. Finally,

Chapter VI summarizes the notable results of the overall body of work and provides the

key takeaways from this set of studies, while acknowledging limitations and outlining

future directions for work in this area of research.

This dissertation includes co-authored work, some which is under review in peer-

reviewed journals. Chapter III has been accepted to a special issue "Mechanisms of

Human Motion Generation" in the journal *Biology*. Chapter IV and V are currently in

preparation for submission to appropriate journals. For all work in this dissertation,

Kathryn A. Farina was the primary investigator, responsible for study design, data

collection, analysis, interpretation, and dissemination. Michael E. Hahn, the co-author of

all studies, advised on all aspects of this dissertation.

CHAPTER II

GENERAL METHODOLOGY

Subjects

To address Specific Aims 1 and 2 (Chapters III-IV), twenty runners were
recruited, nine of which were female (Table 2.1). To be included, subjects had to be
between the ages 18-65, running at least 15 miles/week, and be running pain/injury free
at the time of data collection.

Table 2.1. Subject characteristics (Mean ± SD) for Specific Aims 1 and 2.

Sex	Age (yr)	Height (cm)	Mass (kg)	Weekly Mileage
Male (n = 11)	23.09 ± 5.63	179.61 ± 8.16	71.01 ± 11.46	38.55 ± 20.43
Female (n = 9)	27.11 ± 11.34	166.44 ± 6.25	56.97 ± 3.92	28.33 ± 9.68
Total (n = 20)	24.90 ± 8.66	173.69 ± 9.83	64.69 ± 11.27	34.50 ± 17.08

To address Specific Aim 3 (Chapter V) six runners with Achilles tendon pain
were recruited (Table 2.2).

Table 2.2. Subject characteristics (Mean ± SD) for Specific Aim 3.

Sex	Age (yr)	Height (cm)	Mass (kg)	Weekly Mileage
Male (n = 2)	25.00 ± 2.83	178.00 ± 0.00	69.50 ± 14.85	37.50 ± 3.54
Female (n = 4)	28.25 ± 13.69	159.00 ± 6.27	57.02 ± 2.29	21.25 ± 9.47
Total (n = 6)	27.17 ± 10.95	165.33 ± 10.95	61.18 ± 9.42	26.67 ± 11.25

These runners, between the ages of 18-65, had to have Achilles tendon pain in the mid-
portion of the Achilles tendon (no insertional Achilles tendon pain or retrocalcaneal
bursitis), be capable of running at least five minutes continuously on the treadmill, not
currently have any other running related injuries, had not experienced previously, or
currently have, an Achilles tendon rupture, not scheduled to surgically repair the current
injury, and have been experiencing Achilles tendon pain for greater than four weeks. For

Chapters III and V, written informed consent was obtained from subjects and study protocols were approved by the University of Oregon Institutional Review Board (IRB protocol #04092020.010 & #00000230).

Study Design and Experimental Protocol

Chapter III & V

Subjects ran on an instrumented treadmill (Bertec, Inc., Columbus, OH) at their preferred running speed for three step rate conditions of preferred step rate, +5% increase in step rate, and +10% increase in step rate for three minutes each while motion capture data (Motion Analysis Corp., Rohnert Park, CA) were collected. Subjects were cued by metronome to the goal step rate for both increased step rate conditions. Twenty strides of data were collected during the last minute of each condition. Rest between conditions was self-selected. All participants wore the same neutral cushioned footwear (Brooks Launch 3) with window cut outs for direct placement of retro-reflective markers on the foot.

Chapter V

In addition to the running protocol described above, subjects in this study underwent magnetic resonance imaging (MRI) scans of their injured foot-ankle complex. These MRI scans were used to extract segment geometries of the calcaneus bone and Achilles tendon to create subject-specific models for finite element analysis.

Data Collection

Chapters III & V

Participants were outfit with a bilateral marker set consisting of 43 retro-reflective markers defining nine segments (forefoot, rearfoot, shank, thigh, pelvis). Three-dimensional marker data were collected at 200 Hz using an 8-camera motion capture system (Motion Analysis Corp., Santa Rosa, CA). Ground reaction force data were collected at 1000 Hz using a force-instrumented treadmill (Bertec, Inc., Columbus, OH). All participants wore the same neutral cushioned footwear (Brooks Launch 3).

Chapter IV

Data from Chapter III were used in a unique analysis for Chapter IV. In addition, an MRI scan from a healthy, 30-year-old active male (height: 175 cm; weight: 68 kg) was used to create a generic model for a finite element mesh. The MRI sequence is described below.

Chapter V

An MRI scan of each subject's injured ankle-foot complex was performed using a Siemens Skyra 3.0 Tesla Scanner (Siemens Medical Solutions, Malvern, PA, USA) to obtain sagittal, coronal, and axial images of the injured Achilles tendon and calcaneus. Each subject's ankle was positioned in a non-weight bearing neutral position in a flex coil and stabilized with foam. The 3D True FISP sequence, a steady-state coherent sequence in which balanced gradients (net gradient-induced dephasing over a repetition time

interval is zero) are used along all three axes, was used with 8 mm slice thickness with zero gap between slices, and resolution of 0.8x0.8x0.8 mm.

Data and Statistical Analysis

Chapter III

Analyses were completed using a custom written script in MATLAB (R2020b, The MathWorks, Inc., Natick, MA). Raw marker coordinate and force plate data were filtered using a 4th order lowpass Butterworth filter at 20 Hz. The shank coordinate system origin was defined as the midpoint between the medial and lateral femoral epicondyle markers, and the ankle joint coordinate system origin was defined as the midpoint between the medial and lateral malleoli markers. The rearfoot coordinate system origin was defined as the midpoint between the medial and lateral calcaneus markers. For all segments, x defined the medio-lateral axis, y defined the antero-posterior axis, and z defined the longitudinal axis. For all coordinate systems, an x-y-z Cardan sequence of flexion/extension, eversion/inversion, and internal/external rotation was used for joint angle calculations.

Plantar/Dorsi-flexion and eversion/inversion angles were calculated for the rearfoot segment with respect to the shank. Tibial internal/external rotation was calculated as the rotation of the shank with respect to the rearfoot. Angles were averaged across twenty-right foot strikes, normalized to 101 data points for the stance phase of running, and peak variables were extracted.

A repeated-measures multivariate analysis of variance (MANOVA) ($\alpha = 0.05$) was used to test the effects of the three different step rate conditions (preferred, +5%, and

+10%) on the discrete peak variables. In the case of a significant main effect, a

Bonferroni correction was used in *post-hoc* analysis to determine significant differences

between conditions. SPSS v27 was used for statistical analysis (IBM SPSS Statistics,

Chicago, IL).

In addition, statistical parametric mapping (SPM) was used to analyze differences

in the normalized stance phase curves between conditions for the continuous variables of

interest. The open-source "SPM1D" package was used in MATLAB [106]. In this

approach, a repeated-measures ANOVA over the normalized time series was used to

determine any significant differences between the three conditions. If statistical

significance was reached, *post-hoc* t-tests over the normalized time series were used to

determine significant differences between conditions. Both analyses involve computing a

test statistic at each time point in the curve, calculating a critical threshold at which only

the α % (5%) of smooth random curves would be expected to cross, and finally

calculating the probability that specific points, or clusters of points, could have exceeded

the critical threshold due to random field process. The final analysis effectively produces

suprathreshold clusters, or areas of the time normalized curve, which are significantly

different from each other (if any significant differences are found) [106,107].

Chapter IV

Data previously collected, described in Chapter III, were used to estimate Achilles

tendon force during the stance phase of running. Achilles tendon force was calculated as

the sagittal plane ankle moment divided by the Achilles tendon moment arm:

$$ATF = \frac{M_A}{AT_{MA}}$$

where M_A is the ankle plantar flexor moment, and AT_{MA} is the moment arm of the Achilles tendon. The Achilles tendon moment arm was calculated using a regression equation developed from MRI scans that accounts for changes in moment arm length during stance [108–111]:

$$AT_{MA} = -0.5910 + 0.08297\theta - 0.0002606\theta^2$$

where θ is the sagittal plane ankle flexion angle. Finally, the ankle plantar flexor moment was calculated using a Newtonian-Euler inverse dynamics approach:

$$M_p = I\alpha + \omega \times (I\omega) - M_d - r_d \times F_d - r_p \times F_p$$

where M_p is the moment about the proximal end of the segment (ankle), I is the moment of inertia about the segment center of mass (foot), determined from previously published segment lengths and heights [112], α is the angular acceleration of the segment, ω is the angular velocity of the segment, F_p and F_d are the proximal and distal reaction forces, M_d is the moment about the distal end of the segment, and r_p and r_d are the distances from center of mass of the segment to the proximal or distal joint.

The estimated Achilles tendon force, along with global rotation data of the calcaneus and shank segments previously collected, were then used in a FE analysis to estimate von Mises stress in the Achilles tendon under the varying step rate conditions. The finite element model consisted of an Achilles tendon and calcaneus segment. The model was generated from the MRI scan of a healthy male subject. Digital imaging and communications in medicine (DICOM) files obtained from the MRI were imported into 3D Slicer software (version 4.11) (www.slicer.org) [113,114]. The Fast GrowCut algorithm [115] was used in the segment editor [116] to section the Achilles tendon from the insertion on the calcaneus to the highest point visible from the MRI scans

(approximately 12 cm from the Achilles tendon insertion), and the calcaneus. Segments were smoothed and exported as standard tessellation language (stl) files which described the surface geometry of the 3D objects. The surface files were then imported into FEBio software [117], where the included Tetgen function (tetgen.berlio.de) was used to create a tetrahedral mesh. Surfaces for the Achilles tendon and calcaneus were defined, and material properties assigned in FEBio. The Achilles tendon segment consisted of 3,639 elements, 2,612 faces, and 1,308 nodes. The material property values for the Achilles tendon were selected from previous literature of cadaveric Achilles tendons and have previously been used in FE analysis [79,118,119]. The Achilles tendon was modeled as a neo-Hookean material, with Young's Modulus set to 819 MPa, and Poisson's ratio of 0.4 [119]. The calcaneus was modeled as a rigid body. An additional rigid body segment was created and attached to the proximal surface of the Achilles tendon, emulating a clamp, similar to what may be used in cadaveric studies [120]. This proximal rigid body was created in order to apply rotations and Achilles tendon force to the proximal area of the Achilles tendon.

The boundary conditions for the model were assigned based on the calculated global rearfoot and shank rotations, and Achilles tendon force. The three-dimensional rotation angles of the calcaneus segment (rearfoot), shank tracking system rotations, and Achilles tendon force at peak eversion and peak Achilles tendon force were used to simulate Achilles tendon stress at these two time points. Data to define the motion of the Achilles tendon was not collected, and an assumption was made that the Achilles tendon rotation would follow that of an assumed rigid body shank segment. Therefore, three-dimensional rotation of the shank tracking system was used to define the rotation of the

proximal rigid body fixed to the proximal surface of the Achilles tendon. The displacement in the x-y-z directions of the calcaneus was fixed, as well as the x-y displacements of the proximal rigid body. The z-displacement of the proximal rigid body was assigned a value of 6 mm to imitate lengthening from the contraction of the gastrocnemius and soleus muscles during stance. This displacement was chosen as a previous study has reported a displacement of approximately 6 mm of the Achilles tendon from touch-down to mid-stance during running [121]. Finally, Achilles tendon force was applied as a z-force to the proximal rigid body.

The area of peak von Mises stress was extracted from the simulation results. Only the area from 2 – 6 cm of tendon length (2 cm from the tendon insertion to 6 cm from the tendon insertion) was considered (Figure 2.1), as this area of tendon has been found to be the area of tendon that is most frequently injured [33].
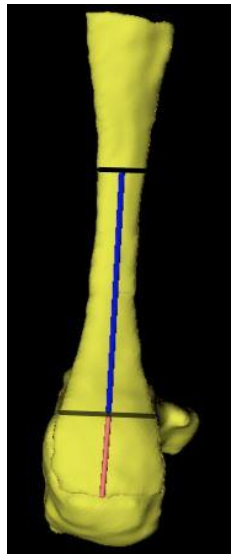
Figure 2.1. Achilles tendon model with distal tendon insertion area (0 – 2 cm) (red) and tendon mid-portion (2 – 6 cm) (blue) marked. Only the mid-portion of the tendon was considered during analysis.

The width and length location of the peak stress area were measured from the lateral edge of the tendon and from the bottom of the insertion. The measured length and width were normalized to tendon length and width, with 6 cm from the distal insertion considered 100% of tendon length. Because the Achilles tendon width is not consistent throughout the length of the tendon, the width of the tendon was measured every centimeter from 2 – 6 cm (2 cm from the distal insertion to 6 cm from the distal insertion). The measured width at peak stress was then normalized to the width at the measured section of tendon length, with 0% corresponding to the most lateral edge of the tendon, and 100% corresponding to the most medial edge of the tendon. For example, if peak stress were measured at a tendon length of 5 cm, the measured width would be normalized to the width of the tendon at 5 cm. This process was repeated for peak eversion and peak Achilles tendon force time points during stance, for each step rate condition, for each of the six subjects.

Cross sectional area (CSA) of the Achilles tendon was measured from the segmented geometry in 3D slicer for the length of the tendon. For analysis, CSA at 3 cm, 4 cm, and 5 cm were used (3 cm from insertion, 4 cm from insertion, 5 cm from insertion). For each CSA, calculated Achilles tendon force was divided by CSA to evaluate Achilles tendon stress at each of the selected lengths of tendon for each step rate condition. This analysis was performed to compare to the results of previous research, and to the FE analysis results.

Repeated measures analyses of variance (ANOVA) ($\alpha = 0.05$) were used to evaluate differences in Achilles tendon stress, locations of stress, peak tendon force, and peak eversion between each of the three step rate conditions. If the assumption of

sphericity was violated, a Greenhouse-Geisser correction was used. In the case of a significant main effect, a Bonferroni correction was used in *post-hoc* analysis to determine significant differences between conditions. Statistical analyses were performed in SPSS v27 (IBM SPSS Statistics, Chicago, IL).

Chapter V

Analysis of rearfoot angles and Achilles tendon stress were completed as described previously. The MRI images for each subject were used in 3D Slicer, as described above. An Achilles tendon and calcaneus model for each subject was generated from their individual MRI scans. In addition, individual subject CSA was calculated from the segmented geometry. The same material properties as described previously were utilized, and similar boundary conditions and model inputs were used as in Chapter IV, but specific to each subject's collected data. One difference in the boundary conditions used in this analysis was the z-displacement of the proximal rigid body was left free, rather than the fixed 6 mm displacement prescribed in the previous study. In the CSA analysis, Achilles tendon stress was calculated at 2, 3, 4, 5, and 6 cm, as opposed to only 3 – 5 cm, and at an average CSA from 2 – 6 cm (with distances referring to distance from the Achilles tendon distal insertion).

CHAPTER III

INCREASING STEP RATE AFFECTS REARFOOT KINEMATICS AND GROUND

REACTION FORCES DURING RUNNING

This work has been accepted to the special issue "Mechanisms of Human Motion

Generation" in the section "Biological Engineering" in the journal *Biology* as of

December 2021. Kathryn A. Farina designed the study and collected and analyzed data.

Michael E. Hahn provided mentorship including assistance with study design, oversight,

and editing and finalizing the final manuscript.

Introduction

Greater frontal and transverse plane motion in the lower limbs during running

have been thought to play a role in the development of some running related injuries

(RRIs) [17,44,70]. Increased tibial rotation during the stance phase of running has been

targeted as a possible mechanism contributing to patellofemoral pain syndrome and

iliotibial band syndrome in runners by causing increased joint compression force on the

patella, and friction over the iliotibial band insertion [76,126,127]. Tibial rotation has

been shown to be coupled to motion at the rearfoot, as these segments are linked through

the subtalar and talocrural axes [124,125]. Thus, motion at the rearfoot may have an

influence on the amount of segmental motion propagating up the kinetic chain [124]. In

normal running locomotion, a slightly supinated foot makes contact with the ground and

the calcaneus everts as the subtalar joint begins to pronate, causing the talus to move

medially and adduct, thus internally rotating the tibia due to the tight articulations

between the subtalar, talocrural, and tibiotalar joints [17]. Similarly, once the foot moves into midstance, the foot begins to supinate and the knee extends to prepare for the foot leaving the ground, causing the tibia to externally rotate [17].

When a mismatch arises in the timing of these coupling events, or one segment displays excessive motion, rotation of the tibia may conflict with rearfoot eversion, and cause increased stresses to be placed on other soft tissues or bones [16]. Indeed, one of the theories for development of Achilles tendinopathy centers around this conflicting motion between the start of tibial external rotation with knee extension and prolonged rearfoot eversion, causing increased stress on the Achilles tendon [16]. Although a causal relationship between increased rearfoot motion and development of running injury has not been firmly established, there is conflicting evidence suggestive of some type of link. Runners with Achilles tendinopathy have been reported to have increased rearfoot eversion, or duration of eversion, compared to healthy controls [38,39]. Similarly, excessive rearfoot eversion has been reported in runners with tibial stress fractures [126], medial tibial stress syndrome [38], and patellofemoral pain syndrome [127].

Attention has been given to rearfoot eversion in evaluating RRIs, and it has often been used as a surrogate measure to describe pronation, which has long been thought to play a role in RRI development [16,17]. However, pronation is a complex motion, involving movement between the forefoot, rearfoot, and ankle; subsequently influencing tibial rotation [124]. Indeed, movement at the subtalar joint involves motion in multiple planes, and has been shown to be linked to tibial rotation in both the transverse and frontal planes [125]. Despite the link between rearfoot and tibial rotation, and the possible effects on RRI development, little is known about methods for altering frontal

and transverse plane rearfoot motion, if such an alteration influences injury risk, or whether such methods could be used for rehabilitation after injury.

For many RRIs that appear to arise from injurious segmental motion patterns, various methods of gait retraining have been employed to alter the movement pattern of interest to decrease pain and return the runner to full training. Promising results have been shown when increased hip adduction has been targeted in an effort to rehabilitate runners with patellofemoral pain and iliotibial band syndrome [6,8,9]. Runners completing a gait retraining program aimed at decreasing excessive hip adduction were able to reduce pain levels, and return to pre-injury training volumes [6,8,9]. These previous investigations have used real-time visual feedback displaying pelvic angles or used a mirror to focus the runners' attention on hip movement. Although successful, these methods generally require the runner to visit a lab or clinic for many gait retraining sessions. One simple, effective, and low-cost gait retraining method requiring minimal supervision is to have runners increase step rate. After foot strike, the ground reaction force propagates through the subtalar joint, contributing to rearfoot eversion, a necessary function enabling foot pronation in order to aid in shock absorption, and help the foot form a rigid lever to prepare for push-off [124]. Increasing step rate has been shown to decrease peak ground reaction forces and loading rates, which may require less energy absorption from the lower extremity musculature and joints [53,69,128–130]. Increasing step rate effectively draws the foot at ground contact closer to the body center of mass, reducing center of mass vertical oscillation, thereby reducing the energy absorbed by the lower limbs, and altering joint kinematics [53,128]. For example, increasing step rate has been shown to decrease peak hip adduction [53,67,71,131], peak knee abduction [132],

and peak rearfoot eversion [70], all of which have been implicated in the development of specific RRIs [6,38,133].

Few studies have looked at how non-sagittal plane rearfoot motion is affected by increasing step rate. With the linkage between rearfoot motion and tibial rotation, and the potential development of RRIs, it is important to discover how these motions can be modified. Therefore, the purpose of this study was to evaluate the effects of increasing step rate on kinematics at the rearfoot in the sagittal, frontal, and transverse planes during the stance phase of running. A secondary purpose was to confirm how ground reaction forces throughout the stance phase are adjusted with increased step rate. We hypothesized there would be significant reductions throughout stance in rearfoot angles and ground reaction forces.

Methods

Twenty runners (nine female) were recruited for participation in this study (Table 3.1).

Table 3.1. Subject characteristics, preferred running pace, and step rates (steps/min).

	Males (n = 11)	Females (n = 9)	Total (n = 20)
Age	23.09 ± 5.63	27.11 ± 11.34	24.90 ± 8.66
Height (cm)	179.61 ± 8.16	166.44 ± 6.25	173.69 ± 9.83
Mass (kg)	71.01 ± 11.46	56.97 ± 3.92	64.69 ± 11.27
Miles per week	38.55 ± 20.43	28.33 ± 9.68	34.50 ± 17.08
Preferred Pace (m/s)	3.56 ± 0.28	3.04 ± 0.26	3.33 ± 0.38
Preferred Step Rate	172 ± 6	177 ± 8	175 ± 7
+5% Step Rate	181 ± 7	187 ± 9	$185 \pm 9*$
+10% Step Rate	190 ± 7	194 ± 11	$192 \pm 9*\#$

* denotes significant difference from preferred condition; # denotes significant difference from +5% condition ($p < 0.05$). Significant differences shown only for the total sample.

Participants had to be between the ages 18-65, running at least 15 miles per week, and be running pain free at the time of data collection. Prior to data collection, participants provided written, informed consent, approved by the University of Oregon Institutional Review Board.

Data Collection

Forty-three retroreflective markers were placed bilaterally on the lower limbs and pelvis to define pelvis, thigh, shank, rearfoot, and forefoot segments. Standardized, neutral running shoes (Brooks Launch) were used by each of the participants, in which windows were cut to place markers directly on the foot [134]. Participants performed a static trial, after which markers on the medial and lateral malleoli, femoral epicondyles, and greater trochanters were removed so as not to interfere with running motion.

Three-dimensional marker trajectories were collected using an 8-camera motion capture system (Motion Analysis Corp., Rohnert Park, CA) and ground reaction force data were collected using an instrumented treadmill (Bertec, Columbus, OH) at 200 and 1000 Hz, respectively. Participants performed three running trials on the treadmill consisting of three minutes each. Kinematic and kinetic data were recorded for twenty strides during the final minute of each trial. The first trial consisted of the participants running at their self-selected easy pace to determine their preferred running step rate. Step rate was assessed by counting the number of foot falls during a 20 second period, and multiplying this number by 3, to determine number of steps per minute. Calculations of +5% and +10% increases over preferred step rate were then determined for each subject. In the following two trials, a metronome was set to the calculated increase in step

rate, and participants were instructed to match their foot falls to the beat of the

metronome. The +5% trial was followed by the +10% trial. Subjects were given the first

two and half minutes of each trial to acclimate to the increased step rate. Step rate was

calculated during the final minute of each trial, once before and once after data were

recorded to ensure participants had modified their step rate.

Data Analysis

A custom MATLAB (The MathWorks, Natick, MA) program was used to

calculate rearfoot kinematics from the right foot throughout the stance phase. The stance

phase was defined as when the vertical ground reaction force exceeded 5% of participant

body weight [135]. This threshold defined the start and end of each foot strike on the

ground. The rearfoot coordinate system origin was defined as the midpoint between the

medial and lateral calcaneus markers, with the *x* axis pointed laterally, *y* axis pointed

anteriorly, and *z* axis directed superiorly. Raw marker coordinate and force platform data

were dual pass filtered using a 4th order lowpass Butterworth filter with a 20 Hz cutoff

frequency. Joint angles were calculated using a Cardan sequence of flexion/extension,

inversion/eversion, adduction/abduction. It has been noted previously that sagittal plane

motion between the tibia and calcaneus primarily occurs through the talocrural joint,

while frontal and transverse plane motion occur at the subtalar joint [136]. In this study,

rearfoot sagittal plane angle primarily reflects talocrural dorsiflexion/plantarflexion, with

inversion/eversion and adduction/abduction reflecting subtalar joint motion [136].

Rearfoot angles were calculated with respect to the shank segment, with the exception of

the transverse plane angle calculated as the shank segment with respect to the rearfoot segment to reflect tibial rotation [136,137].

Foot strike index (FSI) at initial contact was calculated in order to assess changes in foot strike pattern with increasing step rate. Center of pressure (COP) data were first transformed into the rearfoot coordinate system. Then FSI was calculated as the longitudinal difference (heel to toe) between the COP and the heel marker at initial contact with the ground. This difference was then divided by total foot length to obtain a percentage of foot length [138].

Twenty right foot strikes, defined by the stance phase threshold previously described, were identified. Rearfoot angles and ground reaction forces were calculated for each stance phase, averaged the across twenty right foot strikes, and normalized to 101 data points. Peak values for rearfoot dorsiflexion, eversion, and tibial internal rotation, and vertical, braking, and propulsive ground reaction forces were extracted by finding the peak value within each curve.

Statistical Analysis

A repeated measures analysis of variance (ANOVA) ($\alpha = 0.05$) was used to test the effects of the three step rate conditions on the discrete peak values listed above, and FSI at initial contact. In the case of a significant main effect, a Bonferroni correction was used in *post-hoc* analysis to determine significant differences between conditions. Statistical analyses were performed in SPSS v27 (IBM SPSS Statistics, Chicago, IL).

Statistical parametric mapping (SPM) was used to analyze differences in the normalized stance phase time series curves between conditions for the rearfoot angles and

ground reaction forces. The open-source "SPM1D" package was used in MATLAB [106]. In this approach, a repeated-measures ANOVA over the normalized time series was used to determine any significant differences between the three conditions. If statistical significance was reached, *post-hoc* t-tests over the normalized time series were used to determine significant differences between conditions. These analyses involve computing a test statistic at each time point in the curve, calculating a critical threshold at which only the α % (5%) of smooth random curves would be expected to cross, and finally calculating the probability that specific points, or clusters of points, could have exceeded the critical threshold due to random field process. The final analysis effectively produces suprathreshold clusters, or areas of the time-normalized curve, which are significantly different from each other (if any significant differences are found) [106,107].

Results

Peak Variables Analysis Results

Peak rearfoot angles were significantly different between step rate conditions in all planes of motion (Table 3.2). Increasing step rate significantly decreased peak dorsiflexion angle at the +5% (p = 0.010) and +10% step (p = 0.001) rate conditions compared to the preferred condition. The +10% condition showed significantly decreased peak dorsiflexion angle compared to the +5% condition (p = 0.016). Peak eversion was significantly decreased from the preferred step rate condition in the +5% (p = 0.013) and the +10% condition (p = 0.008). Peak tibial internal rotation was significantly decreased in the +10% condition compared to the preferred condition (p = 0.037).

Table 3.2. Peak rearfoot angles (degrees), peak tibial internal rotation (degrees), peak vertical, propulsion, and braking ground reaction forces (BW), and foot strike index (% of foot length) at initial contact for the preferred, +5%, and +10% step rate conditions.

	Preferred Step Rate	+5% Step Rate	+10% Step Rate
Peak Dorsiflexion	25.85 ± 9.28	24.94 ± 9.60*	24.27 ± 9.53*[#]
Peak Eversion	8.97 ± 5.15	8.40 ± 5.44*	8.18 ± 5.52*
Peak Internal Rotation	11.39 ± 5.06	10.94 ± 5.37	10.58 ± 5.27*
Peak Vertical	2.50 ± 0.22	2.47 ± 0.25	2.43 ± 0.24*[#]
Peak Propulsion	0.30 ± 0.04	0.29 ± 0.04	0.28 ± 0.04
Peak Braking	0.35 ± 0.04	0.33 ± 0.04*	0.32 ± 0.05*[#]
Foot Strike Index	35.44 ± 13.75	37.63 ± 18.35	40.95 ± 19.93

* indicates significant difference from the preferred condition; [#] indicates significant difference from the +5% condition ($p < 0.05$).

Peak vertical ground reaction force was significantly decreased in the +10% step rate condition compared to the preferred (p = 0.005) and +5% (p = 0.010) conditions. Peak braking force was significantly reduced in the +5% condition compared to the preferred condition (p = 0.010), and in the +10% condition compared to the preferred (p = 0.002) and +5% condition (p = 0.004). There were no significant differences found for FSI at initial contact between conditions (Table 3.2).

Time Series Analysis Results

The preferred condition displayed significantly increased sagittal plane rearfoot angle between 45.1-59.2% of stance (p = 0.018) compared to the +10% condition. Compared to the +5% condition, sagittal plane rearfoot angle in the +10% condition was significantly reduced between 35.3-51.2% (p = 0.022) and between 90.2-100% of stance (p = 0.037) (Figure 3.1). Frontal plane rearfoot angle was significantly reduced in the +5% condition between 30.8 – 42.1% of stance (p = 0.031) and in the +10% condition between 20.4 – 44.0% of stance (p = 0.0060) compared to the preferred condition (Figure

3.2). Transverse plane tibial rotation angle was significantly reduced in the +10% condition between 2.6 – 34.9% of stance ($p < 0.001$) compared to the preferred condition, and significantly reduced in the +10% condition between 6.1 – 31.4% of stance ($p = 0.0059$) compared to the +5% condition (Figure 3.3).

In the +10% step rate condition vertical ground reaction force was significantly reduced compared to the preferred condition between 6.7 – 12.0% ($p = 0.023$) and between 38.8 – 51.6% ($p < 0.001$) of stance and compared to the +5% condition between 2.6 – 13.3% ($p = 0.0033$) and between 35.0 – 47.8% ($p < 0.001$) of stance. In the anteroposterior direction, the preferred condition displayed significantly greater braking force compared to the +5% and +10% conditions between 21.2 – 26.3% ($p = 0.032$) and 14.6 – 29.9% ($p < 0.001$), respectively. The +10% condition also displayed significantly decreased braking force compared to the +5% condition between 15.5 – 29.4% ($p < 0.001$) of stance. There were no significant differences across the stance phase found between conditions in the mediolateral ground reaction force.

(a)

(b)
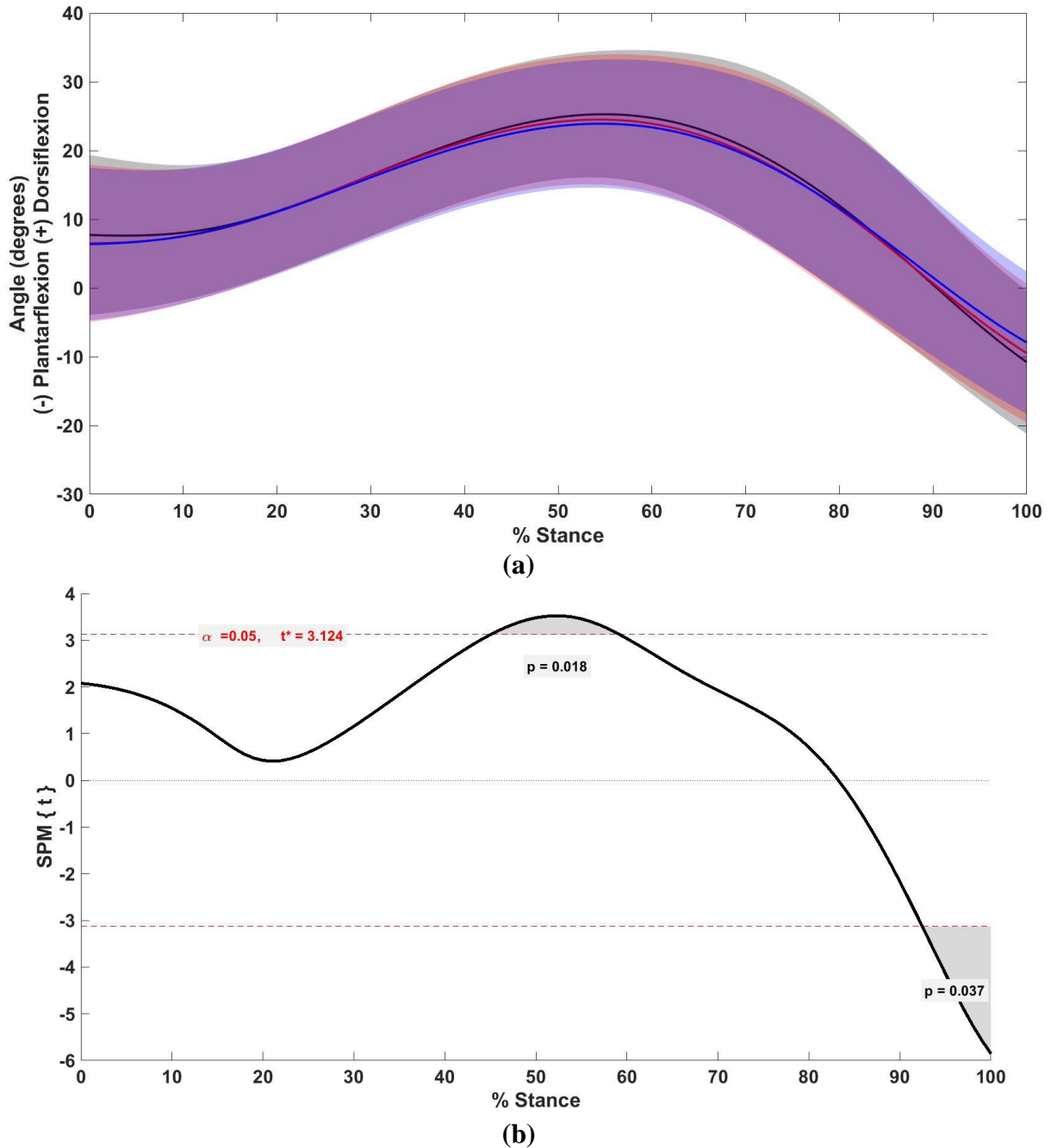
Figure 3.1. **(a)** Mean (solid line) and standard deviation (shaded) sagittal plane rearfoot angle between preferred (black), +5% (red), and +10% (blue) step rate conditions. **(b)** t-values of SPM post-hoc comparison between preferred and +10% conditions for sagittal plane rearfoot angle. Dashed red lines indicate critical threshold ($\alpha = 0.05$). Gray shaded area indicates regions with statistically significant differences between the preferred and +10% condition.

34
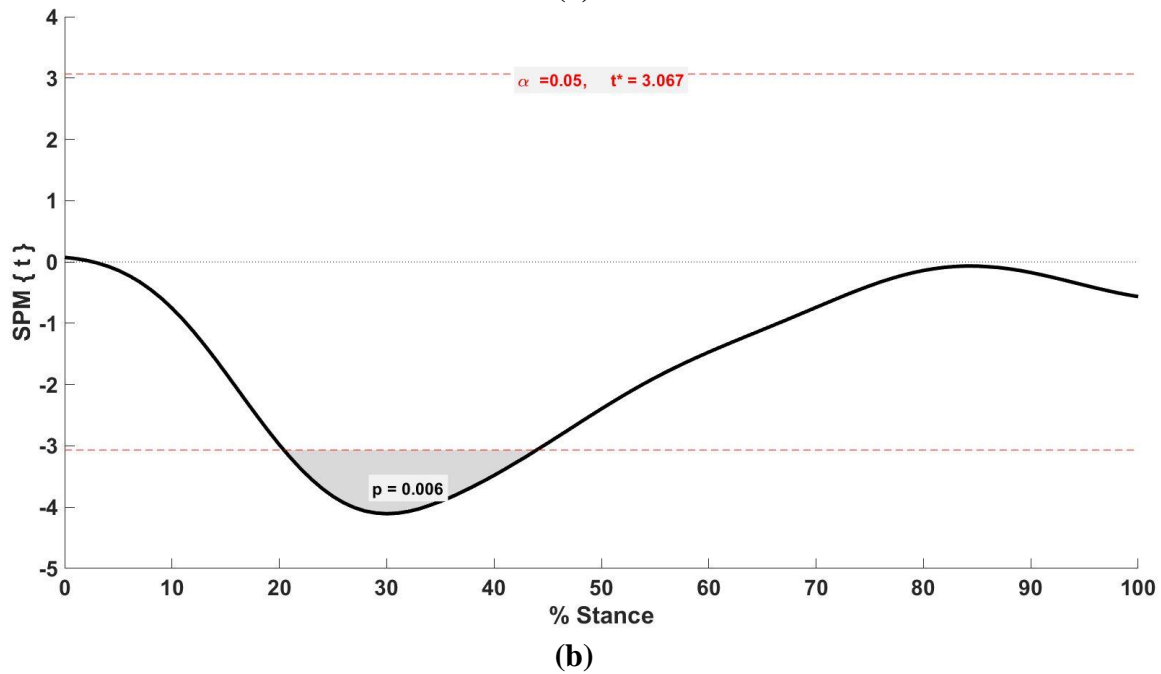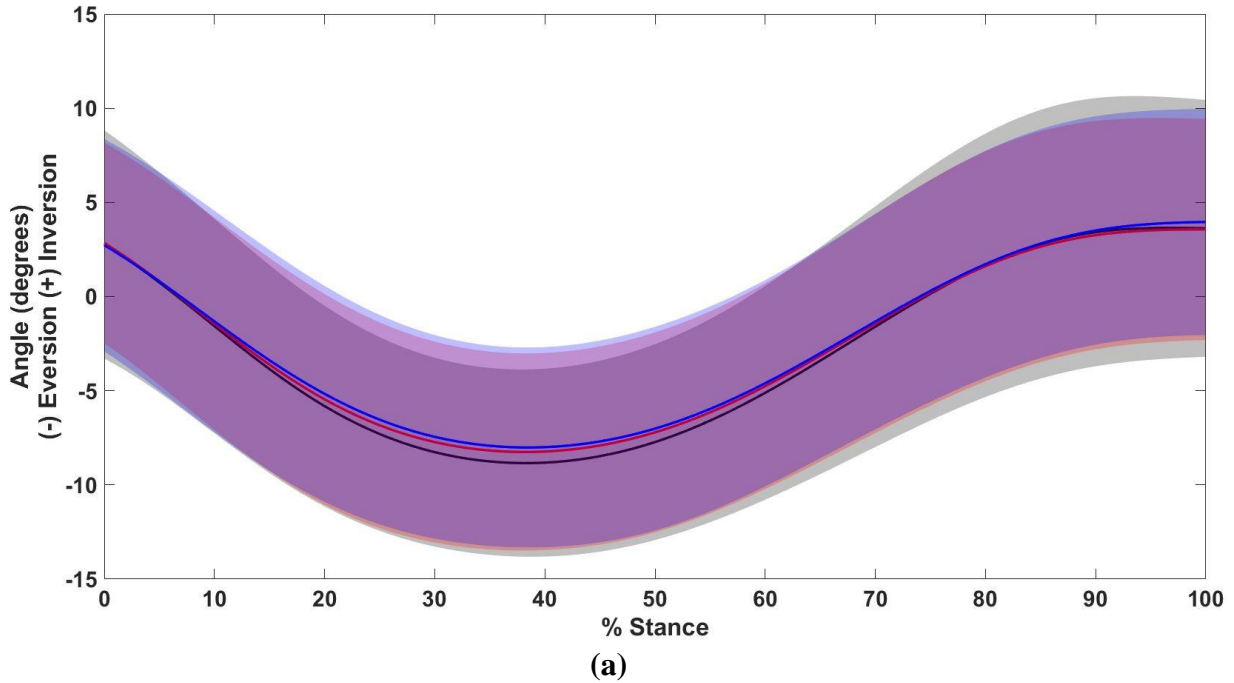
Figure 3.2. (a) Mean (solid line) and standard deviation (shaded) frontal plane rearfoot angle between preferred (black), +5% (red), and +10% (blue) step rate conditions. (**b**) t-values of SPM post-hoc comparison between preferred and +10% conditions for frontal plane rearfoot angle. Dashed red lines indicate critical threshold (α = 0.05). Gray shaded area indicates regions with statistically significant differences between the preferred and +10% condition.

(a)

(b)
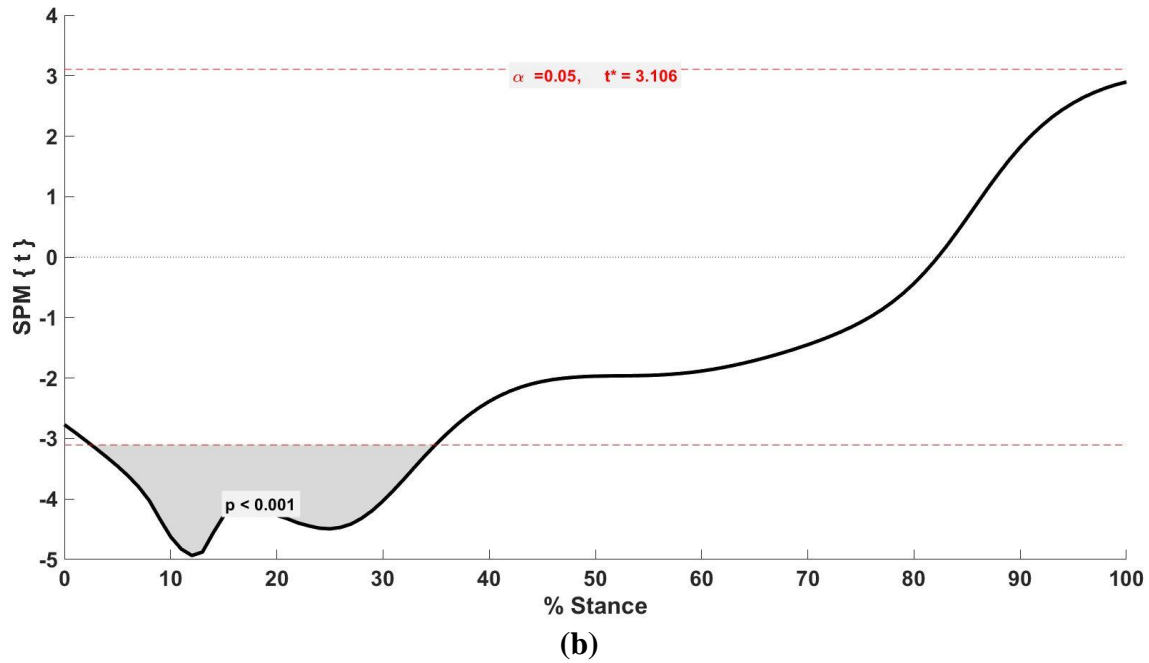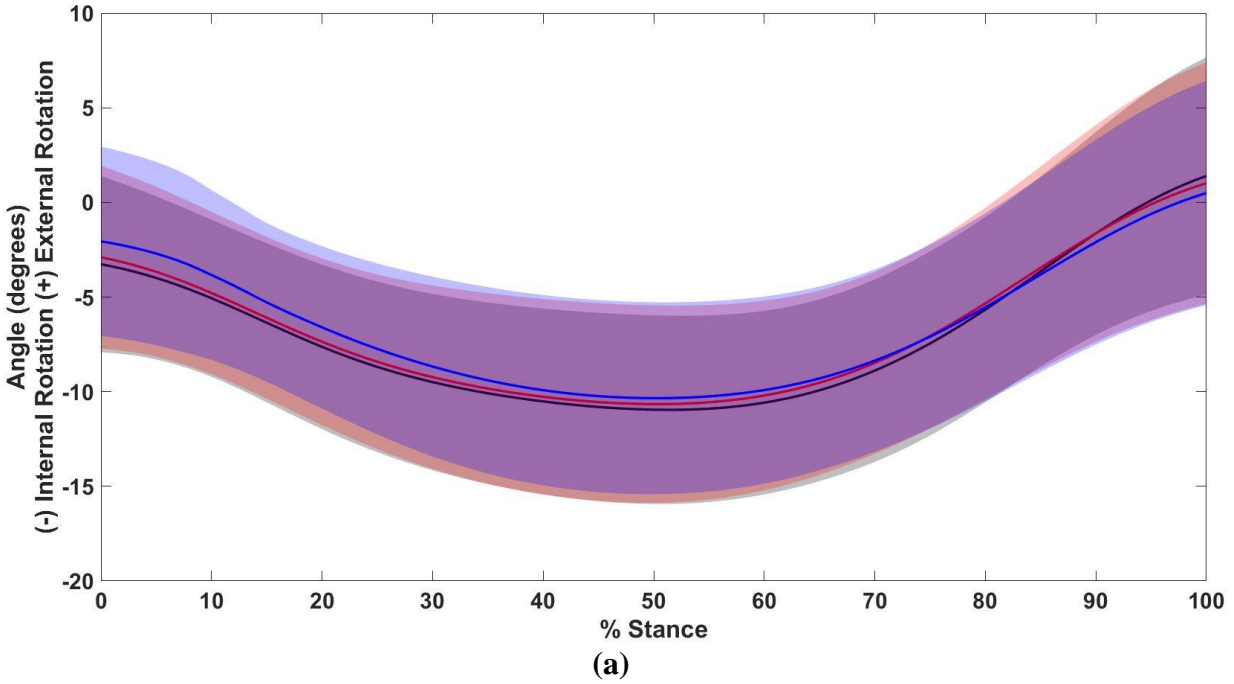
Figure 3.3. (a) Mean (solid line) and standard deviation (shaded) tibial rotation angle between preferred (black), +5% (red), and +10% (blue) step rate conditions. (**b**) t-values of SPM post-hoc comparison between preferred and +10% conditions for tibial rotation angle. Dashed red lines indicate critical threshold (α = 0.05). Gray shaded area indicates regions with statistically significant differences between the preferred and +10% condition.

Discussion

The purpose of this study was to analyze motion of the rearfoot during the stance phase of running with an increased step rate. Supporting our hypothesis, decreases in peak rearfoot angles were observed in the sagittal, frontal, and transverse planes. Similar to previous investigations, peak rearfoot dorsiflexion was decreased with increasing step rate. A +10% increase in step rate was reported to decrease ankle dorsiflexion at midstance by around 8%, corresponding to a 2.5 degree decrease in ankle dorsiflexion at midstance [139]. Likewise, other investigations implementing a +10% increase in step rate reported decreases in peak dorsiflexion angle of approximately 2 – 2.5- degrees, compared to preferred step rate [132,140]. These investigations observed a slightly greater decrease (1 degree) in ankle dorsiflexion than the results observed in the present study. This discrepancy may be due to differences in average preferred running speeds and step rates, both of which were slightly greater in the present study. These previous investigations have also evaluated ankle dorsiflexion, whereas the present study observed rearfoot angles, with an origin in the calcaneus segment. This difference may have influenced the observed differences between the present study and prior work. However, as noted previously, the majority of rearfoot plantar-dorsiflexion occurs at the talocrural joint [136], indicating that there would be little functional difference between these calculated angles.

In the frontal plane, peak rearfoot eversion was decreased in the +5% and +10% conditions compared to the preferred condition. Boyer and Derrick found a significant linear trend for a decrease in peak ankle eversion as stride length was decreased (thereby increasing step rate, assuming a constant speed), and observed a 0.6 degree decrease in

peak rearfoot eversion as stride length decreased [70]. We observed a slightly greater average decrease in peak rearfoot eversion angle from the preferred to +10% condition of 0.79 degrees. Again, this difference may be due to differences in joint measurement definitions. Another investigation comparing a +10% increase and preferred step rate reported only a 0.24 degree decrease from the preferred to increased step rate condition, which was not significant [141]. Although these authors also evaluated rearfoot motion with a coordinate system similar to the present study, participants' preferred step rate was lower than in the present study, and these authors utilized an overground running protocol, differing from our use of the treadmill, which may have an effect on joint kinematics [142].

Few studies have evaluated the effects of increasing step rate on tibial rotation. Boyer and Derrick found peak knee internal rotation angle to decrease by 0.4 degrees from preferred to 10% decreased stride length [70]. The present study observed peak tibial internal rotation to decrease, on average, 0.8 degrees from the preferred to +10% step rate condition. More similar to the results observed in the present study, peak knee rotation during stance was found to decrease approximately 0.5 degrees with a 10% increase in step rate [132]. Although not directly manipulating step rate, Pohl and Buckley found peak tibial internal rotation angle to decrease almost 3 degrees between a rearfoot-strike and toe-strike pattern [143]. It has been suggested that running with an increased step rate may be associated with transitioning from a rearfoot- to a forefoot-strike pattern [69]. We did not observe a significant difference in FSI between step rate conditions in the present study, but there was a trend for subjects to land more anteriorly on the foot, closer to a mid-foot strike pattern. This may indicate that the subjects were

beginning to demonstrate early patterns of transitioning from a rearfoot-strike to forefoot-strike pattern.

Analysis using SPM allows for differences between conditions to be viewed throughout the stance phase, as opposed to only at discrete time points. This approach provides a more complete view of when changes occur throughout the stance phase. There were significant differences throughout the stance phase for rearfoot angles in the sagittal and frontal planes. In the sagittal plane, differences occurred close to peak dorsiflexion at toe-off. Similarly, frontal plane rearfoot angle was significantly reduced near the period of peak eversion in both the +5% and +10% conditions compared to the preferred condition. Tibial rotation angle displayed a greater range of significant differences during stance, with approximately the first 30% of stance being significantly reduced in the +10% condition compared to the preferred and +5% conditions. Interestingly, differences in rearfoot eversion were not observed until the latter part of this early stance period, suggesting there may be other mechanisms contributing to the differences in tibial rotation in the first 30% of stance. Some authors have suggested tibial internal rotation could also be caused by more proximal mechanisms, such as changes at the hip [47]. Increasing step rate has been shown to affect motion at the hip [53,70,131,132], adding support for hip compensation to be affecting these changes seen in tibial rotation early in stance. This period of significance in the first 30% of stance did not include peak tibial internal rotation; however significant differences were observed when the discrete values were compared between conditions. Peak eversion occurred approximately 10% earlier in the stance phase than peak tibial internal rotation. The significant cluster in the frontal plane angle also occurred about 10% earlier in the stance

phase than peak tibial internal rotation, suggesting the changes in rearfoot eversion could have influenced peak tibial internal rotation.

The secondary purpose of this study was to assess changes in ground reaction forces with increased step rate. Peak vertical ground reaction force was significantly reduced in the +10% condition compared to the preferred and +5% conditions. Previous investigations have also reported decreases in peak vertical ground reaction force of 2.6% and 3.5% with a 10% increase in step rate [139,144]. Similarly, a +10% increase in step rate was shown to significantly decrease peak vertical ground reaction force by 0.6 N/kg from the preferred condition [53]. The results from the present study agree well with these previous findings, as we observed an average 0.07 BW decrease from the preferred to +10% condition, corresponding to approximately a 2.8% decrease between conditions. We also observed a significant reduction in peak braking force in the +10% condition compared to the preferred and +5% condition, and the +5% condition compared to the preferred condition. These decreases corresponded to a 5.7% decrease from the preferred to +5% condition, and an additional 3% decrease from the +5% to +10% condition. Additionally, the +10% condition displayed an 8.6% decrease compared to the preferred condition. Lenhart et al observed a 5.5% decrease in the anterior-posterior ground reaction force maximum with a 10% increase in step rate [139]. Other reports have also detected approximately a 9% decrease in peak anterior-posterior ground reaction force with a 10% decrease in stride length [145], aligning well with the results in the present study.

Significant differences in the vertical ground reaction force were observed between 38 – 51% of stance when comparing the preferred and +10% condition. The

+5% condition also displayed significantly decreased vertical ground reaction force between 35 – 47% of stance. These results are likely related to the significant differences observed in the peak ground reaction forces, as these time periods correspond closely to the timing of the peak vertical ground reaction force. There was also a small time period early in stance, between 2 - 13%, found to be significantly different between conditions, possibly indicating differences in rate of loading in the vertical ground reaction force. In the anterior-posterior direction, similar results were observed. Significantly decreased braking force was observed with increasing step rate in the period between 14 – 30% of stance, likely also reflecting both rate of loading and peak braking force.

Both foot pronation and knee flexion are essential components of gait to enable efficient shock absorption upon ground contact when the foot moves through the stance phase during running [146]. As the subtalar joint everts, and the talus adducts, the tibia is forced to internally rotate [124]. Then, as the knee starts to extend after the foot has reached midstance, the tibia begins to externally rotate, just as the foot moves into supination to prepare for toe-off [124]. It has been thought that if the timing is poor between the transitions to pronation/supination and tibial internal/external rotation, the distal and proximal ends of the tibia will experience conflicting rotations from the talus and knee [16,146]. These conflicting rotations could then lead to the development of RRIs [16]. There appears to be a coupling between tibial rotation and rearfoot motion [125]; however, it remains unknown if altering these movements has an impact on RRI development. There is some evidence to suggest adjustments to step rate can influence forces and stresses in the lower extremities associated with common RRIs. Increasing step rate has been shown to decrease peak knee flexion during stance, contributing to a

41

reduction in patellofemoral joint loading[139]. Similarly, tibiofemoral joint forces have been shown to decrease with a 10% decrease in step length [67]. Achilles tendon stress has also been shown to decrease with a 5% increase in step rate [75]. The present study supports these past findings as we found significant reductions in rearfoot motion, tibial rotation, and vertical and braking ground reaction forces with increased step rate. Despite these findings, further research is needed to solidify the connections between changes in rearfoot motion, tibial rotation, and RRI development.

The results from this study indicate increasing step rate has the potential to alter rearfoot and tibial motion, as well as ground reaction forces. The observed decreases in ground reaction forces in the present study could diminish the need for shock absorption, thus leading to a reduction in subtalar joint motion. As motion at the subtalar joint is transferred to the tibia [146], reductions in subtalar joint motion could also lead to decreased tibial rotation. Increasing step rate may allow for proximal changes which influence tibial rotation, as well. Increasing step rate has been shown to decrease both ground reaction forces and knee flexion during stance [139]. With the reduced need for shock absorption, the knee may not be forced into as much flexion. This could alter the timing between the changes in knee flexion/extension, as the knee would not have to move through as great of a range of motion from reduced peak flexion. Improved timing between the shift to external tibial rotation when the knee begins to extend could allow for a reduction in possible conflicting rotations between the proximal and distal ends of the tibia.

A limitation of this study was not controlling for whether runners were habitual rearfoot- or forefoot-strike runners. Differences in ankle and rearfoot kinematics have

been observed between rearfoot- and forefoot-strike runners in previous investigations [143]. However, most runners (n = 16) in this sample, as determined by the foot strike index results, tended to utilize a rearfoot strike pattern, and our participants did not significantly alter their foot strike pattern with the increased step rate. When comparing the rearfoot- and forefoot-strike runners, no differences were observed in the variables of interest. The average step rate of the runners in this study was relatively high before the increased step rate conditions. Although this study was focused on how increased step rate influenced rearfoot kinematics, increasing step rate may have a ceiling effect [130], and it may not be feasible for the average runner to increase their step rates to the level observed in some of the subjects' +10% trials. Screening for runners with lower step rates would increase the applicability of this study, as runners with lower step rates would likely find more benefit from increasing step rate and may experience more pronounced effects from an intervention. This study also only tested the acute effects of increased step rate on measures of rearfoot kinematics and ground reaction forces. Previous investigations implementing at-home or in-lab gait retraining sessions over the course of multiple weeks or months have shown participants are able to effectively alter their step rate [10,11,67,72,130,131,147]. However, the longitudinal effects on rearfoot motion, and whether the modifications in rearfoot angles and ground reaction forces would still be observed after implementing a longer-term gait retraining protocol, remain unknown. Finally, we had participants complete the running protocol on a treadmill. Results from this study may not be generalizable to overground running, as there have been differences observed between treadmill and overground running [148].

Conclusion

The results from this study demonstrate that increasing step rate alters rearfoot motion in the sagittal and frontal planes, and tibial rotation, as well. These outcomes have implications for many RRIs such as Achilles tendinopathy, patellofemoral pain, and tibial stress injuries, as reducing excessive rearfoot motion and tibial rotation may prove beneficial in rehabilitating or preventing some of these common RRIs. Further research is needed to quantify the effects these changes in rearfoot and tibial motion have on soft tissue and bone loads.

44

Bridge

  The goal of this chapter was to investigate how increasing step rate affects rearfoot motion and tibial rotation due to the possible influence the coupling of rearfoot and tibial motion may have on Achilles tendon dynamics and stress. Increasing step rate was shown to effectively reduce peak sagittal and frontal plane rearfoot angles, and peak tibial internal rotation. In addition, this study verified previous findings that increasing step rate reduces peak ground reaction force variables. Data in this chapter support the further investigation of how increasing step rate influences Achilles tendon loading and stress. Chapter IV uses these same data to estimate Achilles tendon stress with the increased step rate conditions. Chapter V then evaluates if similar changes are observed in rearfoot kinematics and Achilles tendon stress with increased step rate in runners with current Achilles tendon injury as to those seen in healthy runners.

CHAPTER IV

EFFECTS OF INCREASING STEP RATE ON ACHILLES TENDON STRESS

DURING RUNNING IN HEALTHY RUNNERS

This chapter is currently in preparation for publication. Kathryn A. Farina designed the study and collected and analyzed the data. Michael E. Hahn provided mentorship and aided in study design, general oversight, and editing and finalizing the final manuscript.

Introduction

Achilles tendon injuries are one of the more common running related injuries, with middle and long distance runners reported to experience a lifetime risk of 50% for developing an Achilles tendon injury[15]. In addition, the annual incidence for Achilles injury in high-level runners has been reported to be between $7 - 10\%$[149]. Despite the strength of the Achilles tendon, which can experience loads near 12 times body weight in dynamic activities[21], it is prone to injury from high stress and strain repetitive loading, creating microstructural damage to the collagenous tendon structure, and without adequate time for recovery can spiral into a state of disrepair and degenerative tendinopathy[12]. Achilles tendinopathy is a difficult condition and can cause intermittent pain for many years or impair physical activity altogether [33,37,150–152]. In addition, the injury is prone to recurrence [19,33,37], as a previous Achilles tendon injury has been reported to be strongly associated with redeveloping symptoms for Achilles tendon injury[13]. One study found having Achilles tendinopathy in the previous 12 months prior to current Achilles tendinopathy injury displayed an odds ratio of 6.3

[13]. Currently, the leading methods of Achilles tendinopathy rehabilitation center around heavy load resistance, or eccentric exercise training in order to stimulate collagen synthesis and repair [18,30,153]. However, as many as 45% of patients may not respond to this treatment [14,20], and if not provided with other avenues of rehabilitation, patients will likely experience continued symptoms. Considering the percentage of patients who don't respond to eccentric load rehabilitation, and the high risk for reinjury[13], modifications in the runner's gait may be necessary to decrease injury risk, help facilitate recovery and reduce risk of reinjury.

The combination of inadequate recovery coupled with excessive loading of the Achilles tendon appears to be a major component in the development of Achilles tendinopathy[12]; however, it remains unknown if some people may be predisposed to Achilles injury risk based on gait mechanics. One theory for placing the Achilles tendon in a vulnerable position to experience increased microtrauma relates to greater frontal plane rearfoot eversion conflicting with tibial rotation in the stance phase of gait during running[16,17]. Adding to this theory, investigations into runners with Achilles tendinopathy have shown increased rearfoot motion or time to reach peak eversion, in comparison to uninjured runners[38,39,41]. In addition, it has been shown that the angle of the calcaneus, whether in inversion or eversion, influences stress distribution within the Achilles tendon[76]. Although more research is still needed to better understand how frontal plane rearfoot motion affects the Achilles tendon, using gait retraining to modify movement patterns may prove beneficial for runners recovering from Achilles tendinopathy, or reduce risk of developing the injury.

Gait retraining interventions have become popular in treating other running related injuries, such as patellofemoral pain syndrome [6,9,11,61,63], iliotibial band syndrome [8,10], and tibial stress fractures [130]. Methods of gait retraining have used real-time visual feedback to adjust joint angles [6,9,57] or loading rates [7,59], modifying foot strike patterns [55,69], or adjusting step rate [10,11,130]. Despite successful interventions in other running related injuries, gait retraining has largely not been explored as a treatment option for Achilles tendinopathy. Recent research has explored the use of transitioning to minimalist shoes as a way to decrease Achilles tendon loading [154,155]. Running in minimalist shoes may have potential positive morphological benefits for the Achilles tendon, if transitioned gradually, such as increased cross sectional area (CSA), stiffness, and Young's modulus [156]. However, some authors have cautioned against the use of minimalist footwear and forefoot strike patterns for patients with Achilles tendinopathy[33], as forefoot strike patterns can increase Achilles tendon load, stress, and strain[75,157–159]. Twelve-weeks of transitioning to minimalist shoes and a forefoot strike pattern produced increased Achilles tendon loading during the stance phase of running, but no morphological changes[154]. Another study using similar gait retraining methods found increases in CSA and production of Achilles tendon force during a maximal isometric contraction test[155]. The authors from these studies propose that the transition to minimalist footwear and forefoot striking could be used to gradually increase load in the tendon[154,155]. However, the previously observed increases in peak force between differences in rearfoot and forefoot strike running must be considered and could place the Achilles tendon at greater risk for injury if adequate recovery and pain and load are not carefully monitored.

Increasing step rate is another popular method of gait retraining which could be employed to target Achilles tendinopathy, as it may modify rearfoot frontal plane motion and stress in the Achilles tendon. A previous study reported a 5% increase in step rate reduced Achilles tendon stress by approximately 3% [75]. Few studies have evaluated the effects of increased step rate on rearfoot frontal plane and transverse motion. One study observed a trend of decreased peak ankle eversion with decreased stride length [70], and a recent study reported that increasing step rate decreases peak rearfoot eversion with a 5 and 10% increase in step rate [160].

Previous studies have evaluated Achilles tendon stress using measures of CSA and Achilles tendon force[75,77,158]. These methods are only able to evaluate Achilles tendon stress at the selected cross section of tendon and may not account for how frontal or transverse plane motion affects stress in the Achilles tendon, or how points of stress may migrate under changing conditions. Finite element (FE) modeling enables the creation of a tendon model in which multi-axial rotation and load can be applied and could allow for a more robust view of how load is distributed in the Achilles tendon. Therefore, the purpose of this study was to evaluate Achilles tendon stress and location of stress in runners using a FE model with three-dimensional rearfoot rotations and estimated Achilles tendon force between increased step rate conditions.

Methods

Data from 15 runners (8 male, 7 female) (Table 4.1) collected in a previous step rate intervention protocol were included in this analysis. These runners were recruited

from the local area, were currently running pain free and without current running related

injury and running at least 15 miles per week.

Table 4.1. Subject characteristics, preferred running pace, and step rates.

	Total (7 females, 8 males, n = 15)
Age (years)	25.60 ± 9.78
Height (cm)	174.6 ± 10.06
Mass (kg)	66.04 ± 10.39
Miles per week (miles)	36.00 ± 18.63
Preferred Running Pace (m/s)	3.32 ± 0.40
Preferred Step Rate (steps/min)	175 ± 7
+ 5% Step Rate (steps/min)	184 ± 8*
+ 10% Step Rate (steps/min)	193 ± 9*#

* denotes significant difference from preferred condition; # denotes significant difference from +5% condition ($p < 0.05$). Significant differences shown only for the total sample.

Full details of the previous protocol can be found elsewhere [160]. Briefly, twenty

healthy runners were recruited to run using three different step rates on a force-

instrumented treadmill (Bertec, Columbus, OH) while motion capture data were collected

(Motion Analysis Corp., Rohnert Park, CA) at 1000 and 200 Hz, respectively.

Retroreflective markers were placed on the lower legs and feet to define thigh, shank,

rearfoot, and forefoot segments for the right and left legs. Markers were placed directly

on the feet by cutting windows in standardized, neutral running shoes (Brooks Launch).

Subjects ran at their preferred running speed and step rate for a three-minute trial, after

which step rate was increased by 5 and 10% for two additional three-minute trials, while

running pace did not change. Subjects were cued by metronome to the increased step rate

conditions. Kinematic and kinetic data were collected of twenty foot-strikes during the

final minute of each trial. Step rate was calculated by counting the number of footfalls in

a 20-second period and was verified before and after recording of data.

A custom MATLAB (The MathWorks, Natick, MA) program was used to calculate rearfoot and shank kinematics from the left foot throughout stance phase. The stance phase was defined as when the vertical ground reaction force exceeded 5% of participant body weight[135]. The rearfoot coordinate system origin was defined as the midpoint between the medial and lateral calcaneus markers, with the x axis pointed laterally, y axis pointed anteriorly, and z axis directed superiorly. A quadrad of four markers on a firm plate attached to the shank was used to define the shank tracking coordinate system, with the same x-y-z orientations applied as described above. Raw marker coordinate and force platform data were dual pass filtered using a 4th order lowpass Butterworth filter with a 20 Hz cutoff frequency. Joint angles of the rearfoot segment were calculated with respect to the shank segment using a Cardan sequence of flexion-extension, inversion-eversion, adduction-abduction. Rearfoot joint angles were averaged across twenty-foot-strikes and time-normalized to 101 data points during the stance phase. Peak values for each rotation direction were extracted. Fifteen runners from the previous study were included for further analysis. Five runners were removed from analysis due to errors in force plate analog data collection.

In the present study, the collected kinematic and kinetic data were further processed to determine changes in Achilles tendon stress with increased step rate by using two different methods: finite element (FE) analysis and a calculation of stress using cross sectional area and Achilles tendon force. For both analyses, Achilles tendon force during the stance phase of running was calculated as the sagittal plane ankle moment divided by the Achilles tendon moment arm:

$$ATF = \frac{M_A}{AT_{MA}}$$

51

where M_A is the ankle plantar flexor moment, and AT_{MA} is the moment arm of the Achilles tendon. The Achilles tendon moment arm (cm) was calculated using a regression equation developed from MRI scans that accounts for changes in moment arm length during stance [108–111]:

$$AT_{MA} = -0.5910 + 0.08297\theta - 0.0002606\theta^2$$

where θ is the sagittal plane ankle flexion angle. Finally, the ankle plantar flexor moment was calculated using a Newtonian-Euler inverse dynamics approach:

$$M_p = I\alpha + \omega \times (I\omega) - M_d - r_d \times F_d - r_p \times F_p$$

where M_p is the moment about the proximal end of the segment (ankle), I is the moment of inertia about the segment center of mass (foot), determined from previously published segment lengths and heights [112], α is the angular acceleration of the segment, ω is the angular velocity of the segment, F_p and F_d are the proximal and distal reaction forces, M_d is the moment about the distal end of the segment, and r_p and r_d are the distances from center of mass of the segment to the proximal or distal joint.

Finite Element Analysis

The calculated Achilles tendon force was used with rotation data from the rearfoot segment and shank segment calculated within the global coordinate system in a FE model. The FE analysis was performed for two time points during the stance phase, peak calcaneal eversion and peak Achilles tendon force, for each of the three step rate conditions (preferred, +5%, +10%) for each of the fifteen subjects.

The FE model consisted of an Achilles tendon and calcaneus segment. The model was generated from the MRI scan of a 30-year-old active, healthy male subject (height:

175 cm; weight: 68 kg). The MRI was performed using a Siemens Skyra 3.0 Tesla

Scanner (Siemens Medical Solutions, Malvern, PA, USA) to obtain sagittal, coronal, and

axial images of the Achilles tendon and calcaneus. The subject's ankle was positioned in

a non-weight bearing neutral position in a flex coil and stabilized with foam. The 3D

True FISP sequence, a steady-state coherent sequence in which balanced gradients (net

gradient-induced dephasing over a repetition time interval is zero) are used along all three

axes, was used with 8-mm slice thickness with zero gap between slices, and resolution of

0.8x0.8x0.8-mm.

Digital imaging and communications in medicine (DICOM) files obtained from

the MRI were imported into 3D Slicer software (version 4.11) (www.slicer.org)

[113,114]. The Fast GrowCut algorithm [115] was used in the segment editor [116] to

section the Achilles tendon from the insertion on the calcaneus to near the highest point

visible from the MRI scans (approximately 12-cm proximal from the Achilles tendon

insertion), and the calcaneus. Segments were smoothed and exported as standard

tessellation language (stl) files which described the surface geometry of the 3D objects.

The surface files were then imported into FEBio software [117], where the included

Tetgen function (tetgen.berlio.de) was used to create a tetrahedral mesh. Surfaces for the

Achilles tendon and calcaneus were defined, and material properties assigned in FEBio

(Table 4.2). Material property values used in this study were selected from literature of

cadaveric Achilles tendons [119] and have previously been used in FE analysis [79,118].

The Achilles was modeled as an isotropic and homogenous Neo-Hookean material. The

calcaneus was modeled as a rigid body.

Table 4.2. Achilles tendon and model properties. The cross sectional areas refer to distance from the Achilles tendon distal insertion.

3 cm CSA (mm^2)	79.96
4 cm CSA (mm^2)	64.09
5 cm CSA (mm^2)	49.44
Young's Modulus (MPa)	819
Poisson's Ratio	0.4
Material	Neo-Hookean
Elements	3639
Faces	2612
Nodes	1308

CSA = Cross Sectional Area.

The boundary conditions for the model were assigned based on the collected kinematic data. The three-dimensional rotation angles of the calcaneus segment at peak eversion and peak Achilles tendon force were extracted. The displacement in the x-y-z directions of the calcaneus was fixed. Data to define the motion of the Achilles tendon was not collected, but an assumption was made that the Achilles tendon rotation would follow that of an assumed rigid body shank segment. Three-dimensional rotation of the shank tracking coordinate system was used to define the rotation angles at peak eversion and peak Achilles tendon force. In order to apply these rotations to the Achilles tendon segment, a rigid body was attached to the proximal surface of the Achilles tendon, emulating a clamp similar to that used in cadaveric studies[120]. In addition, Achilles tendon force was applied as a rigid body force to the proximal rigid body. The x-y displacements of the proximal rigid body were fixed; however, because the Achilles tendon lengthens as the gastrocnemius and soleus muscles contract during stance, the z-displacement of the proximal rigid body was prescribed a displacement of 6-mm. This displacement was chosen as a previous study has reported a displacement of

approximately 6-mm of the Achilles tendon from touch-down to mid-stance during running[121].

The area of peak von Mises stress was extracted from the simulation results. The area of tendon from 2 – 6 cm from the distal insertion was used for analysis (Figure 4.1), as this has been reported to be the area of tendon most frequently injured[33].
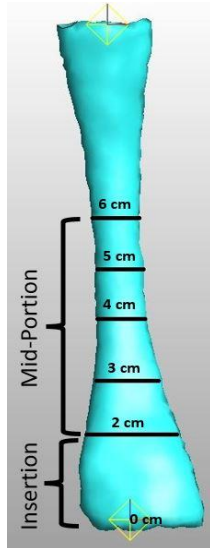
Figure 4.1. Achilles tendon model showing distal tendon insertion from 0 – 2 cm of tendon length, and mid-portion of tendon, used for analysis, from 2 – 6 cm of tendon length, measured from the distal insertion.

The location of the peak stress was measured from the lateral edge of the tendon and from the bottom of the insertion. These measures were normalized to tendon length and width, with 6 cm from the distal insertion considered 100% of tendon length, and 2 cm from the distal insertion considered 0% of tendon length. Because the Achilles tendon width is not consistent throughout the length of the tendon, the width of the tendon was measured each centimeter from 2 – 6 cm from the distal tendon insertion. The measured width at peak stress was then normalized to the width at the measured section of tendon length, with 0% corresponding to the most lateral edge of the tendon, and 100% corresponding to the most medial edge of the tendon. For example, if peak stress were

measured at a tendon length of 5 cm from the insertion, the measured width would be normalized to the width of the tendon at 5 cm from insertion. This process was repeated for peak eversion and peak Achilles tendon force time points during stance, for each step rate condition, for each of the fifteen subjects.

Cross Sectional Area Analysis

Cross sectional area of the Achilles tendon was measured from the segmented geometry in 3D slicer for the length of the tendon. For analysis, CSA at 3 cm, 4 cm, and 5 cm of tendon length from the insertion were used (Table 4.2). For each CSA, calculated Achilles tendon force was divided by CSA to evaluate Achilles tendon stress at each of the selected lengths of tendon for each step rate condition. This analysis was performed to compare to the results of previous research, and to the FE analysis results.

Statistical Analysis

Repeated measures analyses of variance (ANOVA) ($\alpha = 0.05$) were used to evaluate differences in Achilles tendon stress, locations of stress, peak tendon force, and peak eversion between each of the three step rate conditions. If the assumption of sphericity was violated, a Greenhouse-Geisser correction was used. In the case of a significant main effect, a Bonferroni correction was used in *post-hoc* analysis to determine significant differences between conditions. Statistical analyses were performed in SPSS v27 (IBM SPSS Statistics, Chicago, IL).

Results

Kinematic results of the rearfoot segment can be found in Chapter III. Peak Achilles tendon force was significantly reduced ($F_{(2, 30)} = 11.90$, $p < 0.001$) in the +5% ($p = 0.018$) and +10% ($p = 0.004$) conditions compared to the preferred condition, and in the +10% condition ($p = 0.022$) compared to the +5% condition (Table 4.3).

Table 4.3. Peak Achilles tendon force, Achilles tendon moment arm, peak Achilles tendon force at peak eversion and peak tendon force, and width and length locations of peak stress from finite element analysis.

	Preferred Step Rate	+5% Step Rate	+10% Step Rate
Peak Achilles Tendon Force (BW)	5.32 ± 1.08	5.02 ± 0.96*	4.67 ± 1.11*[#]
Achilles Tendon Moment Arm (cm)	4.84 ± 0.22	4.86 ± 0.18	4.83 ± 0.35
Peak Stress at Peak Eversion (MPa)	79.03 ± 7.66	80.45 ± 10.30	80.10 ± 11.19
Width Location at Peak Eversion (% tendon width)	62.46 ± 19.65	64.62 ± 23.01	58.95 ± 27.45
Length Location at Peak Eversion (% tendon length)	87.28 ± 11.71	87.22 ± 12.74	81.80 ± 16.89
Peak Stress at Peak Force (MPa)	76.42 ± 9.20	80.53 ± 11.12	81.19 ± 12.13
Width Location at Peak Force (% tendon width)	69.35 ± 21.08	71.26 ± 21.94	67.74 ± 22.52
Length Location at Peak Force (% tendon length)	88.50 ± 13.13	86.78 ± 13.16	84.31 ± 14.63

* indicates significant difference from the preferred condition; [#] indicates significant difference from the +5% condition ($p < 0.05$). Width and length locations given as % of tendon length, with 0% = 0 cm at insertion of Achilles tendon on calcaneus, and 100% = 6 cm from Achilles tendon insertion. Width values are with respect to tendon width at the measured tendon length, with 0% = most lateral edge of tendon, and 100% = most medial edge of tendon at given length.

Finite Element Analysis

An example of the FE model and results from one subject's simulation are shown in Figure 4.2. Overall, there were no significant differences observed in peak Achilles tendon stress at peak eversion or at peak Achilles tendon force between step rate conditions ($p > 0.05$) (Table 4.3) (Figure 4.3).
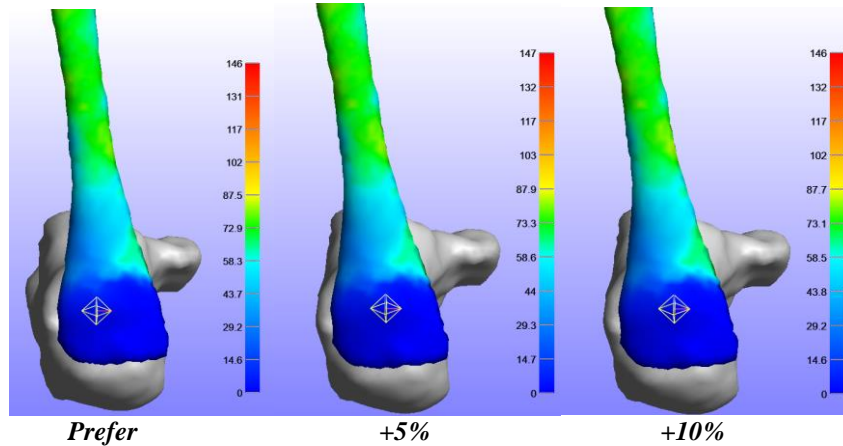
Figure 4.2. Example subject finite element results for the preferred, +5%, and +10% step rate conditions. Note: image shows tendon from insertion to 6 cm of the left calcaneus and tendon.
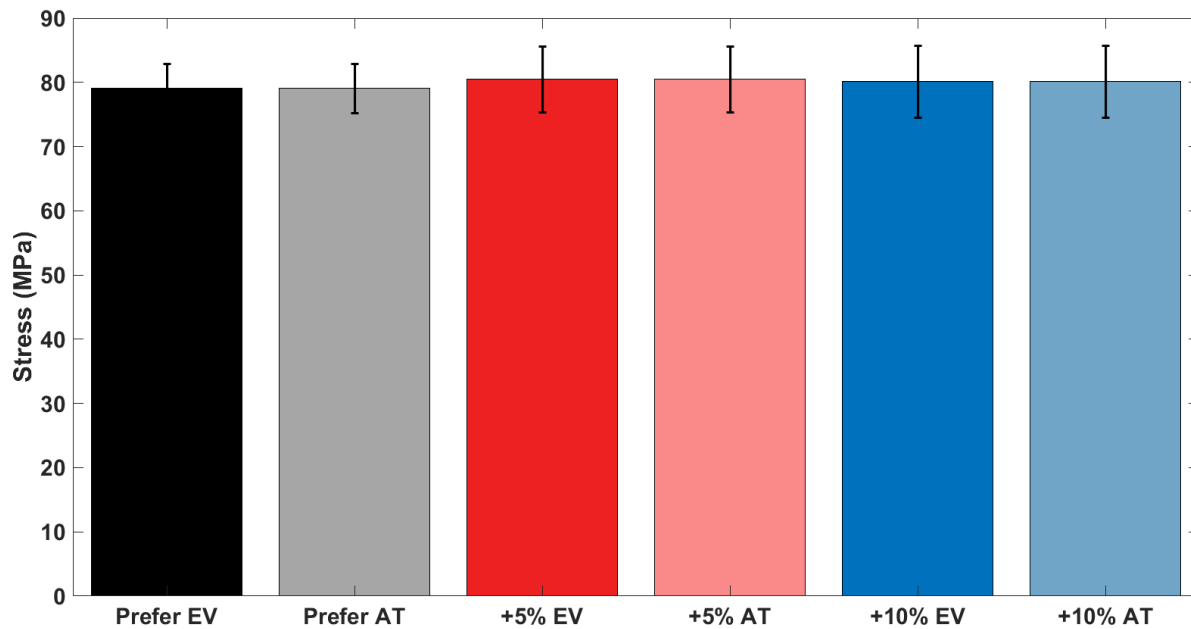
Figure 4.3. Peak Achilles tendon stress (MPa) ± standard deviation (error bars) from finite element analysis for the preferred, +5%, and +10% conditions at peak eversion (EV) and peak Achilles tendon force (AT).

In addition, there were no significant changes in the location of peak Achilles tendon stress between conditions (Table 4.3). The location of peak tendon stress remained near the center portion of the tendon, leaning to the medial side (around 60 - 70% of normalized tendon width), and around 5 cm of tendon length from the distal insertion (corresponding to near 85% of tendon normalized length).

Cross Sectional Area Analysis

The calculated Achilles tendon stress using Achilles tendon peak force and CSA across the length of the tendon from $3 - 5$ cm from the distal insertion is displayed in Figure 4.4. Significant decreases in Achilles tendon stress (F $(1.37, 19.13) = 9.58$, $p = 0.003$) were observed at 3, 4, and 5 cm in the +5% ($p = 0.048$) and +10% step rate
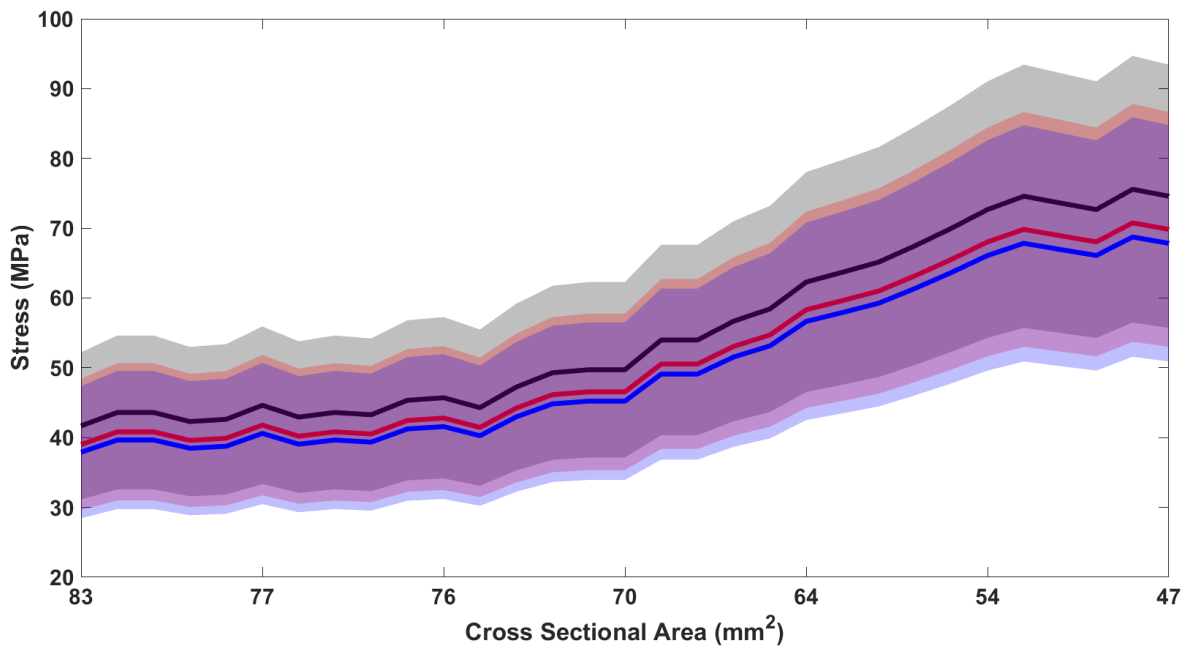
Figure 4.4. Achilles tendon stress (MPa) calculated from cross sectional area (mm²) and peak Achilles tendon force across the length of tendon from $2 - 6$ cm (distance from Achilles tendon insertion) for the preferred (black), +5% (red), and +10% (blue) step rate conditions. 2 cm = 83.00 mm², 3 cm = 79.96 mm², 4 cm = 64.09 mm², 5 cm = 49.44 mm², 6 cm = 47.61 mm². Solid lines show the sample mean with shaded area representing standard deviation.

conditions ($p = 0.014$) compared to the preferred condition (Table 4.4). There was not a

significant difference observed between the +5% and +10% step rate conditions at any of

the tendon lengths ($p = 0.057$).

Table 4.4. Achilles tendon stress at 3, 4, and 5 centimeters (cm) tendon length from distal
insertion calculated with cross sectional area (CSA) and peak Achilles tendon force.

|	**Preferred Step Rate**	**+5% Step Rate**	**+10% Step Rate**
Stress at 3 cm (MPa)	42.94 ± 11.24	40.21 ± 10.02*	37.67 ± 10.83*
Stress at 4 cm (MPa)	49.72 ± 13.01	46.56 ± 11.61*	43.62 ± 12.54*
Stress at 5 cm (MPa)	65.16 ± 17.05	61.01 ± 15.21*	57.16 ± 16.43*

* indicates significant difference from the preferred condition; [#] indicates significant
difference from the +5% condition ($p < 0.05$).

Discussion

This study sought to evaluate the effects of increasing step rate on Achilles tendon

stress in healthy runners. The main findings of this study were conflicting, as using FE

analysis revealed no significant changes in Achilles tendon stress with increasing step

rate, but using CSA and estimated Achilles tendon force revealed significant decreases in

Achilles tendon stress with increasing step rate in the area of 3 – 5 cm of tendon length

from the distal insertion.

Finite Element Analysis Results

A FE model of the Achilles tendon and calcaneus was created from the MRI of a

healthy, active male subject. Data from fifteen runners were used with this model to

estimate Achilles tendon stress at the time points of peak eversion and peak Achilles

tendon stress during the stance phase of running. Despite significant decreases in peak

Achilles tendon force with increasing step rate, similar decreases in peak Achilles tendon

stress were not observed, due in part to larger than expected variation in response to

increased step rate. On average, peak Achilles stress increased with increased step rate at both peak eversion and peak Achilles tendon force time points, although these increases were non-significant. Half of the subjects displayed a decrease in peak Achilles tendon stress at the points of peak eversion and peak Achilles tendon force in response to increased step rate. However, these decreases in peak stress were not consistent between subjects, as some subjects displayed a decrease in peak stress at the point of peak eversion, but an increase in peak stress at the point of peak Achilles tendon force. A possible reason for these results could be related to the boundary conditions and constraints provided for the model. The motion of the proximal portion of the Achilles tendon was defined by attaching the proximal Achilles tendon to a rigid body segment. In reality, the Achilles tendon is connected to muscle proximally, and thus using a rigid body segment to define this motion likely does not accurately represent the muscle-tendon dynamics and subsequent transfer of force. In addition, the motion of the proximal rigid body was assigned rotations of the shank segment, which may misrepresent actual kinematics of the proximal tendon. The lengthening of the tendon was given a value of 6mm displacement based on previous research[121]. This value remained consistent between step rate conditions and may have contributed to inaccuracy in determining changes in Achilles tendon stress, as the tendon may not actually displace the same amount during each condition. This value of 6mm was also not subject-specific and therefore may not accurately represent the tendon dynamics of each individual subject. No other studies have evaluated how Achilles tendon stress is affected by changes in running mechanics using FE analysis, thus it is currently unclear how these results compare to other research in the literature. One study examined Achilles tendon stress

during hopping using FE analysis, and found peak Achilles tendon stress reached values near 50 MPa[80], which was much lower than observed in the present study.

A change in the point of peak Achilles tendon stress was not observed with increasing step rate at peak eversion or at peak Achilles tendon force. It was hypothesized that the area of peak Achilles tendon stress would migrate with increased step rate as changes in kinematics could affect how stress is distributed in the tendon. Despite using data from fifteen different subjects, the areas of peak stress centered around the central midportion of the tendon, from 4.5 – 5.5cm tendon length. This area of the tendon is the most frequently injured[33] and represents the narrowest portion of the tendon. A force applied across a smaller CSA produces increased stress, which could contribute to increased risk of injury to the tissue[161]. The FE analysis showed that the area of peak stress remained in this region with the changes in step rate. As discussed previously, the consistent 6mm of displacement applied to the proximal portion of the tendon could have contributed to these results. Similar to the subject-specific results seen with peak stress, the location of the peak stress changes were variable between subjects. While some subjects experienced little change in peak stress location, others displayed a noticeable shift in peak stress location. There is no other study reporting how stress location changes in the Achilles tendon as a result of changes in running kinematics, making it currently unknown if a change in peak stress location should be expected with increased step rate. However, one study using cadaveric tendons has evaluated the influence of various calcaneal angles on strain in the Achilles tendon, and found that a more everted orientation places greater strain on the medial portion of the Achilles tendon, while a more inverted calcaneus produces greater strain to the lateral portion of the tendon[76]. It

should be noted the results from the present study add some support to this previous finding, as the location of peak stress, measured at time points where the calcaneus would be oriented in an everted position, was slightly towards the medial side of the tendon. In addition, our previous study results [160] indicated a decrease in peak eversion angle from the preferred to the +10% condition, and although non-significant, the location of peak stress in the present study tended to move more centrally in the +10% condition compared to the preferred condition, again, supporting the findings of Lersch and colleagues[76].

Cross Sectional Area Analysis Results

Peak Achilles tendon stress was calculated from CSA and estimated Achilles tendon force to compare with the results from the FE analysis and to previous studies. Peak Achilles tendon stress was calculated in the area between 3 – 5 cm of tendon length from the distal Achilles tendon insertion and was found to significantly decrease at each length position with increasing step rate. One other study has assessed Achilles tendon stress using CSA and Achilles tendon force with changes in step rate. They reported a 5% increase in step rate decreased peak Achilles tendon stress during running compared to preferred step rate [75]. The values for peak Achilles tendon stress at 5cm tendon length observed in the present study compare well with those from Lyght and colleagues, who reported average peak Achilles tendon stress in the range of 55 – 75 MPa [75]. Although not measuring Achilles tendon stress, other groups have reported decreases in overall ankle energy generation with increases in step rate [53], decreases in the peak muscle forces of the triceps surae muscle group [139], and decreased peak plantar flexor moment

[75], all of which may contribute to Achilles tendon loading. Running with an increased step rate draws the center of pressure closer to the body center of mass, decreases vertical center of mass oscillation, and effectively allows for less energy absorption from the lower extremity musculature and joints [69,128–130,139]. Decreased vertical center of mass displacement from increasing step rate may also lend to increases in lower extremity stiffness[162]. Increased tendon stiffness, in general, may be beneficial for force generating and transmission capabilities, as it may allow for the tendon to operate at a more optimal position on the force-length curve[163]. However, it should also be noted that tendons with decreased stiffness may experience greater strain and could lead to greater accumulations of microtrauma overtime, leading to tendon injury[163]. Indeed, a decreased Young's modulus, a measure of stiffness normalized to CSA and length of the tendon[163], is related to an increased failure rate of the tendon[164].

As would be expected, peak Achilles tendon force increased with decreased CSA. At the 5cm location, the area where most subjects experienced peak stress in the FE analysis, peak stress in the CSA analysis was approximately 11 – 30% lower than that calculated in the FE analysis. As mentioned previously, assumptions for the boundary conditions of the FE model and inadequate constraints likely confound the results from the FE analysis, making it unknown if the peak stress values obtained can be considered valid. However, estimating Achilles tendon stress using CSA allows for stress to be determined at a single cross section of tendon, and does not account for tendon stretch, rotation, or displacement which could impart additional stress to the tendon other than Achilles tendon force, and therefore could underestimate stress in the tendon. Although higher than the CSA analysis, the results from the FE analysis point to the need to

consider additional factors contributing to tendon stress. Achilles tendon stress values

obtained using a buckle transducer have been found to be up to 110 MPa during

running[21]. Other studies using methods of CSA and Achilles tendon force have

reported a wide range of values from near 57 – 97 MPa during activity [75,77,158]. The

current values obtained from both the FE and CSA analysis fit within the range of these

measured Achilles tendon stress values.

Limitations

This study was influenced by limitations, in addition to those mentioned

previously. First, a simplified model was used for the FE analysis only consisting of the

Achilles tendon and calcaneus. Additionally, a generic model was used for all subjects

included in the analysis. Similarly, the CSA was not subject-specific, as it was calculated

from the generic Achilles tendon model, and therefore may not represent specific

individual stress for each subject. This model did not consider the Achilles sub-tendons,

the role their twisted structure may have on the tendon and its kinematics, and how force

may not be applied uniformly throughout the tendon as a result of this twisted

structure[27,165]. The Achilles tendon was modeled as a neo-Hookean material which

was consistent throughout the length of the tendon; but tendon material properties may be

anisotropic and change from the proximal to distal end[119,166]. An estimated Achilles

tendon moment arm was calculated from each subject's ankle plantar flexion angle data,

which may not represent actual Achilles tendon moment arm. The Achilles tendon force

applied to the model was estimated from the Achilles tendon moment arm and ankle

plantar flexion angle. Finally, this applied force was assumed to represent the Achilles

tendon force and was assumed to transmit fully to the Achilles tendon, and did not

consider how antagonistic co-contraction of the dorsiflexors may affect Achilles tendon

force [167].

Conclusion

Taken together, the results from this study do not allow for a definitive conclusion

to be made regarding how increasing step rate affects Achilles tendon stress, or how

changes in rearfoot motion may influence location or magnitude of stress. Using a

method of CSA and estimated Achilles tendon force revealed decreases in peak Achilles

tendon stress with increasing step rate, which is in agreement with a previous study [75].

However, this method does not consider how the structures around the tendon may

influence stress. In contrast, the FE analysis method did not result in a decrease in

Achilles tendon stress with increased step rate. This method has the potential to produce a

more realistic picture of Achilles tendon stress by allowing for changes in kinematics to

be included which may affect rotation and displacement of the tendon. However, the

current model likely does not have the appropriate constraints to allow for an accurate

representation of Achilles tendon stress during the stance phase of running. Future

modifications to the model to including more precise kinematics of the tendon will allow

for clearer conclusions to be drawn about how increasing step rate affects stress in the

Achilles tendon. Future efforts should continue to develop more robust methods of

analyzing areas of stress within the Achilles tendon during running, and how alterations

in gait kinematics and kinetics affect stress magnitude and location within the tendon.

Bridge

        The purpose of this chapter was to assess how Achilles tendon stress was affected by increases in step rate during running using a sample of healthy runners and methods of finite element analysis and cross sectional area analysis. The results from this study were conflicting, as the finite element analysis results displayed a non-significant increase in Achilles tendon stress with the increased step rate, and the cross sectional area analysis revealed decreases in Achilles tendon stress with increased step rate. Limitations of this study, including non-subject specific models, likely affected these results. Chapter V combines methods of Chapters III and IV using runners with current Achilles tendon pain. Chapter V improves on the shortcomings of Chapter IV by creating subject-specific models for each subject, and evaluates how runners with current Achilles tendon injury modify rearfoot kinematics and Achilles tendon stress in response to increases in step rate.

CHAPTER V

SUBJECT-SPECIFIC MODELS TO DETERMINE THE EFFECTS OF INCREASING

STEP RATE ON ACHILLES TENDON STRESS IN RUNNERS WITH ACHILLES

TENDON INJURY

This chapter is currently in preparation for publication. Kathryn A. Farina designed the study and collected and analyzed the data. Michael E. Hahn provided mentorship and aided in study design, general oversight, and editing and finalizing the final manuscript.

Introduction

Many running related injuries may stem from repeated cyclical loading without adequate time for recovery and have been termed overuse running injuries [168]. It has been reported that as many as 79% of runners could experience at least one of these overuse running related injuries in a given one-year period [1]. Achilles tendon injuries are one of the most common running related injuries, with estimates of 1 in 20 runners developing Achilles tendinopathy [13]. Achilles tendinopathy is a degenerative process in the Achilles tendon, in which the tenocytes become disorganized and deteriorate, and collagen fibers are disrupted, resulting in pain and weakness in the tendon [12]. These characteristics of the tendinopathic tendon are thought to represent a failed healing response, brought about by a mismatch between cell recovery and breakdown, placing the tendon in a state of degeneration [12]. The cause of this state of disrepair is likely multifactorial, but one theory involves the combined actions of rearfoot eversion and tibial rotation leading to increased damage in the tendon structure [16]. In this model,

prolonged or excessive frontal plane rearfoot motion could conflict with the coupled action of tibial external rotation when the knee begins to extend during stance [16]. These conflicting motions have been proposed to cause microtrauma within the tendon [16] as a result of non-uniform stress or increased frictional forces between fibrils, leading to cumulative damage within the tissue, and ultimately leading to injury [26,27].

Whether excessive eversion is a contributing factor to Achilles tendinopathy or not, stress distributed across the Achilles tendon may influence tendon health and recovery. It is well documented that tendons benefit from mechanical stimulation for collagen synthesis and repair, which is a main reason for the promotion of resistance training in Achilles tendinopathy rehabilitation [18,30,153]. However, this method of rehabilitation may prove ineffective in as many as 45% of patients [14,20], and Achilles tendinopathy is often prone to recurrence [19,33,37]. In fact, one of the major risk factors for developing Achilles tendinopathy is having a prior Achilles tendon injury [13]. This begs for alternative methods of rehabilitation which may address underlying movement abnormalities that may place the tendon in a more vulnerable position or expose the tendon to increased loads.

Gait retraining has become a staple in the rehabilitation of many common running related injuries. Gait retraining involves modification of a runner's movement patterns to address underlying mechanics which may place additional stresses or loads on certain structures. These modifications have come in many forms, with the most common goals being to decrease excessive movements [6,9,62] or loads to body tissues [7,56,59]. Despite the successes observed in other running related injuries with a suspected pathology related to poor mechanics, gait retraining has largely been unexplored for use

in Achilles tendinopathy rehabilitation. Identifying ways to alter running gait to modify stress in the Achilles tendon may prove beneficial for rehabilitating from Achilles tendon injury and decreasing risk for developing an Achilles tendon injury.

Two studies have evaluated the transition to a forefoot strike pattern with minimalist footwear over a 12-week period on Achilles tendon stress. Increases in Achilles tendon force production were observed, which the authors noted may be beneficial for promoting Achilles tendon structural changes to combat injury [154,155]. However, other researchers have observed increased Achilles tendon force, stress, or strain in runners utilizing a forefoot strike pattern in comparison to a rearfoot strike pattern, and generally have recommended against a forefoot strike pattern for runners combating Achilles tendon injury [33,75,157–159]. One study observed decreases in Achilles tendon stress with a 5% increase in step rate [75]. Increasing step rate has been observed to allow the foot to land closer to the body center of mass, decreasing the energy absorption required of the body, and may prove effective in decreasing stress within the Achilles tendon [53,75,128]. These previous observations have been reported from studies involving healthy runners, and it is unknown how runners with current Achilles tendon injury may adapt to gait modifications, and if these modifications translate to a decrease in Achilles tendon stress. Therefore, the purpose of this study was to evaluate Achilles tendon stress in response to an acute increase in step rate in runners currently experiencing Achilles tendon pain. This study utilized two methodologies to evaluate Achilles tendon stress: finite element (FE) analysis using subject-specific models and an approach using cross sectional area (CSA) and Achilles tendon force. The FE model approach provides the benefit of subject specificity, visualizing stress

throughout the tendon structure, and simulating the influence of proximal and distal

motion contributions to Achilles tendon stress, while the CSA analysis allows for

comparison with the FE model results and to previous research which has used a similar

approach.

Methods

Six runners (4 females, 2 males) (Table 5.1) with current Achilles tendon pain

were recruited for participation in this study from the local running community. Subjects

had to be between the ages of 18 – 65 years old, be experiencing Achilles tendon pain

symptoms for more than four weeks, and pain localized to the mid-portion of the Achilles

tendon.

Table 5.1. Subject characteristics, preferred running pace, and step rates.

	Total (4 females, 2 males, n = 6)
Age (years)	27.17 ± 10.95
Height (cm)	165.33 ± 10.95
Mass (kg)	61.18 ± 9.42
Current miles per week (miles)	26.67 ± 11.25
Pre-Injury miles per week (miles)	51.67 ± 22.51
Duration of symptoms (months)	12.00 ± 14.52
Preferred Running Pace (m/s)	3.23 ± 0.39
Preferred Step Rate (steps/min)	174 ± 7
+ 5% Step Rate (steps/min)	186 ± 8*
+ 10% Step Rate (steps/min)	192 ± 8*#

* denotes significant difference from preferred condition; # denotes significant difference from +5% condition ($p < 0.05$). Significant differences shown only for the total sample.

Subjects were excluded if they currently had other running related injuries, Achilles pain

was located at the tendon insertion site, they had a current or previous Achilles tendon

rupture, or if they had previous Achilles tendon surgery or had plans for surgical

intervention for the current injury. Subjects were not required to have had a clinical

diagnosis for participation in this study. Instead, they self-reported general Achilles tendon pain during initial screening procedures. The protocol was approved by the University of Oregon Institutional Review Board, and all subjects provided written, informed consent before taking part in the study. Subjects underwent magnetic resonance imaging (MRI) of their injured foot-ankle complex and completed a running protocol at increased step rates on a treadmill in which segmental position and orientation, and force plate data were collected. The running protocol and MRI collections were performed on the same day.

Magnetic Resonance Imaging

Each subject was provided an MRI scan of their injured Achilles tendon and foot using a Siemens Skyra 3.0 Tesla Scanner (Siemens Medical Solutions, Malvern, PA). Sagittal, coronal, and axial images of the Achilles tendon and calcaneus were obtained using the 3D True FISP sequence with the subject's ankle positioned in a non-weight bearing neutral position in a flex coil stabilized with foam. This sequence uses a steady-state coherent sequence in which balanced gradients (net-gradient induced dephasing over the repetition time interval is zero) were used along all three axes. The parameters for the sequence included 8-mm slice thickness, with zero gap between slices, and resolution of 0.8x0.8x0.8-mm. Each subject's MRI scan was used to create a subject-specific mesh structure of the Achilles tendon and calcaneus for use in a finite element analysis, described below.

Running Protocol

Subjects were equipped with forty-three retroreflective markers placed bilaterally on the lower limbs and pelvis. Markers were used to define pelvis, thigh, shank, rearfoot, and forefoot segments. Participants performed a static trial of stationary standing in the capture volume space on the treadmill, after which markers on the medial and lateral malleoli, femoral epicondyles, and greater trochanters were removed so as not to interfere with running motion. Participants wore standardized, neutral running shoes (Brooks Launch), in which small windows were cut to place markers directly on the posterior calcaneus, medial and lateral calcaneus, first and fifth metatarsal heads, and distal hallux.

Three-dimensional marker trajectories were collected using an 8-camera motion capture system (Motion Analysis Corp., Rohnert Park, CA), and ground reaction force data were collected using an instrumented treadmill (Bertec, Columbus, OH) at 200 and 1000 Hz, respectively. Subjects performed three running trials of approximately three minutes each, with kinematic and kinetic data recorded for twenty strides during the final minute of each trial. The first trial consisted of subjects running at a self-selected easy pace in which preferred running step rate was determined by visually counting the number of steps taken during a 20-second period and multiplied by three to obtain steps per minute. A 5% and 10% increase in step rate over preferred was determined. For the following two trials, subjects were instructed to match their foot falls to sound of a metronome set to the increase in step rate. Subjects were given the first two and half minutes of each trial to acclimate to the increased step rate. Step rate was calculated once before, and once after, data were recorded to ensure subjects had modified their step rate.

Kinematic and Kinetic Data Analysis

Marker trajectories were labeled, and gaps filled using Cortex software (Motion Analysis Corp., Rohnert Park, CA), and exported for further processing in MATLAB (The MathWorks, Natick, MA). A custom script was written in MATLAB to calculate rearfoot and shank kinematics during the stance phase of running. The stance phase was defined as when the vertical ground reaction force exceeded 5% of subject body weight. For global and segment coordinate systems, the *x* axis was directed to the right, *y* axis pointed anteriorly, and *z* axis directed superiorly. The rearfoot coordinate system was defined using the posterior calcaneus, medial and lateral calcaneus markers, with an origin set at the midpoint between the medial and lateral calcaneus markers. The anatomical shank coordinate system origin was set at the midpoint between the medial and lateral femoral epicondyles. The shank tracking coordinate system was placed on a rigid plate consisting of four markers that was firmly wrapped around the subject's shank. Joint angles were calculated using a Cardan sequence of flexion/extension, inversion/eversion, and adduction/abduction (internal/external rotation). Rearfoot motion was calculated as the motion of the rearfoot with respect to the shank. In addition, rearfoot rotation and shank tracking system rotation were calculated in the global coordinate system for use in the finite element software by calculating an axis of rotation, and angle about that axis.

Raw marker coordinate and force platform data were dual pass filtered using a 4th order lowpass Butterworth filter with a 20 Hz cutoff frequency. Rearfoot and shank angles in the global and local coordinate systems were calculated and ensemble averaged across 20-foot strikes of either the right or left foot and normalized to 101 data points.

75

Determination of which foot was analyzed was based upon the injured leg of the subject. Peak rearfoot cardan angles with respect to the shank segment for the sagittal and frontal plane were extracted for statistical analysis. Additionally, peak vertical ground reaction force (GRF), peak propulsive GRF, and peak braking GRF were extracted.

Achilles tendon force during the stance phase of running was calculated as the sagittal plane ankle moment divided by the Achilles tendon moment arm. The sagittal plane ankle moment was determined using an inverse dynamics approach. The Achilles tendon moment arm (AT_{MA}) was determined using a regression equation developed from MRI scans that accounts for changes in moment arm lengths at varying ankle positions during stance [108–111,154]:

$$AT_{MA} = -0.5910 + 0.08297\theta - 0.0002606\theta^2$$

where θ is the sagittal plane ankle flexion angle. Achilles tendon force was averaged across foot strikes, as above. Achilles tendon force normalized to body weight was also determined. Global rearfoot and shank rotations, and Achilles tendon force at peak eversion and peak Achilles tendon force were extracted to be used in the FE analysis.

Magnetic Resonance Imaging Processing

Digital imaging and communications in medicine (DICOM) files obtained from the MRI were imported into 3D Slicer version 4.11 software (www.slicer.org) [113,114]. The Fast GrowCut algorithm [115] was used in the segment editor [116] to segment the Achilles tendon from the Achilles tendon insertion to the highest point visible from the MRI scan (approximately 12-cm from the Achilles tendon insertion), and the calcaneus (Figure 5.1). Segments were smoothed and exported as standard tessellation language

(stl) files which described the surface geometry of the 3D objects. Cross sectional area

(CSA) of the Achilles tendon was measured from the segmented geometry in 3D slicer

for the length of the tendon for further use in estimating Achilles tendon stress using CSA

and Achilles tendon force, described below.
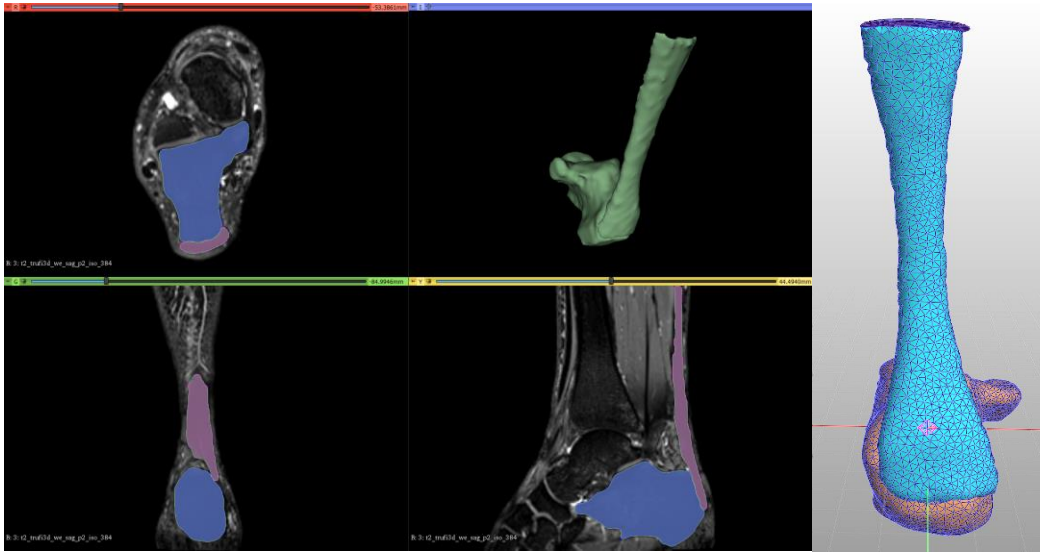
Figure 5.1. Example image of segmentation and creation of Achilles tendon model in 3D Slicer (left). Example Achilles tendon and calcaneus meshed model in FEBio (right).

Finite Element Analysis

The Achilles tendon and calcaneus segments were imported into FEBio software

[117], where the included tetgen function (tetgen.berlio.de) was used to create tetrahedral

meshes for each object. Material properties for the segments were selected from literature

of cadaveric Achilles tendons [119] and have previously been used in FE analysis

[79,118] (Table 5.2). The calcaneus was modeled as a rigid body. An additional rigid

body segment was created and attached to the proximal surface of the Achilles tendon,

emulating a clamp, similar to what may be used in cadaveric studies [120]. This proximal

rigid body was created to apply rotations and Achilles tendon force to the proximal area

of the Achilles tendon.

Table 5.2. Model and material properties for the Achilles and calcaneus segments. Elements, faces, and nodes of the Achilles tendon segment are presented as mean ± standard deviation of each subjects' individual model.

Calcaneus Young's Modulus	7300
Calcaneus Poisson's Ratio	0.3
Calcaneus Material	Rigid Body
Achilles Tendon Young's Modulus (MPa)	819
Achilles Tendon Poisson's Ratio	0.4
Achilles Tendon Material	Neo-Hookean
Elements	4159 ± 778
Faces	2830 ± 525
Nodes	1445 ± 254

The boundary conditions for the model were assigned based on the calculated

global rearfoot and shank rotations, and Achilles tendon force. The three-dimensional

rotation angles of the calcaneus segment (rearfoot), shank tracking system rotations, and

Achilles tendon force at peak eversion and peak Achilles tendon force were used to

simulate Achilles tendon stress at these two time points. The displacement in the x-y-z

directions of the calcaneus were fixed, as well as the x-y displacements of the proximal

rigid body. The z-displacement of the proximal rigid body was left free to allow for the

tendon to exhibit stretch, as the gastrocnemius and soleus muscles would typically

contract during stance, during the simulation. Data to define the motion of the Achilles

tendon was not collected, and an assumption was made that the Achilles tendon rotation

would follow that of an assumed rigid body shank segment. Therefore, three-dimensional

rotation of the shank tracking system was used to define the rotation of the proximal rigid

body fixed to the proximal surface of the Achilles tendon. In addition, Achilles tendon

force was applied as a z-force to the proximal rigid body.

The area of peak von Mises stress was extracted from the simulation results. Only the area from 2 – 6 cm from the distal Achilles tendon insertion was considered, as this area of tendon has been found to be the area of tendon that is most frequently injured [33]. The width and length location of the peak stress area was measured from the lateral edge of the tendon and from the bottom of the insertion. The measured length and width were normalized to tendon length and width, with 6 cm from Achilles insertion considered 100% of tendon length. Because the Achilles tendon width is not consistent throughout the length of the tendon, the width of the tendon was measured every centimeter in the range of tendon length from 2 – 6 cm from the distal insertion. The measured width at peak stress was then normalized to the width at the measured section of tendon length, with 0% corresponding to the most lateral edge of the tendon, and 100% corresponding to the most medial edge of the tendon. For example, if peak stress were measured at a tendon length of 5 cm from the insertion, the measured width would be normalized to the width of the tendon at 5 cm. This process was repeated for peak eversion and peak Achilles tendon force time points during stance, for each step rate condition, for each of the six subjects.

Cross Sectional Area Analysis

Cross sectional area of each subjects' Achilles tendon determined from the segmented geometry was used to calculate a second measure of Achilles tendon stress. Achilles tendon stress was calculated using peak Achilles tendon force divided by CSA. Achilles tendon stress was calculated at each centimeter of tendon length from 2 – 6 cm

from the distal insertion. In addition, average CSA was calculated in the range of $2 - 6$ cm from the insertion and used to calculate Achilles tendon stress with average CSA.

Statistical Analysis

Repeated measures analyses of variance (ANOVA) ($\alpha = 0.05$) were used to evaluate differences in Achilles tendon stress, locations of stress, peak Achilles tendon force, peak vertical, propulsive, and braking GRFs, and peak rearfoot angles. If the assumption of sphericity was violated, a Greenhouse-Geisser correction was used. In the case of a significant main effect, a Bonferroni correction was used in *post-hoc* analysis to determine significant differences between conditions. Statistical analyses were performed in SPSS v27 (IBM SPSS Statistics, Chicago, IL).

Results

Kinematic and Kinetic Results

Peak discrete variables are presented in Table 5.3. Peak rearfoot dorsiflexion angle was significantly reduced ($F_{(2, 10)} = 7.25$, $p = 0.011$) in the +5% ($p = 0.018$) and +10% ($p = 0.048$) conditions compared to the preferred condition. There was no significant difference between the +5% and +10% conditions ($p = 0.872$) (Figure 5.2). No significant differences were observed with increasing step rate for peak rearfoot eversion ($F_{(2, 10)} = 2.62$, $p = 0.121$) (Figure 5.3) or peak tibial internal rotation (rearfoot transverse plane motion) ($F_{(2, 10)} = 1.78$, $p = 0.219$).

Table 5.3. Average (n = 6) peak rearfoot angles (degrees), peak tibial internal rotation (degrees), peak Achilles tendon force (BW), peak vertical ground reaction force (GRF), peak propulsive GRF, and peak braking GRF (BW) for the preferred, +5%, and +10% step rate conditions.

	Preferred Step Rate	+5% Step Rate	+10% Step Rate
Peak Dorsiflexion	19.18 ± 4.25	17.23 ± 5.11*	17.16 ± 5.79*
Peak Eversion	9.92 ± 2.38	8.59 ± 3.49	6.84 ± 5.44
Peak Internal Rotation	7.82 ± 7.45	4.33 ± 9.93	7.39 ± 6.58
Peak Achilles Tendon Force	5.59 ± 1.07	5.63 ± 1.12	5.54 ± 1.20
Peak Vertical GRF	2.60 ± 0.23	2.68 ± 0.24	2.67 ± 0.27
Peak Propulsive GRF	0.26 ± 0.03	0.27 ± 0.04	0.27 ± 0.05
Peak Braking GRF	0.31 ± 0.07	0.30 ± 0.05	0.30 ± 0.05

* indicates significant difference from the preferred condition; [#] indicates significant difference from the +5% condition ($p < 0.05$).
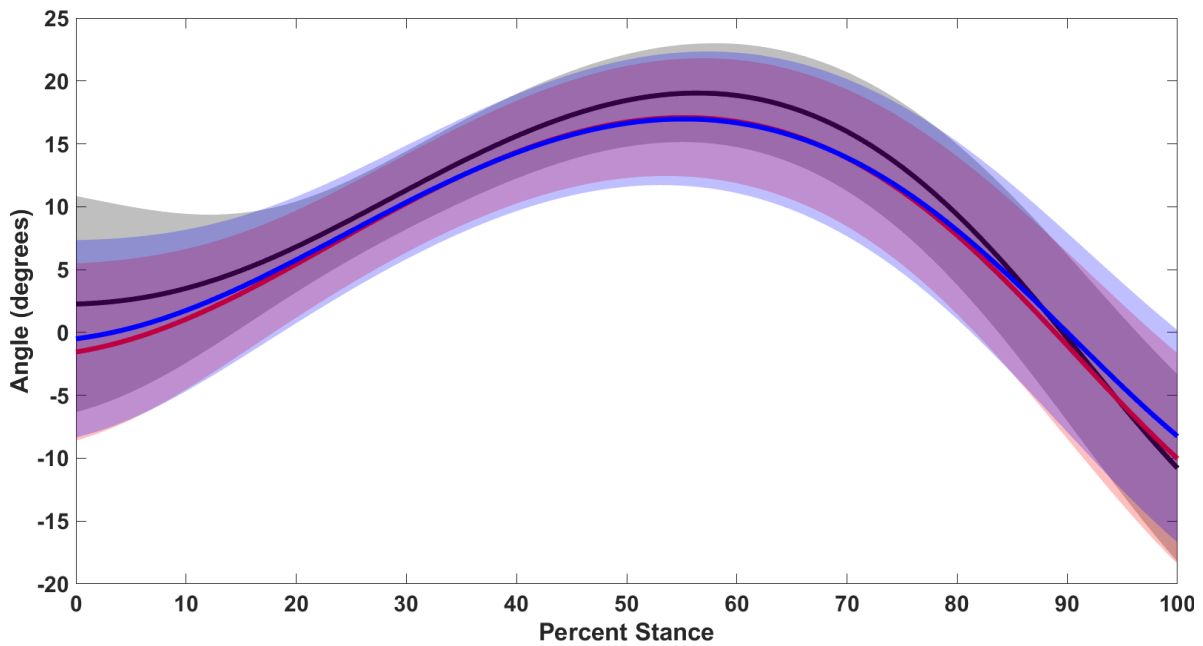
Figure 5.2. Average rearfoot sagittal plane angle across stance phase (solid) ± standard deviation (shaded). Preferred condition displayed in black, +5% in red, and +10% in blue. Dorsiflexion (+), Plantarflexion (-).
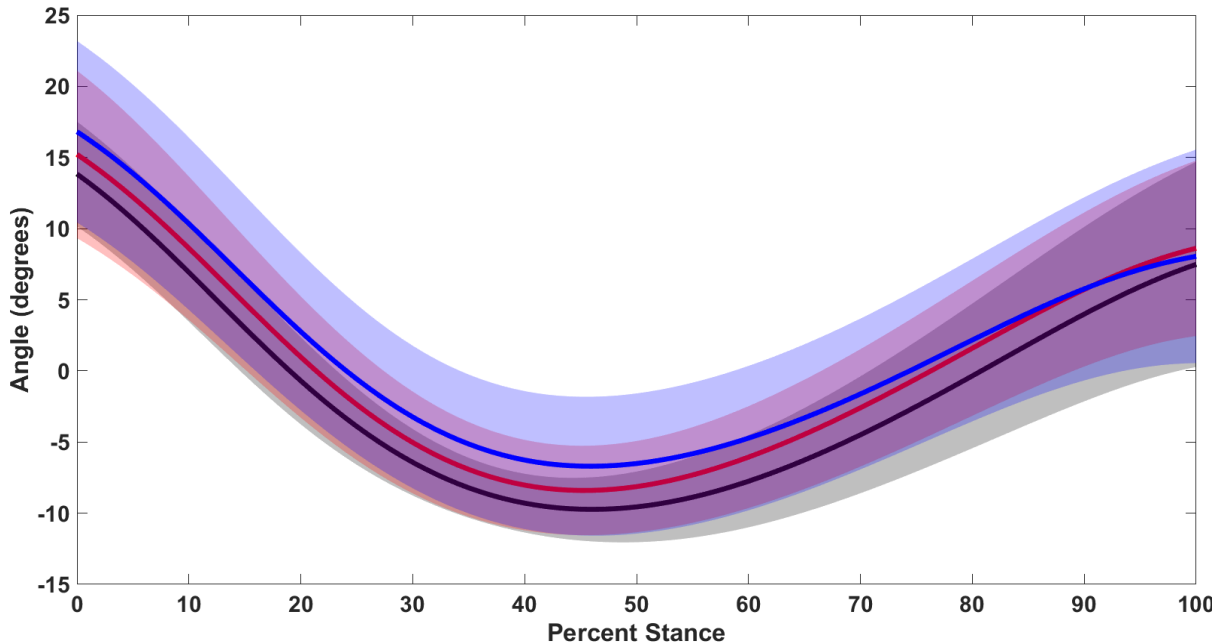
Figure 5.3. Average rearfoot frontal plane angle across stance phase (solid) ± standard deviation (shaded). Preferred condition displayed in black, +5% in red, +10% in blue. Inversion (+), Eversion (-).

Peak Achilles tendon force was also not significantly different between step rate conditions ($F_{(1.09, 5.44)} = 0.20$, $p = 0.822$). No significant differences were observed for any peak GRF variables between conditions ($p > 0.05$).

Finite Element Analysis Results

Finite element analysis results revealed no significant differences in Achilles tendon stress with increased step rate at peak eversion ($F_{(1.10, 5.51)} = 1.26$, $p = 0.315$) or peak Achilles tendon force ($F_{(1.05, 5.25)} = 1.17$, $p = 0.330$) (Table 5.4). Similarly, no significant differences were observed in locations of peak stress for either time point ($p > 0.05$). Individual subject peak Achilles tendon stress responses to increased step rate conditions are displayed in Figure 5.4.

Table 5.4. Average (n = 6) peak Achilles tendon stress at peak eversion and peak tendon force, and width and length locations (% of tendon length) of peak stress from finite element analysis.

	Preferred Step Rate	**+5% Step Rate**	**+10% Step Rate**
Peak Stress at Peak Eversion	71.19 ± 21.33	77.47 ± 17.25	81.51 ± 16.98
Width Location at Peak Eversion	78.64 ± 14.84	71.71 ± 13.74	74.50 ± 10.58
Length Location at Peak Eversion	51.02 ± 8.61	50.46 ± 6.82	52.62 ± 5.95
Peak Stress at Peak Force	75.17 ± 19.86	81.25 ± 16.84	83.40 ± 18.31
Width Location at Peak Force	77.21 ± 16.44	77.24 ± 16.67	74.24 ± 12.43
Length Location at Peak Force	48.44 ± 5.36	48.25 ± 9.81	51.29 ± 6.79

* indicates significant difference from the preferred condition; [#] indicates significant difference from the +5% condition ($p < 0.05$). Width and length locations given as % of tendon length, with 0% = 0 cm at insertion of Achilles tendon on calcaneus, and 100% = 6 cm from Achilles tendon insertion. Width values are with respect to tendon width at the measured tendon length, with 0% = most lateral edge of tendon, and 100% = most medial edge of tendon at given length.

Cross Sectional Area Analysis Results

Using CSA to calculate Achilles tendon stress revealed no significant differences between step rate conditions at any length of the tendon ($p > 0.05$) (Table 5.5) (Figure 5.5). In addition, Achilles tendon stress calculated using average CSA between 2 – 6 cm of tendon length (from the Achilles tendon insertion) did not reveal any significant differences between step rate conditions.
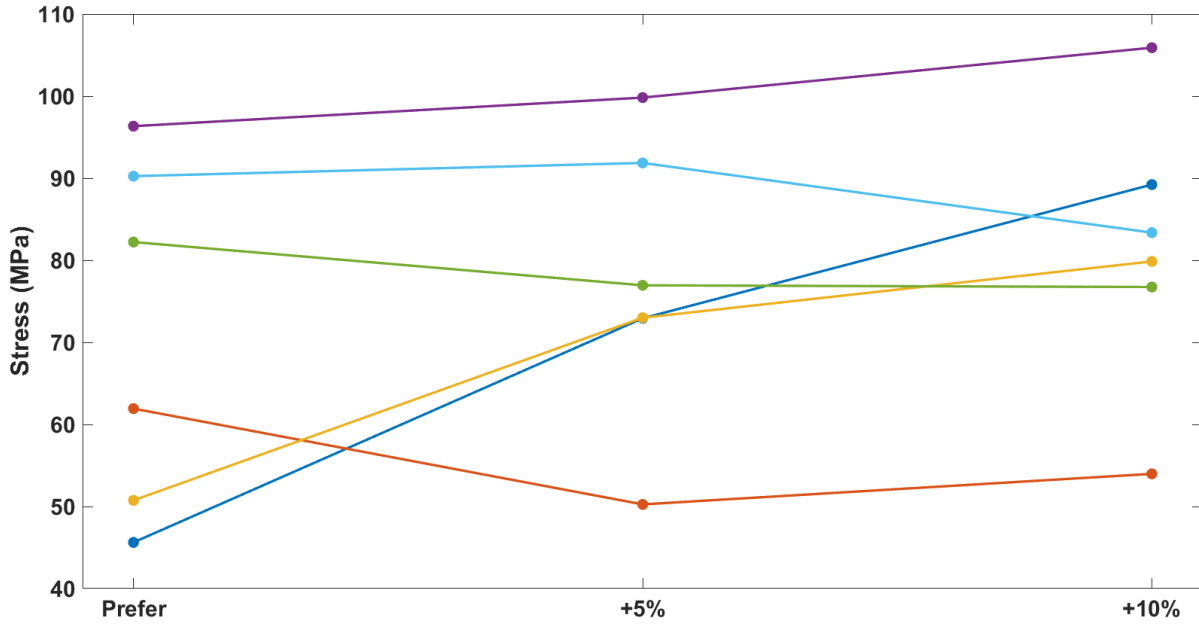
Figure 5.4. Individual subject peak Achilles tendon stress (MPa) in the preferred, +5%, and +10% step rate conditions calculated from finite element analysis, at time of peak eversion.
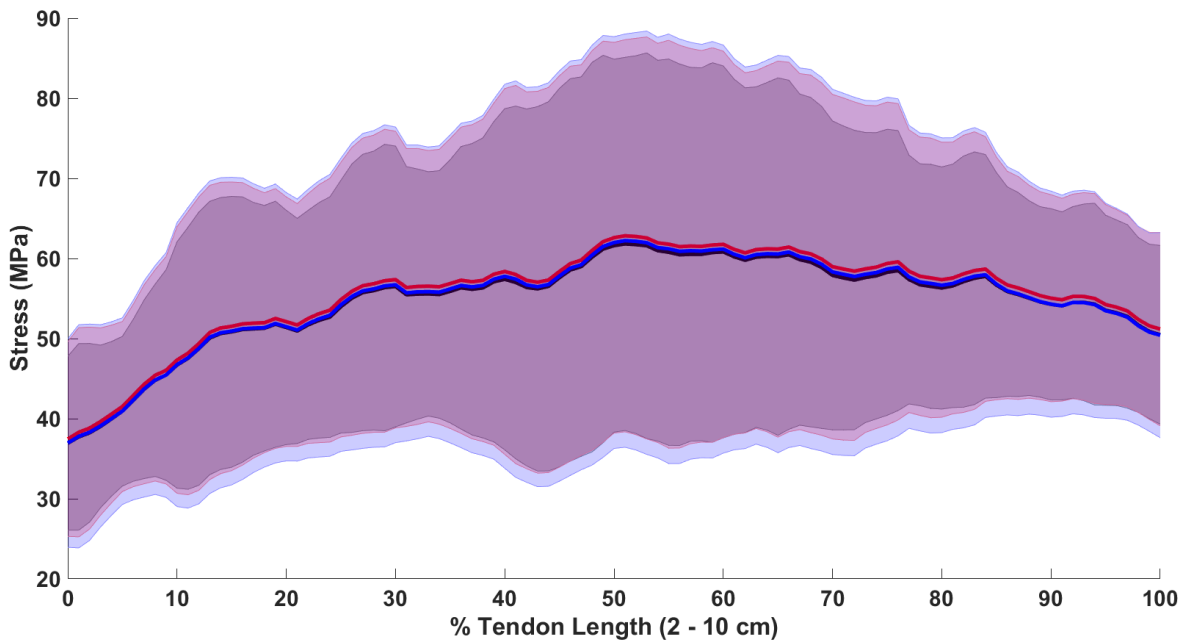
Figure 5.5. Average Achilles tendon stress (solid) ± standard deviation (shaded) across length of tendon from 2 – 10 cm from distal tendon insertion, as percentage of tendon length. Preferred condition displayed in black, +5% in red, +10% in blue.

Table 5.5. Average (n = 6) Achilles tendon stress (MPa) calculated at cross sectional areas (CSA) from 2 – 6 cm, measured from the distal Achilles tendon insertion, and calculated from average cross sectional area (Avg CSA) for 2 – 6 cm for the preferred, +5%, and +10% step rate conditions, and cross sectional area (mm^2) at each interval.

|	CSA	Preferred Step Rate	+5% Step Rate	+10% Step Rate
2 cm	92.99 ± 18.51	36.94 ± 10.85	37.43 ± 12.19	36.96 ± 13.02
3 cm	71.49 ± 17.63	49.37 ± 17.22	50.13 ± 18.64	49.77 ± 19.54
4 cm	65.50 ± 19.92	54.07 ± 15.85	54.95 ± 17.29	54.56 ± 18.18
5 cm	63.68 ± 20.27	56.35 ± 18.41	57.29 ± 19.88	56.88 ± 20.70
6 cm	60.03 ± 20.19	61.09 ± 23.25	61.97 ± 24.15	61.59± 25.18
Avg CSA	63.68 ± 20.59	56.61 ± 19.09	57.50 ± 20.29	56.88 ± 21.51

* indicates significant difference from the preferred condition; # indicates significant difference from the +5% condition ($p < 0.05$).

Discussion

The purpose of this study was to evaluate the effects of increasing step rate during running on Achilles tendon stress in runners with current Achilles tendon pain using subject-specific FE models and measured CSA. Increasing step rate did not have any significant effect on altering Achilles tendon stress in this group of injured runners in either the FE or CSA analysis. The FE analysis revealed no significant differences in peak Achilles tendon stress at the time points of peak eversion and peak Achilles tendon force, and there were no significant differences in the area of peak stress at either time point. Although non-significant, on average, peak Achilles tendon stress showed a trend to increase with the increased step rate conditions. This was unexpected, as a previous study reported a decrease in Achilles tendon stress with a 5% increase in step rate [75]. Similar results were observed in the CSA analysis, with either slight increases in Achilles tendon stress, or little change in stress, between the preferred and increased step rate conditions. However, peak Achilles tendon stress levels were higher in the FE analysis compared to all tendon locations in the CSA analysis. Other studies using methods of

CSA and Achilles tendon force analysis, similar to the CSA analysis in the present study, have reported values of peak Achilles tendon stress near 57 – 97 MPa [75,77,154,158]. The results from the present CSA analysis fit well within this range, and although on the higher end, the FE results are also in this range.

Individual subject responses did not show a consistent trend of increasing with the increased step rate conditions. Two subjects displayed approximately 95% and 57% increases in peak Achilles tendon stress from the preferred to +10% step rate conditions, with one other subject showing a 9% increase from the preferred to +10% step rate condition. The remaining three subjects all showed decreases in Achilles tendon stress from the preferred to +10% conditions ranging from 6 – 12%. It is unknown if the large increases in Achilles tendon stress observed from two of the subjects are accurate representations of changes in Achilles tendon stress with step rate, as these same subjects did not display the same patterns in stress with increased step rate in the CSA analysis. In the CSA analysis, one of these subjects displayed a 15% decrease in Achilles tendon stress with the increased step rate, and the other showed only a 10% increase in Achilles tendon stress with increased step rate. For the remaining subjects, the same trends in either increasing or decreasing Achilles tendon stress with increased step rate were observed; however, the percent changes were less pronounced. For example, the three subjects who displayed decreases in Achilles tendon stress with increased step rate in the FE analysis only showed decreases of 0.76 – 3.5% in the CSA analysis, as opposed to a 6 – 12% decrease.

Larger changes in Achilles tendon stress and higher values of stress observed in FE analysis could be a result of including rotational elements into the model. It has

previously been noted that Achilles tendon stress may be affected by calcaneal angle [76], which could indicate how including the movement of components attached to the Achilles tendon contribute to stress in the tendon. The present model included rotational components at both the distal and proximal ends of the tendon. However, the proximal rotations may not have been representative of how the Achilles tendon moves during running, as it was assumed rotation of the tendon would follow that of a rigid body shank segment. Another factor which could contribute to the values observed in this study is the vertical displacement of the proximal portion of the tendon. The vertical displacement of the rigid body attached to the proximal surface of the tendon was left free to allow the tendon to stretch as it would with muscular contraction from the triceps surae muscle group. Previous research has reported Achilles tendon displacement during the first half of stance during running to be approximately 6 mm [121]. The vertical displacement of the nodes near the proximal portion of the Achilles tendon in this model showed an average displacement of approximately 5.7 mm, which generally agrees with the findings from Farris and colleagues. However, this displacement may not have truly represented stretch and displacement in the tendon, so the accuracy of this component of the model is unknown. In addition, the x and y displacement components of the proximal rigid body and the calcaneus were fixed, and this could also restrict the naturally occurring tendon stretch and movement.

Achilles tendon stress was observed to increase with decreasing CSA, as would be expected [161]. The smallest CSA, and corresponding region with largest stress, was found to be around 6 cm of tendon length from the distal insertion, which previous literature has reported as the narrowest portion of the Achilles tendon [169]. The location

of peak stress observed in the FE analysis tended to be more distal on the tendon, with an average location corresponding to near 3 cm of tendon length from the distal insertion. In addition, the average width location placed peak Achilles tendon stress between the center and medial side of the tendon. Previous research has indicated the area most common to Achilles tendon injuries is in the range of 2 – 6 cm of tendon length from the distal insertion, agreeing with the findings in this study. Unfortunately, no previous literature reports the width location of peak Achilles tendon stress, so the present values are not able to be compared with previous findings.

Peak dorsiflexion angle was observed to significantly decrease with increasing step rate. This finding agrees well with previous literature as a 10% increase in step rate has been reported to decrease peak ankle dorsiflexion by 2 – 2.5 degrees compared to preferred step rate [132,139,140], which is similar to the present results. A significant decrease in peak eversion was not found in this sample of runners; however, on average, peak eversion decreased from the preferred to +10% condition by nearly 3 degrees. Previous research has also shown a trend for decreasing peak eversion [70,141], or a significant decrease [160], with an increase in step rate. The sample size of the present study was small, and while some subjects displayed marked decreases in peak eversion with the increased step rate conditions, one showed little change, and another showed a slight increase, making it difficult to observe significant differences overall.

Unexpectedly, no significant differences were observed in any GRF variables, or peak Achilles tendon force with increased step rate. Previous investigations evaluating GRF variables with step rate interventions have found decreases in peak vertical GRF between 2.6 – 3.5% [139,144,160] and decreases in peak braking forces between 5.5 –

88

9% with increased step rate [139,145,160]. Although non-significant, in the present study peak vertical GRF and peak propulsive GRF were found to increase by approximately 3%, while peak braking GRF decreased near 3%. Similar to the previous observations in this study, individual subject responses were variable and did not follow a systematic trend. Peak Achilles tendon force was not significantly different between conditions, with a slight increase from preferred observed in the +5% condition, and slight decrease in the +10% condition. One study reported a decrease in Achilles tendon force with a 5% increase in step rate [75]. Although not manipulating step rate directly, a previous investigation into differences between overground and treadmill running found increased step rates when running on a treadmill in tandem with an increased Achilles tendon force in treadmill running [170]. The results from the present study cannot confirm or refute either of these previous investigations, as we observed both an increase and decrease in peak Achilles tendon force, depending on the percentage increase in step rate, and neither change was significant. Other investigations have evaluated changes in foot strike pattern from a rearfoot strike to a forefoot strike on Achilles tendon force, and have found a forefoot strike pattern tends to increase Achilles tendon force [75,108,154,157,158]. Forefoot strike patterns have been shown to decrease step length, thereby increasing step rate [171,172], and therefore, it is feasible that an intervention aimed at increasing step rate may increase Achilles tendon force if runners were to switch to a forefoot strike pattern.

Limitations

This study had many limitations that make drawing conclusions from the present results difficult. In addition to those mentioned previously throughout the discussion, the model created for the FE analysis likely did not have the appropriate boundary conditions to fully capture Achilles tendon stress during running. Taking measures of Achilles tendon motion, either using dynamic ultrasound or tracking surface markers on the tendon for motion capture, would make the model more mimetic of anatomical function. This model also did not consider the Achilles sub-tendons and how force may not be applied uniformly through the tendon as a result of the twisted tendon structure [27,165]. The Achilles was modeled using a neo-Hookean material, consistent throughout the length of the tendon, but tendon material properties may differ throughout its length [119,166]. The Achilles tendon moment arm was estimated using a standard equation; however, it may not represent the actual Achilles tendon moment arm for the individuals in this study. The Achilles tendon force was also assumed to be represented by the estimated moment arm and plantar flexor moment, and did not consider how antagonistic co-contraction may affect Achilles tendon force [167]. Finally, this study had a small sample size (n=6), with recruitment restricted to runners who had a current mid-portion Achilles tendon injury. The scope of recruitment was further restricted due to the cost of providing an MRI for each subject, and the time needed to create individual models for each subject. The small sample made observing real chang9es in the group data difficult, as one subject's data could have greater effects on swaying the results.

Conclusion

The results from this study do not lead to a clear conclusion regarding how increasing step rate affects Achilles tendon stress in runners with Achilles tendon injury. On average, Achilles tendon stress was increased with increased step rate; however, subject-specific responses offered a less clear picture, as not all subjects showed an increase in stress with increased step rate. In addition, no significant differences in Achilles tendon stress were observed between step rate conditions using FE analysis with subject-specific models, or CSA analysis. A larger sample size, and a FE model with more realistic boundary conditions should enable a better picture of how the Achilles tendon is affected by increasing step rate, but at this time, it is still unclear how increasing step rate affects Achilles tendon stress.

CHAPTER VI

CONCLUSION

Summary of Results and Findings

This dissertation sought to further explore the relationship between rearfoot kinematics, Achilles tendon stress, and step rate modifications during running in both healthy and injured runners. Previous research has indicated a potential mechanism for development of Achilles tendinopathy to be the coupled actions of rearfoot eversion and tibial rotation, which could cause damage to the tendinous structure with repeated cyclical loading and inadequate recovery time [16]. With the advent and popularity of gait retraining in the rehabilitation, or possible injury prevention, of other RRIs, a need arose to explore the use of gait retraining as a possible tool to decrease risk or aid in recovery of Achilles tendon overuse injuries in runners. Increasing step rate was chosen as a gait retraining intervention to explore because it is easy to implement, affects kinematic and kinetic changes throughout the lower limbs, and has preliminarily been shown to decrease stress in the Achilles tendon [75]. Previously, there was little research available regarding how changes in step rate affect non-sagittal plane motion at the rearfoot. In addition, Achilles tendon stress has primarily been calculated using methods of cross sectional area and Achilles tendon force, neglecting other possible contributors to stress in the tendon, such as rotational elements from proximal and distal components attached to the tendon. To address these gaps, a simple step rate protocol was used to test the acute effects of increasing step rate on rearfoot kinematics in healthy runners. These data were then used in a generic finite element model which employed proximal and distal kinematics of the structures attached to the Achilles tendon to evaluate stress in the

92

Achilles tendon with the increased step rate conditions. Finally, subject-specific models were created for runners with current Achilles tendon pain to assess the effects of increased step rate on Achilles tendon stress in injured runners.

Chapter III revealed increasing step rate significantly decreased peak rearfoot sagittal and frontal plane angles, and peak tibial internal rotation angle. In addition, peak vertical ground reaction force and braking force were significantly reduced, confirming our hypotheses. The results from this study agreed with previous research, which has shown increasing step rate significantly decreases peak dorsiflexion angle and peak ground reaction forces during stance [53,132,139,140,144,145]. Previous research has shown inconclusive results for the effects of increasing step rate on frontal plane rearfoot motion, with non-significant decreases in rearfoot eversion observed [70]. In addition, there has previously been few studies evaluating tibial rotation with increasing step rate protocols. The results from the present study filled the gap for this previously lacking data regarding non-sagittal plane rearfoot motion, and tibial rotation, alterations in response to increased step rate. These findings support further exploring if increasing step rate affects Achilles tendon stress, as peak ground reaction forces and rearfoot angles were significantly reduced.

Chapter IV utilized a finite element model created from a healthy, active 30-year-old male subject to use with the kinematic and kinetic data collected in Chapter III to estimate stress in the Achilles tendon under different step rate conditions. The results from this study were conflicting, as the finite element model analysis showed an increase in stress in the Achilles tendon with an increase in step rate, but the cross sectional area analysis showed decreases in Achilles tendon stress with the increased step rate

conditions. Peak stress in the Achilles tendon region from 2 – 6 cm from the tendon insertion ranged from approximately 76 – 81 MPa in the finite element analysis. Previous research evaluating Achilles tendon stress during hopping using a finite element approach found peak Achilles tendon stress values near 50 MPa [80]. However, the cross sectional area analysis approach revealed peak Achilles tendon stress to be in the range from approximately 37 – 65 MPa, aligning better with previous research. Previous investigations using a similar method with cross sectional area to estimate Achilles tendon stress have found peak stress values near 57 – 97 MPa during running [75,77,158]. These previous investigations using cross sectional area and Achilles tendon force to estimate Achilles tendon stress also align better with the findings for peak stress from the finite element analysis in the present study.

The finite element model may have been under constrained to fully represent how the Achilles tendon would behave, and the model was non-subject-specific, leading to possible inaccuracy. Although the cross sectional area analysis showed a decrease in stress with increased step rate, the cross sectional area used was also not specific to each subject and did not account for contributors to stress other than Achilles tendon force. There were also no significant changes observed in the location of peak stress with the increase in step rate in the finite element analysis. Although non-significant, there did appear to be a shift of the location of peak Achilles tendon stress from the medial side of the tendon towards the center of the tendon with the increased step rate conditions, adding support to previous research which has shown changing calcaneus angle from an everted to inverted position shifts Achilles tendon strain from the medial to lateral side [76]. We had hypothesized if there were alterations in rearfoot kinematics, the location of

stress within the Achilles tendon would be modified. This hypothesis was not supported, as the location of peak stress within the tendon remained relatively unchanged.

Finally, Chapter V combined methods from Chapters III and IV, but recruited runners with current Achilles tendon pain, and created finite element models specific to each subject. The results from this study revealed non-significant increases in Achilles tendon stress, or no change in stress, with the increased step rate conditions. Although the finite element model and the cross sectional areas used were specific to each subject, there was a fair amount of subject variability. While some subjects did increase Achilles tendon stress with increased step rate, others displayed decreases in stress, and these changes were inconsistent between the finite element results and cross sectional area results. Compared to the results from Chapter IV, peak Achilles tendon stress was similar, with values between 71 – 83 MPa, where values in Chapter IV were near 76 – 81 MPa. Peak stress values from cross sectional area analysis were also similar between the two investigations, with values in Chapter V between 36 – 62 MPa, compared to 37 – 65 MPa. Despite using subject specific models in the present study, peak Achilles tendon stress values from both finite element analysis and cross sectional area analysis were similar to the results from using a generic model.

Although the slight increase in Achilles tendon stress with increased step rate, or no change in stress, was unexpected, it could be due to the small sample of runners used, and the need to better constrain the finite element model to represent dynamic tendon motion. However, these results may highlight the necessity for subject-specific rehabilitation protocols, as some runners may benefit from an increased step rate program, while others may find it more detrimental to Achilles tendon health. In addition,

no significant changes were observed in the location of peak Achilles tendon stress in the finite element model with the increase in step rate.

Taken together, the results from this dissertation revealed increasing step rate successfully alters rearfoot kinematics during running. Although the decrease in peak eversion observed in the sample of runners from Chapter V was non-significant, there was an overall larger change in peak eversion angle in the injured runners compared to the significant decrease in peak eversion angle observed in the healthy runner sample in Chapter III. Although kinematics appear to be successfully modified, the results regarding Achilles tendon stress are less clear. An under constrained finite element model in both Chapter IV and V may have contributed to increases in peak Achilles tendon stress with increased step rate, although not significantly. Cross sectional area analysis also delivered contradictory findings between studies. Chapter IV results displayed decreases in peak Achilles tendon stress using cross sectional area and Achilles tendon force with increased step rate, while Chapter V echoed the findings of the finite element analysis for an increase in stress with increased step rate. It is challenging to determine how best to interpret these findings, as the finite element analysis in Chapter IV suffered from non-subject specificity, and the Chapter V analysis was influenced by great variation between subject responses. At present, a recommendation for increasing step rate as a tool to decrease risk for Achilles tendon injury, or rehabilitation from injury, cannot be provided with confidence. However, these findings do highlight the need to further explore subject-specific responses to increased step rate on Achilles tendon stress, especially in runners with current Achilles tendon injury. While the healthy runners in Chapter III primarily decreased Achilles tendon loads with the increased step rate

conditions, the runners with Achilles tendon injury in Chapter V had a more varied response. This finding could point to avenues to explore for why some runners may be more susceptible to Achilles tendon injury than others.

Limitations

  This dissertation experienced limitations that likely confounded the observed results. Beginning with Chapter III, a major limiting factor in this study and its applicability was not screening for runners who had a lower starting step rate. The runners in this sample had average step rates, with some runner's 10% increase in step rates being higher than would be feasible for normal, daily running. Many of the significant changes observed in this study occurred at the +10% step rate, and therefore may not be realistic to interpret, as these step rates would not likely be adopted, or recommended, for these runners. This limitation may mask applicability from this study and recruiting runners with lower step rates could have been more beneficial for making recommendations to clinicians or runners about the utility of increasing step rate to alter rearfoot kinematics.

  In Chapters IV and V, the main limitations relate to the finite element model. First, the model was simplified to only included the calcaneus and Achilles tendon. Muscles surrounding the tendon, namely the triceps surae muscle group, influence the lengthening of the Achilles tendon. In addition, adding other structures to the model could enable a more holistic picture of a full foot strike during running, and allow for other motion and forces to be included. The model was further simplified to not include the Achilles sub-tendons, which may result in force not being applied uniformly through

97

the tendon, nor does it consider that sliding between Achilles sub-tendons could contribute to stress in the tendon. Additionally, the Achilles tendon material properties were simplified. A single material was used to represent the entire length of the tendon; but the Achilles tendon may be anisotropic and display varying material properties from the distal to proximal end.

Further, calculation of the Achilles tendon moment arm was done through a regression equation, which may not represent the true moment arm for individual subjects. The Achilles tendon force was calculated using this moment arm and the plantar flexor moment. This force was assumed to represent Achilles tendon force and did not take into account potential antagonistic co-contraction. In addition, this force was assumed to fully transmit to the Achilles tendon, but other structures surrounding the tendon could either contribute to or offload some of this force. Finally, only two time points were analyzed in the finite element model. The complexity of the running motion made it difficult to represent a full stance phase during running, and therefore only the time points of peak eversion and peak Achilles tendon force were analyzed.

The boundary conditions prescribed for the finite element model were simplified to allow the model to converge. Displacements of the calcaneus in the x-y-z directions were fixed, and only rotations considered. The proximal rigid object was a major limitation to the study, as this does not accurately represent a normal attachment of the proximal Achilles tendon. This rigid object was included to prescribe proximal rotations to the model, and for uniform proximal application of the Achilles tendon force. The rotations of the proximal object were given those of the shank segment as it was assumed the tendon would move with the entire shank rigid body segment. This may not

adequately represent how the Achilles tendon moves naturally. The x-y displacements of the proximal object were fixed, but the z-displacement was given a fixed value of 6 mm, based on previous literature evaluating Achilles tendon displacement during the stance phase of running [121]. However, this displacement was not specific to each subject. In Chapter V, this displacement was left free to allow for tendon lengthening based on the subject-specific model and individual kinematics, but this may also not have been representative of true tendon motion.

Limitations specific to Chapter IV included the use of a non-subject specific model and cross-sectional area. The goal of this chapter was to provide a general view of how a group of healthy runners' Achilles tendon stress responded to increases in step rate; however, not using models specific to each subject may provide an unrealistic picture. In addition, not using subject-specific cross-sectional area sheds little light on how an individual subject may respond to the changing step rate conditions and relies only on the calculated Achilles tendon force to show differences.

In Chapter V, many of the same limitations discussed previously were still present. The subjects in this study self-reported their Achilles tendon pain, and only one had received a clinical diagnosis from a previous MRI scan. The extent of Achilles tendon injury in these subjects is therefore unknown and may have influenced the results. The MRI protocol position each subject's ankle in a neutral, unweighted position, and although this is common to MRI protocols, it could have made the models appear to have more plantar flexion. Taking more MRI images of subjects' ankles in a variety of positions could have allowed for moment arms to be measured for each subject based on

ankle angle, giving a more accurate value to use for each subject's Achilles tendon moment arm.

Limitations pertinent to all the data collected in this study relate to the running protocol being performed on the treadmill. There may be kinematic and kinetic differences between overground and treadmill running, reducing the translation of these results to overground running. In addition, running on treadmills may inflate step rate, and causing subjects' preferred step rate to be higher than normal, and may have elevated the calculations for the increased step rate conditions. Finally, this study evaluated the variables in an acute response to increasing step rate. It is unknown if these findings would be observed over a long-term intervention.

Recommendations for Future Work

This dissertation opens avenues for many different research paths. Using step rate as an intervention in Achilles tendon injuries has been largely unexplored, and there is a need for alternate avenues of rehabilitation, and methods to decrease injury risk, for runners with Achilles tendon injuries. Future research should first look to verify the effects of increasing step rate on rearfoot and tibial motion. It would be sensible to recruit subjects with lower step rates, as these runners may experience the most benefit, and display greater effects, to an increased step rate protocol. Long term interventions are also needed to assess if changes in kinematics or kinetics stand over time. If long term interventions are employed, measures of Achilles tendon morphological properties and strength should be taken, as these would help determine if positive adaptations can occur

to the Achilles tendon structure with increased step rate. Future studies should also perform protocols overground to increase applicability to more runners.

Future work in the finite element space is needed, as this method can allow for a more robust picture of stress in the Achilles tendon and where this stress is occurring. This method also allows for many different boundary conditions to be applied to represent contributors to stress in the tendon. The current model was likely under constrained and was not able to fully represent Achilles tendon motion during running. Further developing the model to allow a more realistic representation of tendon motion will greatly advance conclusions that can be drawn from a similar study. This could be done by collecting data of the Achilles tendon displacement during running, through ultrasound or placing markers directly on the tendon for motion capture. Adding a better option for a proximal attachment of the Achilles tendon in the FE model is likely also needed to allow for Achilles tendon force and proximal motion to be described thoroughly. Finally, adding more segments to the model, such as the tibia and other foot bones, is likely necessary to allow for displacement of segments and other forces to be fully depicted.

Improving the calculation of Achilles tendon force, using electromyography and musculoskeletal models, could improve the accuracy of the Achilles tendon force. This would also eliminate the need to use the Achilles tendon moment arm for deriving the Achilles tendon force. Prescribing more appropriate material properties to the Achilles tendon to better represent its function is paramount and adding the Achilles sub-tendons would greatly improve the strength of the model.

Finally, including more runners with Achilles tendon injuries to test the effects of increasing step rate on Achilles tendon stress is needed, as the small sample used in the present study did not allow for conclusions to be drawn. In addition, recruiting runners with diagnosed Achilles tendon injury, rather than self-reported pain, could decrease variability in the sample. Pursuing these future research areas will allow for recommendations to be made regarding the practicality of using a step rate intervention in the treatment of runners with Achilles tendinopathy, or a way to decrease the risk of Achilles tendon injury.

REFERENCES CITED

1.   van Gent, R.N.; Siem, D.; van Middelkoop, M.; van Os, A.G.; Bierma-Zeinstra, S.M.A.; Koes, B.W.; Taunton, J.E. Incidence and Determinants of Lower Extremity Running Injuries in Long Distance Runners: A Systematic Review. *British Journal of Sports Medicine* **2007**, *41*, 469–480, doi:10.1136/bjsm.2006.033548.

2.   van der Worp, M.P.; ten Haaf, D.S.M.; van Cingel, R.; de Wijer, A.; Nijhuis-van der Sanden, M.W.G.; Staal, J.B. Injuries in Runners; A Systematic Review on Risk Factors and Sex Differences. *PLoS ONE* **2015**, *10*, e0114937, doi:10.1371/journal.pone.0114937.

3.   Hollander, K.; Johnson, C.D.; Outerleys, J.; Davis, I.S. Multifactorial Determinants of Running Injury Locations in 550 Injured Recreational Runners. *Medicine & Science in Sports & Exercise* **2021**, *53*, 102–107, doi:10.1249/MSS.0000000000002455.

4.   Taunton, J.E. A Retrospective Case-Control Analysis of 2002 Running Injuries. *British Journal of Sports Medicine* **2002**, *36*, 95–101, doi:10.1136/bjsm.36.2.95.

5.   Davis, I. Optimising the Efficacy of Gait Retraining. *British Journal of Sports Medicine* **2018**, *52*, 624–625, doi:10.1136/bjsports-2017-098297.

6.   Willy, R.W.; Scholz, J.P.; Davis, I.S. Mirror Gait Retraining for the Treatment of Patellofemoral Pain in Female Runners. *Clinical Biomechanics* **2012**, *27*, 1045–1051, doi:10.1016/j.clinbiomech.2012.07.011.

7.   Crowell, H.P.; Milner, C.E.; Hamill, J.; Davis, I.S. Reducing Impact Loading During Running With the Use of Real-Time Visual Feedback. *Journal of Orthopaedic & Sports Physical Therapy* **2010**, *40*, 206–213, doi:10.2519/jospt.2010.3166.

8.   Hunter, L.; Louw, Q.A.; van Niekerk, S.-M. Effect of Running Retraining on Pain, Function, and Lower-Extremity Biomechanics in a Female Runner With Iliotibial Band Syndrome. *Journal of Sport Rehabilitation* **2014**, *23*, 145–157, doi:10.1123/JSR.2013-0024.

9.   Noehren, B.; Scholz, J.; Davis, I. The Effect of Real-Time Gait Retraining on Hip Kinematics, Pain and Function in Subjects with Patellofemoral Pain Syndrome. *British Journal of Sports Medicine* **2011**, *45*, 691–696, doi:10.1136/bjsm.2009.069112.

10.   Allen, D.J. Treatment of Distal Iliotibial Band Syndrome in a Long Distance Runner with Gait Retraining Emphasizing Step Rate Manipulation. *International Journal of Sports Physical Therapy* **2014**, *9*, 222–231.

11. Bramah, C.; Preece, S.J.; Gill, N.; Herrington, L. A 10% Increase in Step Rate Improves Running Kinematics and Clinical Outcomes in Runners With Patellofemoral Pain at 4 Weeks and 3 Months. *The American Journal of Sports Medicine* **2019**, *47*, 3406–3413, doi:10.1177/0363546519879693.

12. Cook, J.L.; Khan, K.M.; Purdam, C. Achilles Tendinopathy. *Manual Therapy* **2002**, *7*, 121–130, doi:10.1054/math.2002.0458.

13. Lagas, I.F.; Fokkema, T.; Verhaar, J.A.N.; Bierma-Zeinstra, S.M.A.; Middelkoop, M. van; de Vos, R.-J. Incidence of Achilles Tendinopathy and Associated Risk Factors in Recreational Runners: A Large Prospective Cohort Study. *Journal of Science and Medicine in Sport* **2020**, *23*, 448–452.

14. Beyer, R.; Kongsgaard, M.; Hougs Kjær, B.; Øhlenschlæger, T.; Kjær, M.; Magnusson, S.P. Heavy Slow Resistance Versus Eccentric Training as Treatment for Achilles Tendinopathy: A Randomized Controlled Trial. *The American Journal of Sports Medicine* **2015**, *43*, 1704–1711, doi:10.1177/0363546515584760.

15. Kujala, U.M.; Sarna, S.; Kaprio, J. Cumulative Incidence of Achilles Tendon Rupture and Tendinopathy in Male Former Elite Athletes. *Clinical Journal of Sport Medicine* **2005**, *15*, 133–135.

16. Clement, D.B.; Taunton, J.E.; Smart, G.W. Achilles Tendinitis and Peritendinitis: Etiology and Treatment. *The American Journal of Sports Medicine* **1984**, *12*, 179–184.

17. Tiberio, D. The Effect of Excessive Subtalar Joint Pronation on Patellofemoral Mechanics: A Theoretical Model. *Journal of Orthopaedic & Sports Physical Therapy* **1987**, *9*, 160–165, doi:10.2519/jospt.1987.9.4.160.

18. Maffulli, N.; Longo, U.G.; Kadakia, A.; Spiezia, F. Achilles Tendinopathy. *Foot and Ankle Surgery* **2020**, *26*, 240–249, doi:10.1016/j.fas.2019.03.009.

19. Gajhede-Knudsen, M.; Ekstrand, J.; Magnusson, H.; Maffulli, N. Recurrence of Achilles Tendon Injuries in Elite Male Football Players Is More Common after Early Return to Play: An 11-Year Follow-up of the UEFA Champions League Injury Study. *British Journal of Sports Medicine* **2013**, *47*, 763–768, doi:10.1136/bjsports-2013-092271.

20. Sayana, M.K.; Maffulli, N. Eccentric Calf Muscle Training in Non-Athletic Patients with Achilles Tendinopathy. *Journal of Science and Medicine in Sport* **2007**, *10*, 52–58, doi:10.1016/j.jsams.2006.05.008.

21.   Komi, P.V. Biomechanical Loading of the Achilles Tendon during Normal Locomotion. *Clinics in Sports Medicine* **1992**, *11*, 521–531.

22.   Ker, R.F.; Bennett, M.B.; Bibby, S.R.; Kester, R.C.; Alexander, R.M. The Spring in the Arch of the Human Foot. *Nature* **1987**, *325*, 147–149, doi:10.1038/325147a0.

23.   Benjamin, M.; Theobald, P.; Suzuki, D.; Toumi, H. The Anatomy of the Achilles Tendon. *The Achilles Tendon* **2007**, *3*, 5–16.

24.   Dalmau-Pastor, M.; Fargues-Polo, B.; Casanova-Martínez, D.; Vega, J.; Golanó, P. Anatomy of the Triceps Surae. *Foot and Ankle Clinics* **2014**, *19*, 603–635, doi:10.1016/j.fcl.2014.08.002.

25.   Pierre-Jerome, C.; Moncayo, V.; Terk, M.R. MRI of the Achilles Tendon: A Comprehensive Review of the Anatomy, Biomechanics, and Imaging of Overuse Tendinopathies. *Acta Radiologica* **2010**, *51*, 438–454, doi:10.3109/02841851003627809.

26.   Sharma, P.; Maffulli, N. Biology of Tendon Injury: Healing, Modeling and Remodeling. *Journal of Musculoskeletal and Neuronal Interaction* **2006**, *6*, 181–190.

27.   Arndt, A.N.; Komi, P.V.; Brüggemann, G.-P.; Lukkariniemi, J. Individual Muscle Contributions to the in Vivo Achilles Tendon Force. *Clinical Biomechanics* **1998**, *13*, 532–541, doi:10.1016/S0268-0033(98)00032-1.

28.   Haglund-Åkerlind, Y.; Eriksson, E. Range of Motion, Muscle Torque and Training Habits in Runners with and without Achilles Tendon Problems. *Knee Surgery, Sports Traumatology, Arthroscopy* **1993**, *1*, 195–199, doi:10.1007/BF01560205.

29.   Mahieu, N.N.; Witvrouw, E.; Stevens, V.; Van Tiggelen, D.; Roget, P. Intrinsic Risk Factors for the Development of Achilles Tendon Overuse Injury: A Prospective Study. *The American Journal of Sports Medicine* **2006**, *34*, 226–235, doi:10.1177/0363546505279918.

30.   Kjaer, M.; Langberg, H.; Heinemeier, K.; Bayer, M.L.; Hansen, M.; Holm, L.; Doessing, S.; Kongsgaard, M.; Krogsgaard, M.R.; Magnusson, S.P. From Mechanical Loading to Collagen Synthesis, Structural Changes and Function in Human Tendon. *Scandinavian Journal of Medicine & Science in Sports* **2009**, *19*, 500–510, doi:10.1111/j.1600-0838.2009.00986.x.

31.   Baxter, J.R.; Corrigan, P.; Hullfish, T.J.; O'Rourke, P.; Silbernagel, K.G. Exercise Progression to Incrementally Load the Achilles Tendon. *Medicine & Science in Sports & Exercise* **2020**, *Publish Ahead of Print*, doi:10.1249/MSS.0000000000002459.

32. Malliaras, P.; Rodriguez Palomino, J.; Barton, C.J. Infographic. Achilles and Patellar Tendinopathy Rehabilitation: Strive to Implement Loading Principles Not Recipes. *Br J Sports Med* **2018**, *52*, 1232–1233, doi:10.1136/bjsports-2017-098615.

33. Silbernagel, K.; Crossley, K.M. A Proposed Return-to-Sport Program for Patients With Midportion Achilles Tendinopathy: Rationale and Implementation. *Journal of Orthopaedic & Sports Physical Therapy* **2015**, *45*, 876–886, doi:10.2519/jospt.2015.5885.

34. Gravare Silbernagel, K.; Thomee, R.; Eriksson, B.I.; Karlsson, J.; Khan, K. Full Symptomatic Recovery Does Not Ensure Full Recovery of Muscle-Tendon Function in Patients with Achilles Tendinopathy * COMMENTARY. *British Journal of Sports Medicine* **2007**, *41*, 276–280, doi:10.1136/bjsm.2006.033464.

35. Silbernagel, K.G.; Brorsson, A.; Lundberg, M. The Majority of Patients With Achilles Tendinopathy Recover Fully When Treated With Exercise Alone: A 5-Year Follow-Up. *The American Journal of Sports Medicine* **2011**, *39*, 607–613, doi:10.1177/0363546510384789.

36. Woodley, B.; Newsham-West, R.; Baxter, G. Chronic Tendinopathy: Effectiveness of Eccentric Exercise. *British Journal of Sports Medicine* **2007**, *41*, 188–198.

37. Alfredson, H.; Pietilä, T.; Öhberg, L.; Lorentzon, R. Achilles Tendinosis and Calf Muscle Strength. *The American Journal of Sports Medicine* **1998**, *26*, 166–171, doi:10.1177/03635465980260020301.

38. Becker, J.; James, S.; Wayner, R.; Osternig, L.; Chou, L.-S. Biomechanical Factors Associated With Achilles Tendinopathy and Medial Tibial Stress Syndrome in Runners. *The American Journal of Sports Medicine* **2017**, *45*, 2614–2621, doi:10.1177/0363546517708193.

39. Donoghue, O.A.; Harrison, A.J.; Laxton, P.; Jones, R.K. Lower Limb Kinematics of Subjects with Chronic Achilles Tendon Injury During Running. *Research in Sports Medicine* **2008**, *16*, 23–38, doi:10.1080/15438620701693231.

40. McCrory, J.L.; Martin, D.F.; Lowery, R.B.; Cannon, W.D.; Curl, W.W.; Read, Jr., H.M.; Hunter, D.M.; Craven, T.; Messier, S.P. Etiologic Factors Associated with Achilles Tendinitis in Runners. *Med Sci Sports Exerc* **1999**, *31*, 1374–1381.

41. Ryan, M.; Grau, S.; Krauss, I.; Maiwald, C.; Taunton, J.; Horstmann, T. Kinematic Analysis of Runners with Achilles Mid-Portion Tendinopathy. *Foot & Ankle International* **2009**, *30*, 1190–1195, doi:10.3113/FAI.2009.1190.

42. Lattanza, L.; Gray, G.W.; Kantner, R.M. Closed Versus Open Kinematic Chain Measurements of Subtalar Joint Eversion: Implications for Clinical Practice. *Journal of Orthopaedic & Sports Physical Therapy* **1988**, *9*, 310–314, doi:10.2519/jospt.1988.9.9.310.

43. Williams, D.S.B.; Zambardino, J.A.; Banning, V.A. Transverse-Plane Mechanics at the Knee and Tibia in Runners With and Without a History of Achilles Tendonopathy. *Journal of Orthopaedic & Sports Physical Therapy* **2008**, *38*, 761–767, doi:10.2519/jospt.2008.2911.

44. Ferber, R.; Hreljac, A.; Kendall, K.D. Suspected Mechanisms in the Cause of Overuse Running Injuries: A Clinical Review. *Sports Health: A Multidisciplinary Approach* **2009**, *1*, 242–246, doi:10.1177/1941738109334272.

45. Knutzen, K.; Price, A. Lower Extremity Static and Dynamic Relationships with Rearfoot Motion in Gait. *Journal of the American Podiatric Medical Association* **1994**, *84*, 171–180, doi:10.7547/87507315-84-4-171.

46. Hughes, P.E.; Hsu, J.C.; Matava, M.J. Hip Anatomy and Biomechanics in the Athlete. *Sports Medicine and Arthroscopy Review* **2002**, *10*, 103–114, doi:10.1097/00132585-200210020-00002.

47. Bellchamber, T.L.; van den Bogert, A.J. Contributions of Proximal and Distal Moments to Axial Tibial Rotation during Walking and Running. *Journal of Biomechanics* **2000**, *33*, 1397–1403, doi:10.1016/S0021-9290(00)00113-5.

48. Snyder, K.R.; Earl, J.E.; O'Connor, K.M.; Ebersole, K.T. Resistance Training Is Accompanied by Increases in Hip Strength and Changes in Lower Extremity Biomechanics during Running. *Clinical Biomechanics* **2009**, *24*, 26–34, doi:10.1016/j.clinbiomech.2008.09.009.

49. Steinberg, N.; Dar, G.; Dunlop, M.; Gaida, J.E. The Relationship of Hip Muscle Performance to Leg, Ankle and Foot Injuries: A Systematic Review. *The Physician and Sportsmedicine* **2017**, *45*, 49–63, doi:10.1080/00913847.2017.1280370.

50. Azevedo, L.B.; Lambert, M.I.; Vaughan, C.L.; O'Connor, C.M.; Schwellnus, M.P. Biomechanical Variables Associated with Achilles Tendinopathy in Runners. *British Journal of Sports Medicine* **2009**, *43*, 288–292, doi:10.1136/bjsm.2008.053421.

51. Franettovich Smith, M.M.; Honeywill, C.; Wyndow, N.; Crossley, K.M.; Creaby, M.W. Neuromotor Control of Gluteal Muscles in Runners with Achilles Tendinopathy: *Medicine & Science in Sports & Exercise* **2014**, *46*, 594–599, doi:10.1249/MSS.0000000000000133.

52. Creaby, M.W.; Honeywill, C.; Franettovich Smith, M.M.; Schache, A.G.; Crossley, K.M. Hip Biomechanics Are Altered in Male Runners with Achilles Tendinopathy: *Medicine & Science in Sports & Exercise* **2017**, *49*, 549–554, doi:10.1249/MSS.0000000000001126.

53. Heiderscheit, B.C.; Chumanov, E.S.; Michalski, M.P.; Wille, C.M.; Ryan, M.B. Effects of Step Rate Manipulation on Joint Mechanics during Running. *Medicine & Science in Sports & Exercise* **2011**, *43*, 296–302, doi:10.1249/MSS.0b013e3181ebedf4.

54. Chumanov, E.S.; Wille, C.M.; Michalski, M.P.; Heiderscheit, B.C. Changes in Muscle Activation Patterns When Running Step Rate Is Increased. *Gait & Posture* **2012**, *36*, 231–235, doi:10.1016/j.gaitpost.2012.02.023.

55. Huang, Y.; Xia, H.; Chen, G.; Cheng, S.; Cheung, R.T.H.; Shull, P.B. Foot Strike Pattern, Step Rate, and Trunk Posture Combined Gait Modifications to Reduce Impact Loading during Running. *Journal of Biomechanics* **2019**, *86*, 102–109, doi:10.1016/j.jbiomech.2019.01.058.

56. Clansey, A.C.; Hanlon, M.; Wallace, E.S.; Nevill, A.; Lake, M.J. Influence of Tibial Shock Feedback Training on Impact Loading and Running Economy: *Medicine & Science in Sports & Exercise* **2014**, *46*, 973–981, doi:10.1249/MSS.0000000000000182.

57. Hunt, M.A.; Simic, M.; Hinman, R.S.; Bennell, K.L.; Wrigley, T.V. Feasibility of a Gait Retraining Strategy for Reducing Knee Joint Loading: Increased Trunk Lean Guided by Real-Time Biofeedback. *Journal of Biomechanics* **2011**, *44*, 943–947, doi:10.1016/j.jbiomech.2010.11.027.

58. Wood, C.M.; Kipp, K. Use of Audio Biofeedback to Reduce Tibial Impact Accelerations during Running. *Journal of Biomechanics* **2014**, *47*, 1739–1741, doi:10.1016/j.jbiomech.2014.03.008.

59. Creaby, M.W.; Franettovich Smith, M.M. Retraining Running Gait to Reduce Tibial Loads with Clinician or Accelerometry Guided Feedback. *Journal of Science and Medicine in Sport* **2016**, *19*, 288–292, doi:10.1016/j.jsams.2015.05.003.

60. Bonacci, J.; Hall, M.; Saunders, N.; Vicenzino, B. Gait Retraining versus Foot Orthoses for Patellofemoral Pain: A Pilot Randomised Clinical Trial. *Journal of Science and Medicine in Sport* **2018**, *21*, 457–461, doi:10.1016/j.jsams.2017.09.187.

61.   Cheung, R.T.H.; Davis, I.S. Landing Pattern Modification to Improve Patellofemoral Pain in Runners: A Case Series. *Journal of Orthopaedic & Sports Physical Therapy* **2011**, *41*, 914–919, doi:10.2519/jospt.2011.3771.

62.   Fyock, M.; Cortes, N.; Hulse, A.; Martin, J. Gait Retraining With Real-Time Visual Feedback to Treat Patellofemoral Pain in Adult Recreational Runners: A Critically Appraised Topic. *Journal of Sport Rehabilitation* **2019**, 1–5, doi:10.1123/jsr.2019-0094.

63.   Roper, J.L.; Harding, E.M.; Doerfler, D.; Dexter, J.G.; Kravitz, L.; Dufek, J.S.; Mermier, C.M. The Effects of Gait Retraining in Runners with Patellofemoral Pain: A Randomized Trial. *Clinical Biomechanics* **2016**, *35*, 14–22, doi:10.1016/j.clinbiomech.2016.03.010.

64.   Ferber, R.; Noehren, B.; Hamill, J.; Davis, I. Competitive Female Runners With a History of Iliotibial Band Syndrome Demonstrate Atypical Hip and Knee Kinematics. *Journal of Orthopaedic & Sports Physical Therapy* **2010**, *40*, 52–58, doi:10.2519/jospt.2010.3028.

65.   Meardon, S.A.; Campbell, S.; Derrick, T.R. Step Width Alters Iliotibial Band Strain during Running. *Sports Biomechanics* **2012**, *11*, 464–472, doi:10.1080/14763141.2012.699547.

66.   Sharma, J.; Weston, M.; Batterham, A.M.; Spears, I.R. Gait Retraining and Incidence of Medial Tibial Stress Syndrome in Army Recruits: *Medicine & Science in Sports & Exercise* **2014**, *46*, 1684–1692, doi:10.1249/MSS.0000000000000290.

67.   Willy, R.W.; Meardon, S.A.; Schmidt, A.; Blaylock, N.R.; Hadding, S.A.; Willson, J.D. Changes in Tibiofemoral Contact Forces during Running in Response to In-Field Gait Retraining. *Journal of Sports Sciences* **2016**, *34*, 1602–1611, doi:10.1080/02640414.2015.1125517.

68.   Breen, D.T.; Foster, J.; Falvey, E.; Franklyn-Miller, A. GAIT RE-TRAINING TO ALLEVIATE THE SYMPTOMS OF ANTERIOR EXERTIONAL LOWER LEG PAIN: A CASE SERIES. *International Journal of Sports Physical Therapy* **2015**, *10*, 85–94.

69.   Diebal, A.R.; Gregory, R.; Alitz, C.; Gerber, J.P. Forefoot Running Improves Pain and Disability Associated With Chronic Exertional Compartment Syndrome. *The American Journal of Sports Medicine* **2012**, *40*, 1060–1067, doi:10.1177/0363546512439182.

70.   Boyer, E.R.; Derrick, T.R. Select Injury-Related Variables Are Affected by Stride Length and Foot Strike Style During Running. *The American Journal of Sports Medicine* **2015**, *43*, 2310–2317, doi:10.1177/0363546515592837.

71.   Yong, J.R.; Silder, A.; Montgomery, K.L.; Fredericson, M.; Delp, S.L. Acute Changes in Foot Strike Pattern and Cadence Affect Running Parameters Associated with Tibial Stress Fractures. *Journal of Biomechanics* **2018**, *76*, 1–7, doi:10.1016/j.jbiomech.2018.05.017.

72.   Neal, B.S.; Barton, C.J.; Birn-Jeffrey, A.; Daley, M.; Morrissey, D. The Effects & Mechanisms of Increasing Running Step Rate: A Feasibility Study in a Mixed-Sex Group of Runners with Patellofemoral Pain. *Physical Therapy in Sport* **2018**, *32*, 244–251, doi:10.1016/j.ptsp.2018.05.018.

73.   Powers, C.; Witvrouw, E.; Davis, I.; Crossley, K. Evidence-Based Framework for a Pathomechanical Model of Patellofemoral Pain: 2017 Patellofemoral Pain Consensus Statement from the 4th International Patellofemoral Pain Research Retreat, Manchester, UK, Part 3. *British Journal of Sports Medicine* **2017**, *51*, 1713–1723.

74.   Noehren, B.; Davis, I.; Hamill, J. Prospective Study of the Biomechanical Factors Associated with Iliotibial Band Syndrome. *Clinical Biomechanics* **2007**, *22*, 951–956.

75.   Lyght, M.; Nockerts, M.; Kernozek, T.W.; Ragan, R. Effects of Foot Strike and Step Frequency on Achilles Tendon Stress During Running. *Journal of Applied Biomechanics* **2016**, *32*, 365–372, doi:10.1123/jab.2015-0183.

76.   Lersch, C.; Grötsch, A.; Segesser, B.; Koebke, J.; Brüggemann, G.-P.; Potthast, W. Influence of Calcaneus Angle and Muscle Forces on Strain Distribution in the Human Achilles Tendon. *Clinical Biomechanics* **2012**, *27*, 955–961, doi:10.1016/j.clinbiomech.2012.07.001.

77.   Gheidi, N.; Kernozek, T.W.; Willson, J.D.; Revak, A.; Diers, K. Achilles Tendon Loading during Weight Bearing Exercises. *Physical Therapy in Sport* **2018**, *32*, 260–268, doi:10.1016/j.ptsp.2018.05.007.

78.   Kernozek, T.; Gheidi, N.; Ragan, R. Comparison of Estimates of Achilles Tendon Loading from Inverse Dynamics and Inverse Dynamics-Based Static Optimisation during Running. *Journal of Sports Sciences* **2017**, *35*, 2073–2079, doi:10.1080/02640414.2016.1255769.

79.   Chen, W.-M.; Park, J.; Park, S.-B.; Shim, V.P.-W.; Lee, T. Role of Gastrocnemius–Soleus Muscle in Forefoot Force Transmission at Heel Rise — A 3D Finite Element Analysis. *Journal of Biomechanics* **2012**, *45*, 1783–1789, doi:10.1016/j.jbiomech.2012.04.024.

80.   Gu, Y.D.; Li, J.S.; Lake, M.J.; Ren, X.J.; Zeng, Y.J. The Mechanical Response of Achilles Tendon during Different Kinds of Sports. *Communications in Numerical Methods in Engineering* **2008**, *24*, 2077–2085, doi:10.1002/cnm.1096.

81. Handsfield, G.G.; Inouye, J.M.; Slane, L.C.; Thelen, D.G.; Miller, G.W.; Blemker, S.S. A 3D Model of the Achilles Tendon to Determine the Mechanisms Underlying Nonuniform Tendon Displacements. *Journal of Biomechanics* **2017**, *51*, 17–25, doi:10.1016/j.jbiomech.2016.11.062.

82. Lucaciu, A.R. Finite Element Analysis of the Achilles Tendon While Running. *Acta Medica Marisiensis* **2013**, *59*, 8–11, doi:10.2478/amma-2013-0002.

83. Obst, S.J.; Renault, J.-B.; Newsham-West, R.; Barrett, R.S. Three-Dimensional Deformation and Transverse Rotation of the Human Free Achilles Tendon in Vivo during Isometric Plantarflexion Contraction. *Journal of Applied Physiology* **2014**, *116*, 376–384, doi:10.1152/japplphysiol.01249.2013.

84. Obst, S.J.; Newsham-West, R.; Barrett, R.S. Three-Dimensional Morphology and Strain of the Human Achilles Free Tendon Immediately Following Eccentric Heel Drop Exercise. *Journal of Experimental Biology* **2015**, *218*, 3894–3900, doi:10.1242/jeb.127175.

85. Shim, V.B.; Hansen, W.; Newsham-West, R.; Nuri, L.; Obst, S.; Pizzolato, C.; Lloyd, D.G.; Barrett, R.S. Influence of Altered Geometry and Material Properties on Tissue Stress Distribution under Load in Tendinopathic Achilles Tendons – A Subject-Specific Finite Element Analysis. *Journal of Biomechanics* **2019**, *82*, 142–148, doi:10.1016/j.jbiomech.2018.10.027.

86. Yamamura, N.; Alves, J.L.; Oda, T.; Kinugasa, R.; Takagi, S. Effect of Tendon Stiffness on the Generated Force at the Achilles Tendon - 3D Finite Element Simulation of a Human Triceps Surae Muscle during Isometric Contraction. *Journal of Biomechanical Science and Engineering* **2014**, *9*, 13-00294-13–00294, doi:10.1299/jbse.13-00294.

87. Brekelmans, W.A.M.; Poort, H.W.; Slooff, T.J.J.H. A New Method to Analyse the Mechanical Behaviour of Skeletal Parts. *Acta Orthopaedica Scandinavica* **1972**, *43*, 301–317, doi:10.3109/17453677208998949.

88. Antunes, P.J.; Dias, G.R.; Coelho, A.T.; Rebelo, F.; Pereira, T. *Non-Linear Finite Element Modelling of Anatomically Detailed 3D Foot Model*; 2007; pp. 1–11;.

89. Ellison, M.A.; Akrami, M.; Fulford, J.; Javadi, A.A.; Rice, H.M. Three Dimensional Finite Element Modelling of Metatarsal Stresses during Running. *Journal of Medical Engineering & Technology* **2020**, 1–10, doi:10.1080/03091902.2020.1799092.

90. Filardi, V. Finite Element Analysis of the Foot: Stress and Displacement Shielding. *Journal of Orthopaedics* **2018**, *15*, 974–979, doi:10.1016/j.jor.2018.08.037.

91.   Gefen, A. Biomechanical Analysis of Fatigue-Related Foot Injury Mechanisms in Athletes and Recruits during Intensive Marching. *Medical and Biological Engineering and Computing* **2002**, *40*, 302–310, doi:10.1007/BF02344212.

92.   Giddings, V.L.; Beaupré, G.S.; Whalen, R.T.; Carter, D.R. Calcaneal Loading during Walking and Running: *Medicine & Science in Sports & Exercise* **2000**, *32*, 627–634, doi:10.1097/00005768-200003000-00012.

93.   Hannah, I.; Harland, A.; Price, D.; Schlarb, H.; Lucas, T. Evaluation of a Kinematically-Driven Finite Element Footstrike Model. *Journal of Applied Biomechanics* **2016**, *32*, 301–305, doi:10.1123/jab.2015-0002.

94.   Li, Y.; Leong, K.; Gu, Y. Construction and Finite Element Analysis of a Coupled Finite Element Model of Foot and Barefoot Running Footwear. *Proceedings of the Institution of Mechanical Engineers, Part P: Journal of Sports Engineering and Technology* **2019**, *233*, 101–109, doi:10.1177/1754337118803540.

95.   Morales-Orcajo, E.; Souza, T.R.; Bayod, J.; Barbosa de Las Casas, E. Non-Linear Finite Element Model to Assess the Effect of Tendon Forces on the Foot-Ankle Complex. *Medical Engineering & Physics* **2017**, *49*, 71–78, doi:10.1016/j.medengphy.2017.07.010.

96.   Morales-Orcajo, E.; Becerro de Bengoa Vallejo, R.; Losa Iglesias, M.; Bayod, J.; Barbosa de Las Casas, E. Foot Internal Stress Distribution during Impact in Barefoot Running as Function of the Strike Pattern. *Computer Methods in Biomechanics and Biomedical Engineering* **2018**, *21*, 471–478, doi:10.1080/10255842.2018.1480760.

97.   Ramlee, M.H.; Kadir, M.R.A.; Harun, H. Three-Dimensional Modeling and Analysis of a Human Ankle Joint. In Proceedings of the 2013 IEEE Student Conference on Research and Developement; IEEE: Putrajaya, Malaysia, December 2013; pp. 74–78.

98.   Vijayaragavan, E.; Gopal, T.V. Biomechanical Modeling of Human Foot Using Finite Element Methods. *Indian Journal of Science and Technology* **2016**, *9*, doi:10.17485/ijst/2016/v9i31/93412.

99.   Wong, D.W.-C.; Niu, W.; Wang, Y.; Zhang, M. Finite Element Analysis of Foot and Ankle Impact Injury: Risk Evaluation of Calcaneus and Talus Fracture. *PLOS ONE* **2016**, *11*, e0154435, doi:10.1371/journal.pone.0154435.

100.   Yettram, A.L.; Camilleri, N.N. The Forces Acting on the Human Calcaneus. *Journal of Biomedical Engineering* **1993**, *15*, 46–50, doi:10.1016/0141-5425(93)90092-D.

101. Zhang, X.; Wu, H.; Zhang, L.; Zhao, J.; Zhang, Y. Calcaneal Varus Angle Change in Normal Calcaneus: A Three-Dimensional Finite Element Analysis. *Medical & Biological Engineering & Computing* **2017**, *55*, 429–437, doi:10.1007/s11517-016-1527-4.

102. Shim, V.B.; Fernandez, J.W.; Gamage, P.B.; Regnery, C.; Smith, D.W.; Gardiner, B.S.; Lloyd, D.G.; Besier, T.F. Subject-Specific Finite Element Analysis to Characterize the Influence of Geometry and Material Properties in Achilles Tendon Rupture. *Journal of Biomechanics* **2014**, *47*, 3598–3604, doi:10.1016/j.jbiomech.2014.10.001.

103. Firminger, C.R.; Fung, A.; Loundagin, L.L.; Edwards, W.B. Effects of Footwear and Stride Length on Metatarsal Strains and Failure in Running. *Clinical Biomechanics* **2017**, *49*, 8–15, doi:10.1016/j.clinbiomech.2017.08.006.

104. Chen, T.L.-W.; Wong, D.W.-C.; Wang, Y.; Lin, J.; Zhang, M. Foot Arch Deformation and Plantar Fascia Loading during Running with Rearfoot Strike and Forefoot Strike: A Dynamic Finite Element Analysis. *Journal of Biomechanics* **2019**, *83*, 260–272, doi:10.1016/j.jbiomech.2018.12.007.

105. Chen, W.-M.; Lee, P.V.-S. Explicit Finite Element Modelling of Heel Pad Mechanics in Running: Inclusion of Body Dynamics and Application of Physiological Impact Loads. *Computer Methods in Biomechanics and Biomedical Engineering* **2015**, *18*, 1582–1595, doi:10.1080/10255842.2014.930447.

106. Pataky, T.C. Generalized N-Dimensional Biomechanical Field Analysis Using Statistical Parametric Mapping. *Journal of Biomechanics* **2010**, *43*, 1976–1982.

107. Pataky, T.C.; Vanrenterghem, J.; Robinson, M. Statistical Parametric Mapping (SPM): Theory, Software, and Future Directions. Presented at the International Society of Biomechanics, Brisbane, 2017.

108. Rice, H.; Patel, M. Manipulation of Foot Strike and Footwear Increases Achilles Tendon Loading During Running. *American Journal of Sports Medicine* **2017**, *45*, 2411–2417, doi:10.1177/0363546517704429.

109. Rugg, S.G.; Gregor, R.J.; Mandelbaum, B.R.; Chiu, L. In Vivo Moment Arm Calculations at the Ankle Using Magnetic Resonance Imaging (MRI). *Journal of Biomechanics* **1990**, *23*, 495–501, doi:10.1016/0021-9290(90)90305-M.

110. Self, B.P.; Paine, D. Ankle Biomechanics during Four Landing Techniques: *Medicine and Science in Sports and Exercise* **2001**, *33*, 1338–1344, doi:10.1097/00005768-200108000-00015.

111. Starbuck, C.; Bramah, C.; Herrington, L.; Jones, R. The Effect of Speed on Achilles Tendon Forces and Patellofemoral Joint Stresses in High-performing Endurance Runners. *Scand J Med Sci Sports* **2021**, 1–9, doi:10.1111/sms.13972.

112. de Leva, P. Adjustments to Zatsiorsky-Seluyanov's Segment Inertia Parameters. *Journal of Biomechanics* **1996**, *29*, 1223–1230, doi:10.1016/0021-9290(95)00178-6.

113. Fedorov, A.; Beichel, R.; Kalpathy-Cramer, J.; Finet, J.; Fillion-Robin, J.-C.; Pujol, S.; Bauer, C.; Jennings, D.; Fennessy, F.M.; Sonka, M.; et al. 3D Slicer as an Image Computing Platform for the Quantitative Imaging Network. *Magn Reson Imagining* **2012**, *30*, 1323–1341.

114. Kikinis, R.; Pieper, S.; Vosburgh, K. 3D Slicer: A Platform for Subject-Specific Image Analysis, Visualization, and Clinical Support. In *Intraoperative Imaging Image-Guided Therapy*; Jolesz, F.A., Ed.; Springer: New York, NY, 2014; pp. 277–289 ISBN 978-1-4614-7657-3.

115. Zhu, L.; Gao, Y.; Kikinis, R.; Tannenbaum, A. An Effective Interactive Medical Image Segmentation Method Using Fast GrowCut. In Proceedings of the Interactive Medical Image Computing Workshop; 2014.

116. Pinter, C.; Lasso, A.; Fichtinger, G. Polymoprh Segmentation Representation for Medical Image Computing. *Computer Methods and Programs in Biomedicine* **2019**, *171*, 19–26.

117. Maas, S.; Ellis, B.; Ateshian, G.; Weiss, J. Finite Elements for Biomechanics. *Journal of Biomechanical Engineering* **2012**, *134*.

118. Gozar, H.; Derzsi, Z.; Chira, A.; Nagy, Ö.; Benedek, T. Finite-Element-Based 3D Computer Modeling for Personalized Treatment Planning in Clubfoot Deformity: Case Report with Technique Description. *Medicine* **2018**, *97*, e11021, doi:10.1097/MD.0000000000011021.

119. Wren, T.A.L.; Yerby, S.A.; Beaupré, G.S.; Carter, D.R. Mechanical Properties of the Human Achilles Tendon. *Clinical Biomechanics* **2001**, *16*, 245–251, doi:10.1016/S0268-0033(00)00089-9.

120. Wren, T.A.L.; Lindsey, D.P.; Beaupré, G.S.; Carter, D.R. Effects of Creep and Cyclic Loading on the Mechanical Properties and Failure of Human Achilles Tendons. *Annals of Biomedical Engineering* **2003**, *31*, 710–717, doi:10.1114/1.1569267.

121. Farris, D.J.; Trewartha, G.; McGuigan, M.P. The Effects of a 30-Min Run on the Mechanics of the Human Achilles Tendon. *Eur J Appl Physiol* **2012**, *112*, 653–660, doi:10.1007/s00421-011-2019-8.

122. Fischer, K.M.; Willwacher, S.; Hamill, J.; Brüggemann, G.-P. Tibial Rotation in Running: Does Rearfoot Adduction Matter? *Gait & Posture* **2017**, *51*, 188–193, doi:10.1016/j.gaitpost.2016.10.015.

123. Hamill, J.; Miller, R.; Noehren, B.; Davis, I. A Prospective Study of Iliotibial Band Strain in Runners. *Clinical Biomechanics* **2008**, *23*, 1018–1025.

124. Dugan, S.A.; Bhat, K.P. Biomechanics and Analysis of Running Gait. *Physical Medicine and Rehabilitation Clinics of North America* **2005**, *16*, 603–621, doi:10.1016/j.pmr.2005.02.007.

125. Fischer, K.M.; Willwacher, S.; Arndt, A.; Brüggemann, G.-P. Calcaneal Adduction and Eversion Are Coupled to Talus and Tibial Rotation. *Journal of Anatomy* **2018**, *233*, 64–72, doi:10.1111/joa.12813.

126. Milner, C.E.; Ferber, R.; Pollard, C.D.; Hamill, J.; Davis, I.S. Biomechanical Factors Associated with Tibial Stress Fracture in Female Runners: *Medicine & Science in Sports & Exercise* **2006**, *38*, 323–328, doi:10.1249/01.mss.0000183477.75808.92.

127. Barton, C.J.; Levinger, P.; Crossley, K.M.; Webster, K.E.; Menz, H.B. The Relationship between Rearfoot, Tibial and Hip Kinematics in Individuals with Patellofemoral Pain Syndrome. *Clinical Biomechanics* **2012**, *27*, 702–705, doi:10.1016/j.clinbiomech.2012.02.007.

128. Derrick, T.R.; Hamill, J.; Caldwell, G.E. Energy Absorption of Impacts during Running at Various Stride Lengths. *Medicine & Science in Sports & Exercise* **1998**, *30*, 128–135.

129. Hobara, H.; Sato, T.; Sakaguchi, M.; Sato, T.; Nakazawa, K. Step Frequency and Lower Extremity Loading During Running. *International Journal of Sports Medicine* **2012**, *33*, 310–313, doi:10.1055/s-0031-1291232.

130. Willy, R.W.; Buchenic, L.; Rogacki, K.; Ackerman, J.; Schmidt, A.; Willson, J.D. In-Field Gait Retraining and Mobile Monitoring to Address Running Biomechanics Associated with Tibial Stress Fracture: In-Field Gait Retraining and Monitoring. *Scandinavian Journal of Medicine & Science in Sports* **2016**, *26*, 197–205, doi:10.1111/sms.12413.

131. Hafer, J.F.; Brown, A.M.; deMille, P.; Hillstrom, H.J.; Garber, C.E. The Effect of a Cadence Retraining Protocol on Running Biomechanics and Efficiency: A Pilot Study. *Journal of Sports Sciences* **2015**, *33*, 724–731, doi:10.1080/02640414.2014.962573.

132. dos Santos, A.; Nakagawa, T.; Nakashima, G.; Maciel, C.; Serrão, F. The Effects of Forefoot Striking, Increasing Step Rate, and Forward Trunk Lean Running on Trunk and Lower Limb Kinematics and Comfort. *Int J Sports Med* **2016**, *37*, 369–373, doi:10.1055/s-0035-1564173.

133. Noehren, B.; Pohl, M.B.; Sanchez, Z.; Cunningham, T.; Lattermann, C. Proximal and Distal Kinematics in Female Runners with Patellofemoral Pain. *Clinical Biomechanics* **2012**, *27*, 366–371, doi:10.1016/j.clinbiomech.2011.10.005.

134. Bishop, C.; Arnold, J.B.; Fraysse, F.; Thewlis, D. A Method to Investigate the Effect of Shoe-Hole Size on Surface Marker Movement When Describing in-Shoe Joint Kinematics Using a Multi-Segment Foot Model. *Gait & Posture* **2015**, *41*, 295–299, doi:10.1016/j.gaitpost.2014.09.002.

135. Day, E.M.; Hahn, M.E. A Comparison of Metatarsophalangeal Joint Center Locations on Estimated Joint Moments during Running. *Journal of Biomechanics* **2019**, *86*, 64–70, doi:10.1016/j.jbiomech.2019.01.044.

136. McClay, I.; Manal, K. Coupling Parameters in Runners with Normal and Excessive Pronation. *Journal of Applied Biomechanics* **1997**, *13*, 109–124, doi:10.1123/jab.13.1.109.

137. Pohl, M.B.; Messenger, N.; Buckley, J.G. Forefoot, Rearfoot and Shank Coupling: Effect of Variations in Speed and Mode of Gait. *Gait & Posture* **2007**, *25*, 295–302, doi:10.1016/j.gaitpost.2006.04.012.

138. Altman, A.R.; Davis, I.S. A Kinematic Method for Footstrike Pattern Detection in Barefoot and Shod Runners. *Gait & Posture* **2012**, *35*, 298–300, doi:10.1016/j.gaitpost.2011.09.104.

139. Lenhart, R.L.; Thelen, D.G.; Wille, C.M.; Chumanov, E.S.; Heiderscheit, B.C. Increasing Running Step Rate Reduces Patellofemoral Joint Forces. *Medicine & Science in Sports & Exercise* **2014**, *46*, 557–564, doi:10.1249/MSS.0b013e3182a78c3a.

140. Bowersock, C.D.; Willy, R.W.; DeVita, P.; Willson, J.D. Independent Effects of Step Length and Foot Strike Pattern on Tibiofemoral Joint Forces during Running. *Journal of Sports Sciences* **2017**, *35*, 2005–2013, doi:10.1080/02640414.2016.1249904.

141. Hafer, J.F.; Freedman Silvernail, J.; Hillstrom, H.J.; Boyer, K.A. Changes in Coordination and Its Variability with an Increase in Running Cadence. *Journal of Sports Sciences* **2016**, *34*, 1388–1395, doi:10.1080/02640414.2015.1112021.

142. Sinclair, J.; Richards, J.; Taylor, P.; Edmundson, C.; Brooks, D.; Hobbs, S. 3-D Kinematic Comparison of Treadmill and Overground Running. *Sports Biomechanics* **2013**, *12*, 272–282, doi:10.1080/14763141.2012.759614.

143. Pohl, M.B.; Buckley, J.G. Changes in Foot and Shank Coupling Due to Alterations in Foot Strike Pattern during Running. *Clinical Biomechanics* **2008**, *23*, 334–341, doi:10.1016/j.clinbiomech.2007.09.016.

144. Adams, D.; Pozzi, F.; Willy, R.W.; Carrol, A.; Zeni, J. Altering Cadence or Verticall Oscillation during Running: Effects on Running Related Injury Factors. *International Journal of Sports Physical Therapy* **2018**, *13*, 633–642, doi:10.26603/ijspt20180633.

145. Thompson, M.A.; Gutmann, A.; Seegmiller, J.; McGowan, C.P. The Effect of Stride Length on the Dynamics of Barefoot and Shod Running. *Journal of Biomechanics* **2014**, *47*, 2745–2750, doi:10.1016/j.jbiomech.2014.04.043.

146. Stergiou, N.; Bates, B.T.; James, S.L. Asynchrony between Subtalar and Knee Joint Function during Running. *Medicine & Science in Sports & Exercise* **1999**, *31*, 1645, doi:10.1097/00005768-199911000-00023.

147. Baumgartner, J.; Gusmer, R.; Hollman, J.; Finnoff, J.T. Increased Stride-rate in Runners Following an Independent Retraining Program: A Randomized Controlled Trial. *Scandinavian Journal of Medicine & Science in Sports* **2019**, *29*, 1789–1796, doi:10.1111/sms.13509.

148. Nigg, B.M.; De Boer, R.W.; Fisher, V. A Kinematic Comparison of Overground and Treadmill Running. *Medicine & Science in Sports & Exercise* **1995**, *27*, 98–105, doi:10.1249/00005768-199501000-00018.

149. Lysholm, J.; Wiklander, J. Injuries in Runners. *The American Journal of Sports Medicine* **1987**, *15*, 168–171, doi:doi: 10.1177/036354658701500213.

150. Longo, U.G.; Ronga, M.; Maffulli, N. Achilles Tendinopathy. *Sports Medicine and Arthroscopy Review* **2009**, *17*, 112–126, doi:10.1097/JSA.0b013e3181a3d625.

151. Silbernagel, K.; Thomeé, R.; Eriksson, B.; Karlsson, J. Continued Sports Activity, Using a Pain-Monitoring Model, during Rehabilitation in Patients with Achilles Tendinopathy: A Randomized Controlled Study. *American Journal of Sports Medicine* **2007**, *35*, 897–906, doi:http://dx.doi. org/10.1177/0363546506298279.

152. Lagas, I.F.; Fokkema, T.; Bierma-Zeinstra, S.M.A.; Verhaar, J.A.N.; Middelkoop, M.; Vos, R. How Many Runners with New-onset Achilles Tendinopathy Develop Persisting Symptoms? A Large Prospective Cohort Study. *Scandinavian Journal of Medicine & Science in Sports* **2020**, doi:10.1111/sms.13760.

153. Alfredson, H.; Lorentzon, R. Chronic Achilles Tendinosis: Recommendations for Treatment and Prevention. *Sports Med* **2000**, *2*, 135–146.

154. Zhang, X.; Deng, L.; Yang, Y.; Xiao, S.; Li, L.; Fu, W. Effects of 12-Week Transition Training with Minimalist Shoes on Achilles Tendon Loading in Habitual Rearfoot Strike Runners. *Journal of Biomechanics* **2021**, *128*, 110807, doi:10.1016/j.jbiomech.2021.110807.

155. Deng, L.; Zhang, X.; Xiao, S.; Yang, Y.; Li, L.; Fu, W. Changes in the Plantar Flexion Torque of the Ankle and in the Morphological Characteristics and Mechanical Properties of the Achilles Tendon after 12-Week Gait Retraining. *Life* **2020**, *10*, 159, doi:10.3390/life10090159.

156. Histen, K.; Arntsen, J.; L'Hereux, L.; Heeren, J.; Wicki, B.; Saint, S.; Aerni, G.; Denegar, C.; Joseph, M. Achilles Tendon Properties of Minimalist and Traditionally Shod Runners. *Journal of Sport Rehabilitation* **2016**, *26*, 159–164.

157. Almonroeder, T.; Willson, J.D.; Kernozek, T.W. The Effect of Foot Strike Pattern on Achilles Tendon Load During Running. *Annals of Biomedical Engineering* **2013**, *41*, 1758–1766, doi:10.1007/s10439-013-0819-1.

158. Kernozek, T.W.; Knaus, A.; Rademaker, T.; Almonroeder, T.G. The Effects of Habitual Foot Strike Patterns on Achilles Tendon Loading in Female Runners. *Gait & Posture* **2018**, *66*, 283–287, doi:10.1016/j.gaitpost.2018.09.016.

159. Sinclair, J.; Richards, J.; Shore, H. Effects of Minimalist and Maximalist Footwear on Achilles Tendon Load in Recreational Runners. *Comparative Exercise Physiology* **2015**, *11*, 239–244, doi:10.3920/CEP150024.

160. Farina, K.; Hahn, M. Increasing Step Rate Affects Rearfoot Kinematics and Ground Reaction Forces during Running. *Biology* **2022**, *11*, 8, doi:10.3390/biology11010008.

161. Reeves, N.D.; Cooper, G. Is Human Achilles Tendon Deformation Greater in Regions Where Cross-Sectional Area Is Smaller? *The Journal of Experimental Biology* **2017**, *220*, 1634–1642, doi:10.1242/jeb.157289.

162. Farley, C.T.; González, O. Leg Stiffness and Stride Frequency in Human Running. *Journal of Biomechanics* **1996**, *29*, 181–186, doi:10.1016/0021-9290(95)00029-1.

163. Arya, S.; Kulig, K. Tendinopathy Alters Mechanical and Material Properties of the Achilles Tendon. *Journal of Applied Physiology* **2010**, *108*, 670–675, doi:10.1152/japplphysiol.00259.2009.

164. LaCroix, A.; Duenwald-Kuehl, S.; Lakes, R.; Vanderby, R.Jr. Relationship between Tendon Stiffness and Failure: A Metaanalysis. *Journal of Applied Physiology (1985)* **2013**, *115*, 43–51, doi:doi:10.1152/japplphysiol.01449.2012.

165. Bojsen-Møller, J.; Magnusson, S.P. Heterogeneous Loading of the Human Achilles Tendon In Vivo. *Exercise and Sport Sciences Reviews* **2015**, *43*, 190–197, doi:10.1249/JES.0000000000000062.

166. Khayyeri, H.; Longo, G.; Gustafsson, A.; Isaksson, H. Comparison of Structural Anisotropic Soft Tissue Models for Simulating Achilles Tendon Tensile Behaviour. *Journal of the Mechanical Behavior of Biomedical Materials* **2016**, *61*, 431–443, doi:10.1016/j.jmbbm.2016.04.007.

167. Gerasimyuk, B.; Lazarev, I.; Movchan, O.; Skyban, M. Stress-Strain Distribution in the Model of Retrocalcaneal Bursitis by Using Heel-Elevation Insoles. *EUREKA: Health Sciences* **2020**, 31–39, doi:10.21303/2504-5679.2020.001444.

168. Hreljac, A. Impact and Overuse Injuries in Runners. *Medicine & Science in Sports & Exercise* **2004**, 845–849, doi:10.1249/01.MSS.0000126803.66636.DD.

169. Del Buono, A.; Chan, O.; Maffulli, N. Achilles Tendon: Functional Anatomy and Novel Emerging Models of Imaging Classification. *International Orthopaedics* **2013**, *37*, 715–721, doi:10.1007/s00264-012-1743-y.

170. Willy, R.W.; Halsey, L.; Hayek, A.; Johnson, H.; Willson, J.D. Patellofemoral Joint and Achilles Tendon Loads During Overground and Treadmill Running. *Journal of Orthopaedic & Sports Physical Therapy* **2016**, *46*, 664–672, doi:10.2519/jospt.2016.6494.

171. Ahn, A.N.; Brayton, C.; Bhatia, T.; Martin, P. Muscle Activity and Kinematics of Forefoot and Rearfoot Strike Runners. *Journal of Sport and Health Science* **2014**, *3*, 102–112, doi:10.1016/j.jshs.2014.03.007.

172. De Wit, B.; De Clercq, D.; Aerts, P. Biomechanical Analysis of the Stance Phase during Barefoot and Shod Running. *Journal of Biomechanics* **2000**, *33*, 269–278, doi:10.1016/S0021-9290(99)00192-X.